

AD A118372

Report No. CG-D-28-82

12

BREAK-UP OF OIL ON ROUGH SEAS -
SIMPLIFIED MODELS AND STEP-BY-STEP CALCULATIONS

by

K. Aravamudan, P. Raj, J. Ostlund
E. Newman, and W. Tucker



Document is available to the public through the
National Technical Information Service,
Springfield, Virginia 22151

DTIC
SELECTED
AUG 19 1982
S A

DTIC FILE COPY

Prepared for

U.S. DEPARTMENT OF TRANSPORTATION
United States Coast Guard
Office of Research and Development
Washington, D.C. 20590

82 08 19 008

NOTICE

This document is disseminated under the sponsorship of the Department of Transportation in the interest of information exchange. The United States Government assumes no liability for its contents or use thereof.

The contents of this report do not necessarily reflect the official view or policy of the Coast Guard; and they do not constitute a standard, specification, or regulation.

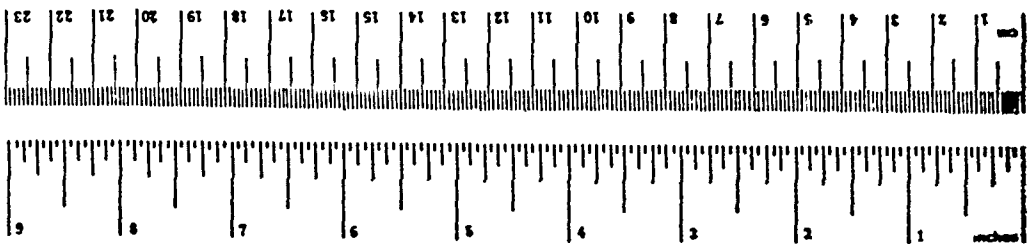
This report, or portions thereof may not be used for advertising or sales promotion purposes. Citation of trade names and manufacturers does not constitute endorsement or approval of such products.

Technical Report Documentation Page

1. Report No. CG-D-28-82	2. Government Accession No. AD-A118372	3. Recipient's Catalog No. 83066
4. Title and Subtitle Breakup of Oil on Rough Seas - Simplified Models and Step-by-Step Calculations	5. Report Date March 1982	6. Performing Organization Code DOT/USCG
	8. Performing Organization Report No.	
7. Author(s) K. Aravamudan, P. Raj, J. Ostlund, E. Newman, and W. Tucker	10. Work Unit No. (TRAIS)	
9. Performing Organization Name and Address Arthur D. Little, Inc. Acorn Park Cambridge, MA 02140	11. Contract or Grant No. DOT-CG-843466-A	
	13. Type of Report and Period Covered Final Report	
12. Sponsoring Agency Name and Address U. S. Coast Guard Office of Research and Development Washington, DC 20593	14. Sponsoring Agency Code G-DMT-4	
15. Supplementary Notes		
16. Abstract <p>In this study, an attempt has been made to integrate the existing theoretical and experimental information regarding behavior of oil spills in the ocean into a unified, sequential calculation procedure. Major consideration has been given in the study to developing the least sophisticated calculation procedures which maintain a reasonable description of the totality of the physical processes. The principal phenomena included in the prediction of oil spill behavior are: combined spreading and evaporation, the interaction of waves within the slick with the slick and formation of oil droplets, dispersion of droplets in the water column and finally the formation and dispersion of slicklets due to turbulence in the ocean. The model has been exercised for four types of oils: light crude, heavy crude, #2 fuel oil, and #6 fuel oil.</p>		
17. Key Words Oil Spills, Water Pollution, Oil Slick Dispersion, Evaporation, Breaking Waves, Globulation, Oil Pollution	18. Distribution Statement This document is available to the public through the National Technical Information Service, Springfield, VA 22161	
19. Security Classif. (of this report) UNCLASSIFIED	20. Security Classif. (of this page) UNCLASSIFIED	21. No. of Pages 200
		22. Price

METRIC CONVERSION FACTORS

Approximate Conversions to Metric Measures		Approximate Conversions from Metric Measures		
Symbol	When You Know	Multiply by	To Find	Symbol
LENGTH				
in	inches	2.5	centimeters	cm
ft	feet	30	centimeters	cm
yd	yards	0.9	meters	m
mi	miles	1.6	kilometers	km
AREA				
sq in	square inches	6.5	square centimeters	cm ²
sq ft	square feet	0.09	square meters	m ²
sq yd	square yards	0.8	square meters	m ²
sq mi	square miles	2.6	square kilometers	km ²
acres	acres	0.4	hectares	ha
MASS (weight)				
oz	ounces	28	grams	g
lb	pounds	0.45	kilograms	kg
	short tons (2000 lb)	0.9	tonnes	t
VOLUME				
tblsp	tablespoons	5	milliliters	ml
fl oz	fluid ounces	15	ml	ml
c	cups	30	milliliters	ml
pt	pints	0.24	liters	l
qt	quarts	0.47	liters	l
gal	gallons	0.95	liters	l
cu ft	cubic feet	3.8	liters	l
yd ³	cubic yards	0.03	cubic meters	m ³
		0.76	cubic meters	m ³
TEMPERATURE (exact)				
°F	Fahrenheit temperature	5/9 (after subtracting 32)	Celsius temperature	°C
°C	Celsius temperature	9/5 (then add 32)	Fahrenheit temperature	°F



* 1 in = 2.54 exactly. For other exact conversions and more detailed tables, see NBS Misc. Publ. 286, Units of Weight and Measure, Price \$2.25, NO Catalog No. 013,10,206.

Acknowledgement

This study was performed by Arthur D. Little Inc., for the Environmental Technology Branch of the U. S. Coast Guard Office of Research and Development, Washington, D. C., under contract number DOT-CG-843466-A.

The project study team at Arthur D. Little Inc. was headed by Dr. P. K. Raj and included Drs. K. S. Aravamudan, W. A. Tucker, M. Bonazountas, Mr. J. Ostlund and Ms. E. Neuman. Professor R. Van Houten of the Massachusetts Institute of Technology was a technical consultant for the project.

Mr. R. Griffiths and Lt. G. Marsh of the U. S. Coast Guard acted as technical monitors for this project. Lt. (j.g.) K. E. Schleiffer and Lt. Cmdr. C. Doherty of the U. S. Coast Guard provided many useful inputs to the development of the computer program. Their helpful support and guidance are gratefully acknowledged.



Accession No.	<input checked="" type="checkbox"/>
1. TITLE	<input type="checkbox"/>
2. AUTHOR	<input type="checkbox"/>
3. SUBJECT	<input type="checkbox"/>
4. ABSTRACT	<input type="checkbox"/>
5. NOTES	<input type="checkbox"/>
6. REFERENCES	<input type="checkbox"/>
7. INDEXING	<input type="checkbox"/>
8. OTHER	<input type="checkbox"/>
A	

TABLE OF CONTENTS

	<u>Page</u>
List of Tables	iv
List of Figures	v
SUMMARY	0-1
MODEL APPLICABILITY AND LIMITATIONS	0-4
CONCLUSIONS	0-4
RECOMMENDATIONS	0-6
1. Experimental Investigations	0-5
2. Theoretical Investigations	0-6
3. Comprehensive Oil Spill Model	0-6
1. INTRODUCTION	
1.1 Background	1-1
1.2 Objectives of the Study	1-3
1.3 Scope of the Work	1-3
2. ANALYSIS	
2.1 Qualitative Description of Oil Spill Behavior on Rough Seas	2-1
2.2 Review of Literature	2-3
3. EVAPORATION MODEL	
3.1 Introduction	3-1
3.2 Model Development	3-2
3.2.1 Loss of Oil due to Evaporation	3-2
3.2.2 Loss of Oil due to Aerosol Formation	3-6
3.3 Model Limitations	3-6
3.3.1 Prediction of the Density of the Residual Oil	3-6
3.3.2 Prediction of the Vapor Pressure Variation of the Oil.	3-8
3.4 Application of the Simple Algorithm	3-9
3.5 Conclusions	3-11
4. DROPLET FORMATION MODEL	
4.1 Introduction	4-1
4.2 Model Development	4-1
4.2.1 Determination of the Largest Diameter of Droplet	4-1
4.2.2 Determination of the Smallest Diameter of the Droplets	4-2
4.2.3 Size Distribution of Droplets	4-4
4.3 Model Limitations	4-5
4.4 Application of the Simple Algorithm	4-5
4.5 Conclusions	4-7
5. DROPLET DISTRIBUTION MODEL	
5.1 Introduction	5-1
5.2 Model Development	5-1
5.2.1 Assumptions	5-1
5.2.2 Depth of Dispersion	5-3
5.2.3 Dispersed Oil Volume	5-5
5.3 Model Limitations	5-10
5.4 Applications of the Simple Algorithm	5-13
5.5 Conclusions	5-15

6.	SURFACE OIL DISTRIBUTION MODEL	
6.1	Introduction	6-1
6.2	Assumptions on the Parameters	6-1
6.3	Model Development	6-3
6.3.1	Interface with Evaporation Model	6-3
6.3.2	Initial Horizontal Diffusion of the Slick	6-3
6.3.3	Transition Time to Gaussian Distribution	6-9
6.3.4	Gaussian Dispersion Formula	6-9
6.4	Model Limitations	6-11
6.5	Applications of the Simple Algorithm	6-12
6.6	Conclusions	6-13
7.	TABLE OF DISPERSION PREDICTIONS	
7.1	Introduction	7-1
7.2	Step-by-Step Procedure Illustration	7-5
7.2.1	Statement of Problem for the Example	7-5
7.2.2	Calculations from Spreading/Evaporation Model	7-5
7.2.3	Calculations from Droplet Formation	7-13
7.2.4	Calculations from Droplet Distribution Model	7-19
7.2.5	Calculations from Surface Oil Distribution Model	7-25
	REFERENCES	R-1
	NOMENCLATURE	N-1
	APPENDIX A - RELATIONSHIP BETWEEN VARIOUS SEA STATE PARAMETERS AND CALCULATION OF OCEAN TURBULENCE	
A.1	Relationship Between Various Sea State Parameters	A-1
A.2	Calculation of Ocean Turbulence Parameters for a Specified Sea State	A-2
	APPENDIX B - DEVELOPMENT OF A MULTI-COMPONENT OIL SLICK EVAPORATION MODEL	
B.1	Formulation of the Multi-Component Oil Slick Model	B-1
B.2	Solution of the Multi-Component Oil Slick Model	B-6
B.3	Discussion of Results	B-7
	APPENDIX C - THE EFFECT OF OIL VISCOSITY AND SLICK THICKNESS ON THE DAMPING OF BREAKING WAVE TURBULENCE	C-1
	APPENDIX D - THE EFFECT OF WAVE DAMPING ON THE PROBABILITY OF BREAKING	D-1
	APPENDIX E - COMPUTERIZATION OF CALCULATION PROCEDURE	E-1
	APPENDIX F - DROPLET NUMBER DISTRIBUTION FUNCTIONS	F-1

LIST OF TABLES

<u>Table</u>		<u>Page</u>
<u>No.</u>		
3.1	Constants to be Used in Equations (3.12) and (3.13)	3-7
3.2	Maximum Residual Density of Various Oils	3-7
3.1	Constants to be Used in Equations (3.24) and (3.25)	7-3
7.1	Summary of Evaporation Model Results	7-11
7.2	Droplet Size Distribution	7-16
7.3	Table of Error Functions	7-17
7.4	Summary of Results for Light Crude Spill in Various States	7-28
7.5	Summary of Results for Light Crude Spill in Various States	7-32
7.6	Summary of Results for Light Crude Spill in Various States	7-36
B.1	Composition of Various Types of Oils	B-8
E.1	Physical/Environmental Input Parameters	E-5
E.2	Program Control Input Parameters	E-6
E.3	Sample Input Parameters	E-9
E.4	Sample Slick Volume Distribution	E-10
E.5	Sample Oil Spreading and Droplet Distribution Information	E-11
E.6	Sample Slick Characteristics	E-12
E.7	Sample Droplet Dispersion and Slick Distributioun	E-13
E.8	Sample Component Mass Concentrations	E-14
E.9	Sample Droplet Terminal Velocities	E-15
E.10	Sample Droplet Dispersion Depths	E-16
E.11	Sample Volume Distribution	E-17

LIST OF FIGURES

Figure		<u>Page</u>
<u>No.</u>		
3.1	Duration of Oil Spread in the Gravity-Inertia Region	3-4
5.1	Variation of Droplet Terminal Velocity With Diameter	5-6
5.2	Number Distribution of Oil Droplets as a Function of Their Diameter	5-9
5.3	Distribution of Dispersed Mass as a Function of Droplet Diameter	5-11
6.1	Schematic of Surface Distribution Model	6-4
6.2	Schematic Diagram Showing the Expected Variation of Coefficient of Correlation Between Turbulent Velocity at One Instant and Another	6-6
6.3	Growth of Oil Slick Under Influence of Horizontal Diffusion	6-10
5.1	Variation of Droplet Terminal Velocity with Diameter	7-18
7.1	Volume of Light Crude Oil Remaining on the Surface as a Function of Time After Spill	7-40
7.2	Volume of Heavy Crude Oil Remaining on the Surface as a Function of Time After Spill	7-41
7.3	Volume of #2 Fuel Oil Remaining on the Surface as a Function of Time After Spill	7-42
7.3	Volume of #6 Fuel Oil Remaining on the Surface as a Function of Time After Spill	7-43
7.5	Surface Area of a Light Crude Oil Slick as a Function of Time After Spill	7-44
7.6	Surface Area of a Heavy Crude Oil Slick as a Function of Time After Spill	7-45
7.7	Surface Area of a #2 Fuel Oil Oil Slick as a Function of Time After Spill	7-46
7.8	Surface Area of a Heavy Crude Oil Slick as a Function of Time After Spill	7-47

A.1	Definition of Wind-Wave Field	A-3
B.1	Flowchart of the Computer Program of the Multi- Component System Evaporation Model	B-5
B.2	Variation of the Density Ratio of Light Crude Oil with Nondimensional Time; Slick Temperature of 25°C, Wind Velocity 5 m/s	B-9
B.2	Variation of the Vapor Pressure of Light Crude Oil with Nondimensional Time; Slick Temperature of 25°C, Wind Velocity 5 m/s	B-10
E.1	Flowchart of Main Program	E-2
F.1	Droplet Number Density Distribution Model	F-2

SUMMARY

Spills of large quantities of oil on the ocean are one of the major sources of pollution affecting both the beaches and the water. Current technology is inadequate to recover the oil spilled on rough seas. The U.S. Coast Guard is conducting research to understand the behavior of oil spills on the ocean as a complementary effort to improving the technology of spill cleanup. The work presented in this report forms part of the continuing efforts to predict the fate of the oil using physical models.

In the past, both theoretical model and laboratory scale experiments have been conducted to determine the processes that an oil spill is subjected to in rough sea conditions. Several results highlighting the importance of various physical phenomena that tend to disperse the oil slick permanently or in non-recoverable fashion have been obtained. The most important finding has been the dispersion of the surface oil into the water in the form of small oil droplets. Breaking waves have been identified as the principal mechanism by which the coherent slick is broken up into these droplets. Studies to date have developed mathematical models to explain the various phenomena, and to analyze the scaling laws and data from laboratory experiments involving oil-water-wave interactions. Each study focuses on certain specific phenomena. No single, comprehensive procedure was available which would treat all of the phenomena occurring and predict the fate of oil spilled on a turbulent ocean.

The current study was undertaken with the objective of integrating the theoretical and experimental information available into a unified, sequential calculation model. Major consideration has been given in the study to developing the least sophisticated calculation procedures which maintain a reasonable description of the totality of the physical process. The study was conducted in two phases. In the first phase, the emphasis was on developing a calculator-based algorithmic calculating procedure for determining the fate of the oil. In the second phase the models developed were computerized for ease of operation. The simplifications made in the first phase analyses were removed in the computerized version in favor of solutions to the full equations.

The principal phenomenon of interest in the early stages of oil spread/dispersion on the ocean is evaporation. A model was developed to describe the combined effects of spreading and evaporation from an oil slick containing multiple components (hydrocarbons of several different vapor pressures). This model takes into account the effects of wind speed, ambient temperature, and the concentration of the various hydrocarbon components in the oil at any particular instant in time. The coupled spreading, evaporation, and composition equations are solved (numerically) to determine for any given time the area of spread, evaporation rate, density of the mixture, and its' composition. This model cannot be exercised on a hand calculator. The multi-component model was exercised for four specific oils (light crude, heavy crude, #2 fuel oil, and #6 fuel oil), and certain dimensionless parameters were determined for use in the simple model. The simple model treats the oil as a single-component fluid with its evaporation rate modified by the parameters determined from multiple component evaporation. The results from this model are expressed in closed-form equations. A comparison of the results (for the four oils of interest) obtained from the two models, over a range of spread times, indicate close agreement.

In the analyses performed the sea state is described by the well-known Pierson-Moskowitz spectrum for a fully developed sea. The sea state is defined by the significant wave height, which represents the average height of the highest one-third of the waves occurring in the sea. Based on this correlation, the probability of encountering a breaking wave at any particular time instant within the oil slick is determined. In the presence of very large oil slicks, the sea state and related parameters are expected to be affected. The possible damping effect is not considered in the analysis of ocean wave or sea turbulence characteristics.

Predictions of the size of oil droplets formed by wave breaking are made utilizing the models developed in earlier studies. The effect of slick thickness on the formations of oil droplets is taken into account explicitly by modifying the kinematic viscosity of water due to the presence of the oil on a breaking wave. Most of the fine droplets are formed on the breaking wave bore. Under typical sea conditions (1m to 3m waves) the diameter of droplets formed vary between 1 centimeter and 50 microns.

The results from the droplet formation model are used in a model for predicting the amount of oil dispersed into the water. This analysis considers the total area of oil slick spread, determined from the evaporation model, estimates the average number of breaking waves occurring within the slick at any instant, and from these determines the total amount of oil dispersed into the water at a given time and the depth of penetration of the drops produced. Lacking specific experimental data, it is assumed that the number density spectrum for drops of a given size decreases linearly with droplet size from the smallest to the largest. The model can be exercised for a broad spectrum of input data calculated from the previous steps. The equations presented are such that the dependant parameter can be evaluated with reasonable ease.

It is a common observation that the final stage of oil slick formation occurs after the slick has thinned sufficiently by spreading, and consists of patches of floating oil with no apparent connecting film. A model has been developed to describe the overall sea area occupied by these slicklets under specified ocean conditions, spill quantity, and time after spill. Data available from a single series of ocean spill experiments have been utilized to develop scaling parameters.

The calculation sequence is structured so that it follows the various stages the oil slick goes through. The results from one model form part of the input for the next. The specific calculation steps are illustrated for the hypothetical spill scenario involving the spill of 10,000 cubic meters of light crude oil on a 1 meter significant wave height sea. A table of the predictions of the dispersion parameters at several time instances (2, 4, 8, 16, 32, and 72 hours) after the spill has been generated. The parameters evaluated include the slick area, thickness, density, total volume dispersed in water, and the volume remaining on the surface. In addition, the total sea surface area covered by slicklets is also evaluated. Graphical output displaying the variation of the floating oil volume and slick area with time are also presented. Finally, the time required to reach 50% droplet dispersion and 90% droplet dispersion are evaluated for different sea states.

MODEL APPLICABILITY AND LIMITATIONS

The methodology presented in this report is general and is applicable to any type of oil and specific sea conditions. The calculations shown and the results presented here are specific to the particular oil chosen and for the environmental conditions used. In developing the models, we have made several key assumptions, which have significant impact on the results.

For example, it has been assumed that the presence of oil does not alter either the size of the breaking wave or the probability of the wave breaking. While this may be acceptable when the oil slick is very thin, it is certainly not correct when the thickness exceeds a few millimeters. Similarly the models presented assume a linear distribution for the droplet number spectrum with droplet size. The total volume dispersed in the water depends, very sensitively, on the number of drops and their sizes. Lack of experimental data and theoretical models prevents us from evaluating the differences between actual results and our predictions.

There are other, less serious assumptions. These include: 1) fully developed sea state is described by the Pierson-Moskowitz spectrum rather than by the more accurate, but highly complicated JONSWAP spectrum, 2) evaporation terminates when the total mass release rate starts to decrease with time, and 3) the droplets follow the wake generated by breaking waves. The models presented will overpredict the dispersion into the water column in most situations. Significant improvements can be made in the predicting schemes by incorporating field experimental data when they become available. Substantial change in the methodology of calculations is not anticipated.

CONCLUSIONS

The major conclusions from the study presented in this report can be summarized as follows:

- o It is possible to make a reasonable estimation of the fate of the oil at given times after the spill, and for specified sea states with the current knowledge of the behavior of oil slick-subjected waves in the ocean. These predictions can be made with the simplified models presented, using only a hand calculator. About two man hours may be required for each set of calculations.

- o The accuracy of all the predictions cannot be verified without data from either spills of opportunity (accidental spills in which data are gathered) or from controlled spills on the ocean. Parts of the model, such as the spreading model, are sufficiently accurate for the purpose of practical predictions.
- o Evaporation loss is significant only in the first twelve to twenty hours for the range of environmental conditions and volumes of spill analyzed. No measureable droplet dispersion is likely to occur within this period. Total evaporation rate is a strong function of the volume of the spill.
- o Oils containing low vapor pressure components (for example, those boiling at temperatures above 420°K) lose a lower proportion of oil by evaporation than an oil containing components with high vapor pressures.
- o The volume of oil predicted to be dispersed in the water column is very sensitive to the assumption of linear droplet size distribution. Lack of data in this area presents a serious limitation on the accuracy of the predictions.
- o Calculating the volume of oil dispersed in the water column is simple in principle, but tedious to implement in a non-programmable calculator. Automating the calculation procedure substantially reduces the time spent on repetitive calculations.

RECOMMENDATIONS

Based on the analysis performed in this project in predicting the fate of oil in rough seas, we recommend that further research be directed towards the following areas:

1. Experimental Investigations

We recommend that the following be measured in controlled experiments or in spills of opportunity.

- o Effects of oil slick on sea state: The presence of an oil slick will reduce the significant wave height and the wave period. This will reduce the probability of a wave breaking within the slick. We recommend that the sea wave spectrum be measured both within the slick and outside the slick. If this is not feasible, gross characteristics, such as the maximum wave-height and period within and outside of the slick should be measured.

- o The size distribution of oil droplets soon after their formation by wave breaking: the amount of oil lost in the water column is directly related to the size distribution of droplets. Controlled experiments should focus on measuring the size distribution of droplets and verify the assumed criteria to determine the size of the largest and the smallest droplets.
- o Effect of emulsification: the formation of an extremely viscous oil-in-water emulsion from wave agitation contributes greatly to the difficulty of cleanup operations. We recommend a study of the effect of sea state on emulsification be conducted.

2. Theoretical Investigations

We recommend that the following theoretical investigations be undertaken:

- o The effects of slick thickness on the wave energy of breaking waves: the present theoretical assumption is that the effect of oil in breaking of waves is insignificant, but field observations indicate otherwise. We recommend that a comprehensive theoretical investigation be undertaken to study the effect of thickness of an oil slick on damping of breaking waves.
- o The effect of prolonged spills: the present analysis assumes an instantaneous spill of known volume. In the event of a continuous spill, the extent of spread will be affected by the spill rate and the advection of the slick due to current.

3. Comprehensive Oil Spill Model

The current state of the art in oil spill models is such that, while very accurate predictions of the oil behavior is still far off, reasonable determination of the fate of the oil can be made. There are numerous models for predicting slick trajectories, and there are models for mass loss by evaporation or dispersion of globules in water. There is no comprehensive model dealing with the total, three-dimensional behavior of oil slicks. For a realistic assessment of potential damage to the environment such a model is essential. We recommend that the USCG undertake the development of a general and comprehensive oil spill fate model.

1. INTRODUCTION

1.1 BACKGROUND

The United States Coast Guard (USCG) has statutory responsibility for regulating marine transportation of hazardous materials. This includes potential pollutants, such as crude oil. The Deep Water Port Act of 1974 gives the Department of Transportation, and through delegation the USCG, regulatory responsibility for most aspects of the deep water ports, including licensing, design, construction, testing, and operation.

The necessary and important part of the USCG regulatory work is assuring minimum oil spillage onto the ocean as well as developing technology to contain and remove any oil that may be spilled accidentally. In order to develop sound regulations, and prepare for reducing oil spill probabilities and ecological damage from such spills, the USCG must have a quantitative understanding of the dispersion of oil under a range of sea and weather conditions.

The USCG has undertaken research on the dispersion of oil spills on rough seas. The objectives of the studies have been to understand: 1) the sea parameters that affect the dispersion of an oil slick, 2) the types of dispersion that ensue, and 3) the extent to which oil would be dispersed to a non-recoverable state, in any given sea state. To achieve these objectives, the USCG initiated a series of contract studies in 1976.

The first of this series was conducted by Arthur D. Little, Inc. (ADL). Theoretical analyses were performed to study such phenomena as the stability of oil slicks on the ocean, the effects of ocean turbulence on the oil, globule formation, and vertical dispersion into the water. The critical conditions under which globules of oil are formed from the slick were identified, and a criterion was developed to predict the minimum sea state in which the globular dispersion would begin. It was also noted that significant oil dispersion would occur under breaking waves. Areas for further laboratory and field experiments were indicated.

Subsequently, the Massachusetts Institute of Technology (MIT) conducted an experimental study of the dispersion of oil caused by breaking waves. A detailed literature survey was initiated as well. The principal finding from these experiments was the significant depth to which the oil globules

were carried by the wake flow generated by breaking waves. The experiments and studies provided information to: 1) make qualitative estimates about the relative ease of dispersion of slicks of various properties, 2) identify the salient physical and chemical phenomena about the dispersion process, and 3) take important countermeasures following an oil spill.

Flow Research Company (FRC) performed an experimental investigation to study the air/water interaction, the characteristics of turbulence in water generated by wind and waves, and the effect of the presence of oil on the turbulence parameters. The principal findings from this work included the relationship between wind speed and the root-mean-square value of turbulent intensity of the water, the effect of wave motions, and the spectral distribution of energies in turbulence generated by simple wind shear as well as by breaking waves.

The experiments conducted by MIT and by FRC were relatively small-scale laboratory experiments. More recently, the U. S. Navy has conducted a series of field measurements of the upper ocean turbulence.

The current experimental data and theoretical knowledge of oil-spill research is scattered in various reports, and is not easily utilized for analyzing the fate of a spill. It was felt that with a relatively modest additional effort involving the development of simple models and synthesis of the results from recent studies, a comprehensive predictive model could be developed. The calculation procedure, elaborated in such a model, would provide a tool for predicting the behavior of oil spilled onto rough seas. The comprehensive model could be utilized in planning controlled experimental spills on the ocean and provides a guide to optimize data collection and their analyses.

Recognizing the importance of comprehensive models and the need for synthesizing existing knowledge into a single predictive calculation scheme, the Coast Guard issued a solicitation (number CG-843466-A) in August of 1978. Arthur D. Little, Inc. was awarded the contract (number DOT-CG-843466-A) in March 1979. This report describes the models and the step-by-step calculation procedure developed under this contract.

1.2 Objectives of the Study

The principal objective of this study was to develop a comprehensive model, using the results from recent investigations, and by additional modeling effort to determine the fate of an instantaneously spilled oil volume on a rough sea. Specifically, the focus of the analyses and methodology is to generate simplified algorithms, based on the model, so that a step-by-step calculation procedure can be executed on a desk calculator.

1.3 Scope of the Work

The work in this report primarily involves the integration of data, results, and the scaling laws developed by recent studies on the behavior of oil spills in the ocean. Several submodels have been developed to obtain a continuity in the description of the various physical phenomena, and to simplify complex calculations.

The calculation procedures in this report are structured to follow the physical processes that an oil spill in the ocean undergoes. The different phenomena are analyzed and the integrated calculations for determining the dispersion parameters are worked out. Four key physical phenomena (spread and evaporation, globule formation, globule penetration and distribution, and surface dispersion) are discussed separately in four chapters. Sample calculations for specific conditions of spills are illustrated, step-by-step, in a separate chapter. A table of dispersion parameters for several time durations of interest is also given. Four different types of oil are included in the calculations.

Oil spilled in large quantities and in a very short duration of time (an "instantaneous spill") spreads initially on the water. Oils which contain fractions of volatile components, such as the light crude, begin to evaporate during spreading. The rate of mass loss by evaporation increases initially because of increasing surface area due to spreading, and subsequently diminishes due to the reduction of volatile fractions remaining on the surface. The combined phenomena of spread and evaporation are explored in Chapter 3. Involved calculations are required to solve the total problem due to: 1) the interdependent relationship between spread and evaporation, and 2) the complex nature of the evaporation of a mixture of

components. A multi-component spread/evaporation variation model is developed. A simplification of this model to easily calculate the spreading characteristics of four specific oils (given initial compositions) is also indicated. For any given time after the spill, parameters, such as the volume of oil remaining, its density, and the slick area, can be calculated.

During the spreading on the ocean, the oil will be subject to wave action. If a large number of breaking waves are present, the oil slick is likely to be broken up and will result in the formation of globules of oil. The extent to which the slick undergoes globulation depends on the sea state and the thickness of the slick. The criteria for globule formation, the expected maximum and minimum sizes of oil drops formed in a given sea state and the effect of slick thickness on sizes of drops, are discussed in Chapter 4. While most of the analysis is a repetition of work performed in previous investigations, some new ideas and insights have been incorporated into the relationship between the breaking wave energy and the slick thickness for the formation of globules.

Oil globules generated by breaking waves or other instabilities in the slick tend to be dispersed in the water column. The wake flow generated by breaking waves seems to be the dominant mechanism for transporting oil drops to considerable depths in the ocean. The turbulence in the ocean tends to maintain a spatial distribution (with depth) of oil drops. Chapter 5 discusses this phenomenon of droplet penetration and distribution. The major effort of this chapter is to simplify the complicated equations, so that sequential calculations can be performed with ease on a calculator. The principal result calculated in this chapter is the total portion of oil dispersed in the water column at a given instant. The number density (probability) distribution with droplet size is assumed to decrease linearly, from a high value for the smallest drops formed, to zero, for the largest diameter drops that may result. The equations for the motion of the drops are obtained from previous investigations. A modified model for the depth-wise distribution of oil drops of different sizes is presented.

It is a common observation in large oil slicks caused by accidental spills that when the slick thickness becomes small, a relatively large number of small patches of oil begin to form. These patches separate from one another by water surface motions caused by currents and turbulence. This phenomenon of surface dispersion of a large number of thin patches is

discussed in Chapter 6. In this treatment, it is assumed that the thin patches do not spread significantly for further thinning, but are separated by surface velocity fluctuations. The principal result calculated is the total ocean area encompassed by these oil patches ("slicklets") at any given time.

In Chapter 7 the detailed, step-by-step procedures are illustrated for a specified initial volume of spill, type of oil, and assumed ocean conditions. This chapter illustrates the order in which the equations, derived and developed in the earlier chapters, should be used. Specific calculations are made for the description of a 10,000 cubic meter spill of light crude oil, every two hours under a 3 meter significant wave height sea. Similar results are also indicated for three other types of oil: heavy crude, number 2 fuel oil, and number 6 fuel oil. A table of dispersion parameters is developed.

The work indicated in this report was performed in two phases. In the first phase the models were developed and simplified algorithms were worked out to enable calculations to be performed on a hand-held calculator. In order to achieve this, certain simplifications were made. Following the Phase I work, the models were computerized in Phase II. The models for exercising on the computer retained their full rigor and no numerical simplifications were incorporated. The details of the computer program, the operational procedure, and the results are indicated in Appendix E.

The scope of the work did not consider of oil breakup by chemical mechanisms, formation of emulsions ("mousse"), or significant losses due to peculiar geographic conditions. The sea state must be assumed to be fully developed.

Finally, specific conclusions are discussed, and recommendations for future work are made.

2. ANALYSIS

2.1 QUALITATIVE DESCRIPTION OF OIL SPILL BEHAVIOR ON ROUGH SEAS

The release of oil from accidental spills (e.g., grounding of ships or well blow-out from offshore oil drilling) is seldom instantaneous. In the case of spills from damaged tankers, the rate depends on the size and location of the hole, the number of tanks damaged, and the local sea conditions. If the total duration of release is relatively short compared to the duration over which the total volume of oil remains on the ocean, calculations based on "instantaneous" release models are probably conservative.

When oil is released onto a relatively calm sea, it tends to spread more uniformly in all directions. The presence of winds and water currents promote non-uniform spreading. In instances where wind directions may vary significantly over short durations, fingering of oil slicks or streaking could also occur. The movement of oil slicks caused by non-breaking waves is relatively insignificant compared to that from other mechanisms. The initial thickness of oil slicks can be significant (order of centimeters). Thick slicks are not, in general, affected by the waves. In fact, oil slicks dampen most of the small wave length waves, and reduce the tendency of breaking for larger waves.

Crude oil is a mixture of a variety of components (hydrocarbons) with a range of volatilities. After the spill, all of the components tend to evaporate in proportion to their vapor pressures. The rate of mass loss with time increases as the area of slick spread increases. The evaporation rate increases with increased wind speed and with increased ambient (sea water) temperature. The net effect of this fractional evaporation of the volatile components is a reduction in the mass of oil on the water as well as an increase in its specific gravity.

Simultaneously with spreading and evaporation, oil is subject to waves, breaking waves in particular if the sea is rough. Breaking waves are the dominant agent causing the initial dispersion of oil in the form of submerged droplets. Oil droplet formation, by breaking waves, becomes more pronounced as the oil thickness decreases. As the oil film is torn by the intense turbulence on the bore of the breaking wave, air is entrained. The

mixing of oil, water, and air could produce an oil-in-water emulsion in addition to oil droplets.

Once the oil droplets are dispersed into the water, their subsequent motion is largely influenced by the turbulent flow in the water. This turbulence can be generated by winds, currents, and breaking waves. The initial downward motion of oil drops is substantially influenced by the wake flow and turbulence caused by the breaking waves. All droplets which are less dense than water tend to rise; large ones rise faster than small ones. In completely calm water, the rise rates for different sizes can be calculated easily. In the presence of turbulence, some drops tend to rise faster and some of the same size will rise slower. This results in a distribution of oil droplet concentration in the water. When a dispersed oil droplet does rise to the surface, it generally encounters the floating slick and has a tendency to recombine with the slick. During the time the droplet is against the slick, but before recombination, turbulent motion in water can easily resubmerge the droplet. Oil droplet behavior in the open ocean is poorly understood.

Some of the oil drops driven to considerable depths may be carried away by a current. This will result in a permanent loss of oil. Also it is conceivable, that some part of the oil drop population may be adsorbed on sediments and remain on the bottom. Some of the components of oil may dissolve in water, but this process is very slow. It is also possible that oil may be lost from the slick in the form of fine aerosols to the atmosphere. While there is no data to confirm this, it is conceivable that gusts of wind and wave breaking may produce oil aerosols, much the same way as salt sprays are generated.

The slick floating on the surface is undergoing physical expansion by spreading, and a change in properties, due to increasing concentration of heavy components. Such a slick may exhibit a variation in properties over its area causing instabilities in its film. Also, when the slick is thin and is broken by breaking waves, small slicklets may be formed. The combined effect of property variation and physical separation probably results in the formation of a large number of the smaller slicks ("pancakes") that have been observed in large spills. These pancakes are subjected to the surface turbulence and are dispersed horizontally over a wider area than the actual oil surface area, corresponding to a single

coherent slick. The spread rate of individual pancakes, with respect to their center, is low and can be treated as non-expanding.

In conclusion, it can be said that an oil spill on an ocean: 1) loses mass by evaporation, 2) is dispersed vertically in the form of oil globules, and 3) is dispersed horizontally over a wide area by surface turbulence after the slick has spread by gravitational and surface-tension forces. Any model utilized in the prediction of the fate of the oil must consider all three phenomena.

2.2 REVIEW OF LITERATURE

Exhaustive reviews of the literature relevant to the problem of oil spill on the ocean have been given by Raj (1977), Milgram et. al. (1978), and Lin et. al. (1978). These reviews cover such topics as the quantitative descriptions of the wind wave interactions, sea states, ocean turbulence, breaking wave probabilities, energy dissipation, characteristics of ocean turbulence, scaling laws, parameters, and other related subjects. Also included in the survey are the qualitative and quantitative observations from large accidental spills, and the chemical phenomena of importance. It is not intended to reiterate the material in these surveys, but to discuss only those results which have been developed since the publication of the above studies. Also, the studies used directly in this investigation will be discussed.

The first mechanism which leads to the ultimate degradation of oil is spreading. An initial model describing the behavior of oil on calm water was developed by Blokker (1964). The model is based on the assumption that most of the potential energy is lost by friction, and that the substantial duration of spreading occurs when the oil thickness is less than 2 cms. The spreading rate was assumed to be proportional to the mean film thickness. Blokker extended the analysis to include the effects of the evaporation of oil.

Blokker's model for evaporation is an extension of the models generally used for the evaporation of water from a lake or for petroleum distillation processes. Blokker assumed the oil to be a single component and developed a complex relationship between spread and evaporation.

Fay (1970) and later Hoult (1972) improved the spreading model, considering the four different types of forces (i.e., gravity, inertia, friction, and surface tension) that act on oil. Milgram and Van Houten (1974) considered the effect of swell waves on spreading oil and concluded that it had little effect.

McKay and Matsugu (1973) conducted laboratory experiments on the effects of wind speed and oil pool sizes on the evaporation rate. A correlation involving the evaporation rate, wind speed and pool area was proposed. There is no comprehensive spreading evaporation analysis which includes the multi-component nature of crude oil (with fractions which have a whole range of vapor pressures), and the effect of varying physical properties.

A comprehensive theoretical analysis of the various (physical) ways in which an oil slick on the ocean can be dispersed has been discussed by Raj (1977). The purpose of the study was to: 1) identify the various phenomena which influence oil dispersion, 2) develop a first generation of physical models, and 3) indicate the parameters that have significant effect on the dispersion process.

The results of the study indicate that the oil globule formation could begin in a 3 meter significant wave height sea caused by non-breaking waves. It is concluded that breaking waves would be the significant mechanism by which oil globules would be formed and driven into the water column.

Models were developed to evaluate the maximum size of droplets formed, the probability of slick fracture by a series of breaking waves, and the distribution of oil droplets in the water column. It was concluded that slick breakup into slicklets by breaking waves was almost impossible in the middle of the ocean. Much of the required information (an assessment of the fate of the oil) is identified. This includes the nature and characteristics of upper ocean turbulence, the effect of the presence of oil on the sea state parameters, wind wave interactions, and other information.

The most extensive series of experiments, involving the dispersion of oil by breaking waves in a laboratory wave channel was performed by Milgram et. al. (1978). The experiments were designed to study the effect of variation on oil properties on the degree of dispersion under similar breaking waves. These tests indicate that the slick thickness is the single most important parameter influencing the amount of floating oil dispersed

into the water. Increasing slick thickness from 0.5 millimeters to 5.5 millimeters reduces dispersion by 96%.

These tests also indicate that the amount of oil dispersed was quite viscosity sensitive with less oil being dispersed for high oil viscosity. This has considerable significance since aging of the oil on the ocean (also evaporation) increases the viscosity and reduces the propensity for droplet dispersion.

The experiments indicate the relative importance of wake flow caused by the breaking waves in dispersing the oil drops to great depths. Milgram et. al. have developed an expression for the depth of penetration of a globule of given size, and correlated it with the rate of momentum lost by the breaking wave.

This study contains the expressions for the smallest size oil drop formed by breaking waves. This is based on the equilibrium of the surface-tension force that tends to maintain the drop and the turbulent fluctuation (dynamic pressure) over a scale comparable to the micro-scale of turbulence.

The relationship between oil properties and the recoalescence time between droplets and the slick was also investigated. It was discovered that the coalescence time increased as the cube of the droplet size increased and with increased oil viscosity. No particular trend was observed with slick thickness. This work by Milgram et. al. has provided qualitative and quantitative information on the formation of oil droplets by breaking waves and their dispersion in water.

The interaction between the wind and waves and the spectral energy in wind generated turbulence in water were measured experimentally by Lin et. al. (1978). Measurements have been made in water, both in the presence of and absence of an oil slick on water. The principal findings from this experimental work were as follows:

-In a wind-generated turbulence within the water, the maximum intensity of turbulence is about 0.7% of the wind speed. The water surface drift speed is about 3.2% of wind speed (measured typically at 10 meters above surface in field conditions). The boundary layers in air and water were similar.

-Dominant turbulence in water is generated by breaking waves. The turbulence spectrum shows a significant peak at the wave frequency and a spectrum which (for about two decades) decreases as the $-5/3$ power of the frequency.

-The presence of oil reduces the amplitude of the water waves and the peak energy density in the wave spectrum for identical excitation conditions.

This series of experiments provides quantitative data on the nature and level of turbulence in water generated by wind shear and breaking waves. The extrapolation of the laboratory results to full-scale sea conditions is indicated in Appendix A of this report.

Shonting (1979) has conducted the field study to measure surface layer turbulence associated with wind stress and breaking waves in the ocean. Measurements were made from a fixed location off Gould Island (Narragansett Bay) in 1 meter waves and under 9 meters per second to 12 meters per second wind speeds. His results indicate that the dominant frequency in the turbulent spectrum corresponds to the wave frequency. The vertical kinetic energy is found to decrease exponentially with depth, and the surface kinetic energy is proportional to the wind speed. The results also show the dependence of the vertically integrated kinetic energy with the cube of the wind speed. Measurements of Reynolds stresses were also made. These results are in agreement with the predictions made by Shonting (1970).

The behavior of oil patches on the ocean is an important area of study for clean up purposes but a systematic study has not been undertaken. On the other hand, the behavior of pollutant clouds, subjected to turbulent atmosphere is reasonably well understood. Csanady (1973) has discussed the growth of an instantaneously released finite-size cloud of particles. It can be seen that the variance of the cluster of particles grows proportional to the square of the diffusion time. Limited quantitative information on the dispersion of small patches of oil are available from tests conducted to evaluate the performance of oil recovery equipment. The results indicate two distinct dispersion regimes with time, similar in character to the two regimes of dispersion postulated by Csanady for finite-size cloud dispersion. An analysis similar to the ones used for three dimensional cloud dispersion is applicable, with certain modifications, to the description of oil slicklet dispersion on the ocean surface.

The brief discussion of the pertinent literature and the findings from more recent studies directly related to oil dispersion in the ocean indicate that substantial progress has been made in understanding this phenomenon. The knowledge is far from complete. For example, there are no models which consider the (significant) effect of wave damping by oil. It is not certain how the size of the breaking wave that will occur within the oil slick is related to the oil film thickness and oil properties. Measurements are not available from experiments on the ocean or from accidental spills indicating the size distribution of oil droplets that may be formed by breaking waves. Similarly, field data does not exist on the effect of an oil slick on damping the near surface turbulence. Finally, the mechanism of turbulence generation on the bore of the breaking wave, and its characterization in terms of intensity, scales and spectra are very poorly understood.

In the succeeding chapters, analyses are presented to calculate the effects of the various phenomena that the oil is subject to on the ocean. Where it is relevant, appropriate references are made to the specific works on which the analyses are based.

3. EVAPORATION MODEL

3.1 Introduction

In this chapter we develop a model to predict the loss of oil due to evaporation. The model assumes an instantaneous oil spill of known volume and composition, and accounts for the simultaneous spreading and evaporation. The output of the model is the remaining volume of oil, the area and thickness of the slick, and the average density of the oil remaining in the slick.

In selecting a model our objective is based on developing a simple, sequential algorithm to predict the rates of evaporation as a function of time. We approached the problem in the following manner:

-By developing a multi-component oil slick model which considers the combined effects of evaporation and spreading. The resulting equations are nonlinear and coupled. Further, the model requires additional data on the vapor pressure, density, and concentration of various components. The solution of the model equations were obtained with the aid of a digital computer. The governing differential equations and the method of obtaining the solutions are discussed explicitly in Appendix B.

-By developing a simple model to predict residual volume, area of the slick, and average density of the oil as a function of the time after the spill. The implicit assumption is that the properties of the oil (such as vapor pressure and average density of the residual oil) are weak functions of time. The variations of these properties were determined empirically using the results of the multi-component oil-slick model. The results of the simplified evaporation model were compared with the multi-component oil-slick model to determine the limitations and the accuracy of the simple model.

The formulation of the simple evaporation model is discussed below. The computation procedure is demonstrated in section 3.4.

3.2 Model Development

3.2.1 Loss of Oil Due to Evaporation

In formulating the simple evaporation model we made three assumptions:

-The oil slick is homogeneous in the horizontal and vertical directions and is of uniform height.

-The spill is radially symmetric.

-The oil can be characterized by a single component and the physical properties of the oil can be taken as quasi-steady.

These assumptions enable us to solve the equations analytically. Rewriting the conservation of mass equation, we obtain:*

$$\frac{dV}{dt} = - \frac{k}{\rho} A(t) \quad (3.1)$$

Further, we assume that the evaporation flux is given as:

$$k = k_0 U P \quad (3.2)$$

Here k_0 is an empirical evaporation constant. Fay's model (1971) was used to evaluate the area of spreading in equations (3.1). In essence, the spreading is broken down artificially into three stages: the gravity-inertia, gravity-viscous, and the surface tension regimes. The expressions for the radius of the slick in these regimes are given in Appendix B. Only the results of the analysis are presented in this section. We introduce the following variables:

$$\bar{V} = V / V_0$$

$$T = v_0^{1/6} / G^{1/2}$$

$$\Delta = \rho_0 / \rho_w$$

$$\tau = t / T$$

$$R = \rho / \rho_0$$

$$G = g (1 - \Delta)$$

Using Fay's expressions, the time of transition from the gravity-inertia regime to the gravity-viscous regime is given by:

* For identification of symbols, see "Nomenclature", page N-1

$$t_0 = 0.546 (V / G \nu_w)^{1/3} \quad (3.3)$$

The transition time t_0 as a function of the initial volume V_0 for various types of oils is plotted in Figure 3.1. Even for the large spill volumes (e.g. 10,000 cubic meters) the transition time t_0 is typically less than 1/2 hour (see Figure 3.1). We assume that there is no evaporation during the initial gravity-inertial spreading. The expressions for the remaining volume and the area of the slick in the gravity-viscous and surface tension regimes are:

Gravity-viscous regime:

$$V = V_0 \left(1 - c_1 g_1 f_1 h_1 \text{UP} (\tau^{3/2} - \tau_0^{3/2}) \right)^3 \quad (3.4)$$

$$A = c_2 f_2 g_2 h_2 \nu_w^{2/3} \tau^{1/2} \quad (3.5)$$

where the symbols used in equations (3.4) and (3.5) are defined as:

$$\left. \begin{aligned} c_1 &= 0.670 k_0 / (\nu_w^{1/6} g^{-5/12} \rho_w) \\ c_2 &= 3.02 g^{-1/12} / \nu_w^{1/6} \\ f_1 &= V_0^{-1/12} & f_2 &= V_0^{1/12} \\ g_1 &= \frac{1}{\Delta (1 - \Delta)^{3/4}} & g_2 &= \frac{1}{(1 - \Delta)^{1/4}} \\ h_1 &= (1 - \Delta R)^{1/3} / R & h_2 &= (1 - \Delta R)^{1/3} \end{aligned} \right\} \quad (3.6)$$

and

$$\tau_0 = 0.546 (V_0 G / \nu_w^2)^{1/6} \quad (3.7)$$

Surface tension regime:

$$V = V_0 \left(V_1 / V_0 - c_3 f_3 g_3 h_3 \text{UP} (\tau^{5/2} - \tau_1^{5/2}) \right) \quad (3.8)$$

$$A = c_4 f_4 g_4 h_4 \tau^{3/2} \quad (3.9)$$

where:

$$\left. \begin{aligned} c_3 &= 3.217 k_0 \nu_w^{-1/12} \rho_w^{-2} g^{5/4} \\ c_4 &= 8.04 \nu_w^{-1/12} \rho_w^{-1} g^{3/4} \end{aligned} \right\} \quad (3.10)$$

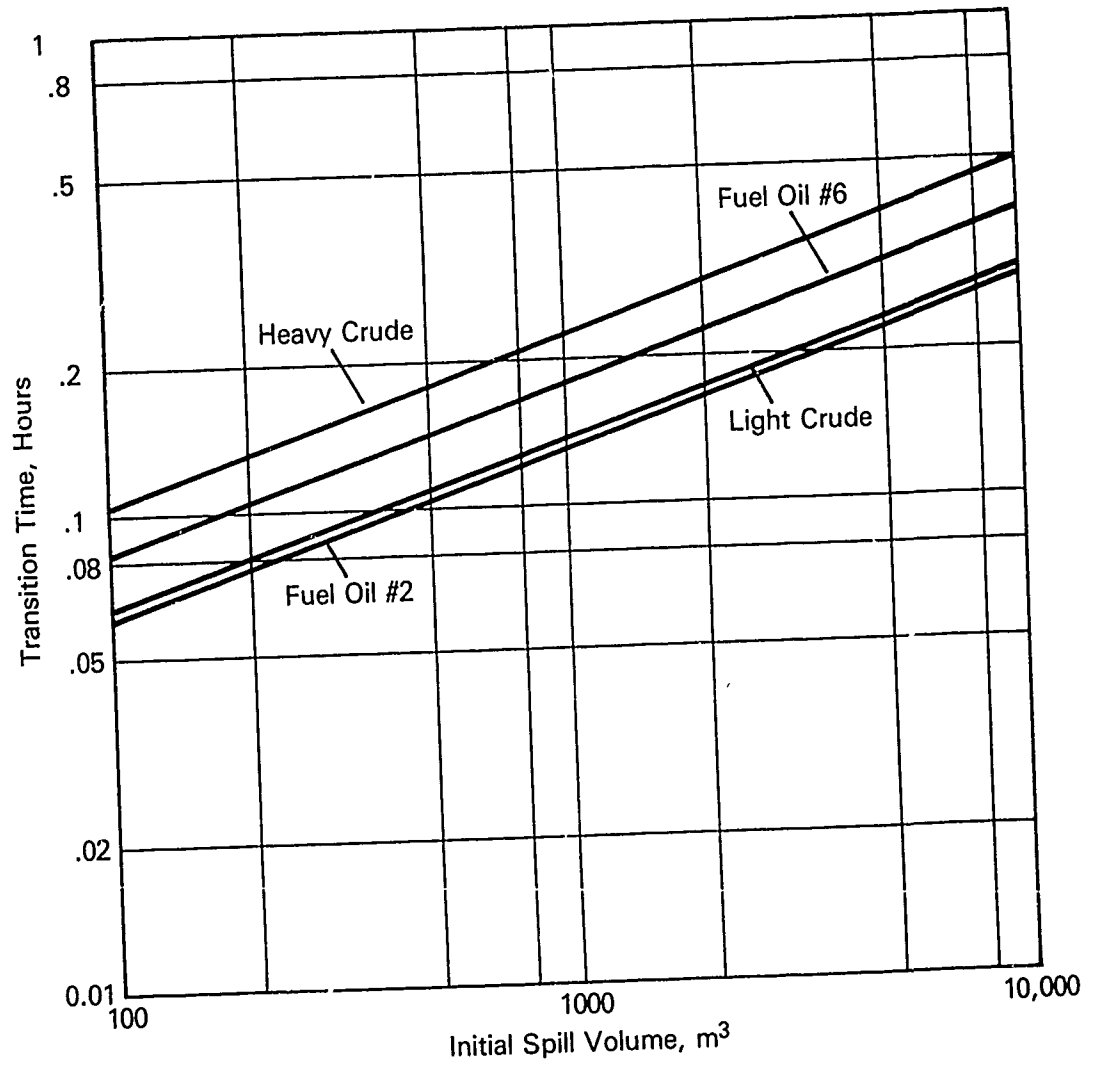


Figure 3.1 Duration of Oil Spread in the Gravity-Inertia Region

$$\begin{aligned}
 f_3 &= V_0^{-7/12} & f_4 &= V_0^{1/4} \\
 g_3 &= \sigma / \Delta (1 - \Delta)^{5/4} & g_4 &= \sigma / (1 - \Delta)^{3/4} \\
 h_3 &= 1/R
 \end{aligned}
 \tag{3.10}$$

Here τ_1 is the transition time from the gravity-viscous regime to the surface tension regime and V_1 is the residual volume at τ_1 . The transition time is given by the expression:

$$\tau_1 = 0.375 \frac{\rho_w}{\sigma} G^{5/6} V_w^{1/3} V^{2/3} / V_0^{1/6}
 \tag{3.11}$$

Equation (3.11) shows the transition time τ_1 as dependant on the residual volume given by equation (3.4). In principle, it is necessary to solve equations (3.4) and (3.11) simultaneously to obtain an accurate value of τ_1 . Because P and R are functions of τ , it is very difficult to solve equations (3.4) and (3.11) simultaneously. However, a greater degree of accuracy in estimating τ_1 is not needed. In practice, one can obtain a value of τ_1 on a trial and error basis.

The two quantities that are not defined in equations (3.4) and (3.8) are P and R. R, by definition, is the ratio of the average density of the remaining oil in the slick to the initial density of the oil. Since light fractions evaporate rapidly, the density of the remaining oil increases with time. The other factors which affect the functional dependance of R are the wind velocity and the slick temperature. P, the vapor pressure of the oil, is a function of the nondimensional time, τ . The initial value of P is very high and corresponds to the vapor pressure of the lightest fraction in the oil. As the lighter fractions evaporate, the vapor pressure decreases and the tendency to evaporate also decreases. The vapor pressure is a function of the temperature of the oil slick. The variation of P and R with nondimensional time τ are determined empirically using the results of the multi-component oil slick analysis. The functional forms of P and R are:

$$P(\tau) = a_1 T_s^{0.66} \exp(-a_2 T_s^{0.22} (\tau - \tau_0))
 \tag{3.12}$$

$$R(\tau) = 1 + b_1 T_s^{0.22} U^{0.32} (\tau - \tau_0)^{b_2}
 \tag{3.13}$$

Here a_1 , a_2 , b_1 , and b_2 are dependant on the type of oil and T_s is the temperature of the slick in degrees Celcius. The numerical values of these constants for different types of oils are provided in Table 3.1.

3.2.2 Loss of Oil Due to Aerosol Formation

Small droplets of oil are formed because of the impact of breaking waves on the oil slick and whitecaps on the ocean. No theoretical model or experimental evidence is available to estimate the loss of oil due to aerosol formation.

Based on some of the information available on salt sprays in the ocean, we estimate the droplet density flux to be 10^2 to 10^3 droplets per square meter per second. The typical diameter of the droplets is about 50 microns. The total oil loss due to aerosol formation can be estimated once the area of the slick is known. For a 10,000 cubic meter spill, at the end of 2 hours, the total amount of oil loss in the form of aerosols is about 1 cubic meter. At the end of 24 hours, the oil loss has increased to about 20 cubic meters. These losses are small compared to the oil loss due to evaporation, and we will ignore the effect of oil loss due to aerosol formation.

3.3 Model Limitations

In the preceding section, we developed a simple model to account for the loss of oil due to evaporation. The expressions derived in section 3.2.1 were based on the premise that the properties of oil, such as the decrease in the vapor pressure and the increase in the density, were very slow varying functions of the nondimensional time. The functional forms of these properties were determined empirically, using the results of the multi-component slick model.

The validity of the simple model is tested over a range of initial volumes (100 to 10,000 cubic meters), wind speeds (5 to 20 meters per second), and slick temperatures (10 to 25 degrees Celcius). The remaining volume, R , and density of the oil slick predicted by the simple model were compared with the results obtained by the multi-component slick model. Because of the nature of the assumptions made in developing the simple model, the model has certain limitaions, which are discussed below.

Table 3.1
Constants to be Used in Equations (3.12) and (3.13)

<u>Type of Oil</u>	<u>Coefficients</u>			
	<u>a₁</u>	<u>a₂</u>	<u>b₁</u>	<u>b₂</u>
Light Crude	350	9.67×10^{-5}	4.2×10^{-5}	0.62
Heavy Crude	27	2.47×10^{-5}	3.5×10^{-7}	1.05
Fuel Oil #2	4.6	1.56×10^{-6}	(no change in density)	
Fuel Oil #6	(no evaporation)		(no change in density)	

Table 3.2
Maximum Residual Density of Various Oils

<u>Type of Oil</u>	<u>Maximum Density</u> <u>ρ_{\max} (kg/m³)</u>
Light Crude	965
Heavy Crude	1060
Fuel Oil #2	890
Fuel Oil #6	970

3.3.1 Prediction of the Density of the Residual Oil

The nondimensional density of the residual oil was given by equation (3.13) which is repeated here:

$$\rho/\rho_0 = 1 + b_1 T_s^{0.22} U^{0.32} (\tau - \tau_0)^{b_2} \quad (3.13)$$

This equation indicates that for a given slick temperature and wind velocity, the density of the residual oil in the slick increases with time. However, the upper bound for the average density is the density of the heaviest hydrocarbon present in the oil. If ρ_{\max} is the density of the heavy fraction, then the time to reach ρ_{\max} can be calculated using the above expression. The time to reach maximum density can be calculated by inverting equation (3.13):

$$\tau_{\rho_{\max}} = (\rho_{\max} / \rho_0 - 1) / (b_1 T_s^{0.22} U^{0.32})^{(1/b_2)} + \tau_0 \quad (3.14)$$

For nondimensional times exceeding that associated with ρ_{\max} , the density will be constant and is equal to ρ_{\max} . The maximum permissible density for various types of oils is indicated in table 3.2.

3.3.2 Prediction of the Vapor Pressure Variation of the Oil

The vapor pressure variation of the oil is

$$P(\tau) = a_1 T_s^{0.66} \exp(-a_2 T_s^{0.22} (\tau - \tau_0)) \quad (3.12)$$

As mentioned above, the evaporation flux is directly related to the vapor pressure and decreases with time. The evaporation rate increases with time due to the enhanced area of the slick. The implicit assumption in this expression is that evaporation flux decreases exponentially. This is true during the initial period of evaporation when the light fractions in the oil are evaporating rapidly. The heavier fractions do not evaporate to any appreciable degree and the variation predicted by the above expression is not valid. In fact, it is possible to estimate an upper limit for the nondimensional time beyond which the present evaporation model is not valid. This is given by equating the derivative of equations (3.4) and (3.8) to zero. The approximate solutions to the resulting algebraic equations are:

$$\begin{aligned} \tau_c &\approx 3/2 a_2 T_s^{0.22} && \text{in gravity-viscous regime} \\ \tau_c &\approx 5/2 a_2 T_s^{0.22} && \text{in surface tension regime} \end{aligned} \quad (3.15)$$

The evaporation model developed in this chapter will not yield satisfactory results for times greater than the critical times defined above.

The limitation on the applicability of the evaporation model does not present a serious problem. Even for moderate initial volumes of spill (10,000 cubic meters), an average slick thickness of about 3 to 4 millimeters is reached when the nondimensional time is equal to the critical time shown above. When the thickness of the oil slick is this small the interaction of ocean waves with the slick, may become a more dominant mechanism by which the oil.

3.4 Application of the Simple Algorithm

In this section we demonstrate the use of the simple algorithm developed in section 3.2 to predict the residual volume and surface area of an oil slick. The relevant equations are redefined and given new numbers.

Step 1 Using the user-defined quantities, determine the following parameters:

$$\Delta = \rho_0 / \rho_w \quad (3.16)$$

$$G = g(1 - \Delta) \quad (3.17)$$

$$T = V_0^{1/6} G^{-1/2} \quad (3.18)$$

Unless otherwise specified use these properties of water:

$$\begin{aligned} \rho_w &= 1000 \text{ kg/m}^3 && g = 9.81 \text{ m/s}^2 \\ \nu_w &= 1 \times 10^{-6} \text{ m}^2/\text{s} \end{aligned}$$

k_0 is an empirical constant to determine the evaporation flux, equal to 1×10^{-8} seconds squared per meter squared.

Using Table 3.1, determine the constants a_1 , a_2 , b_1 , b_2 . Unless otherwise specified use $\rho_{\text{max}} = 990$ kilograms per cubic meter.

Step 2 Determine the times for transition from gravity-inertia to gravity-viscous and from gravity-viscous to surface tension regimes:

$$\tau_0 = 0.546 (V_0 G / \nu_w^2)^{1/6} \quad (3.19)$$

To determine τ_1 , assume that there is no evaporation and use the original volume V_0 in equation (3.11). This leads to:

$$\tau_1 = 0.375 (\rho_w / \sigma) G^{5/6} \nu_w^{1/3} V_0^{1/2} \quad (3.20)$$

Typically 10 to 20 per cent of the original volume evaporates in the gravity-viscous regime, so this procedure will overestimate the value of τ_1 by about 5 to 10 per cent. A more accurate value of τ_1 may be calculated at a later stage using the following expression:

$$\tau_1 = 0.375 (\rho_w / \sigma) G^{5/6} \nu_w^{1/3} V_0^{-1/6} \quad (3.21)$$

Determine τ_c and $\tau_{\rho_{\max}}$:

$$\tau_c = 3/2 a_2 T_s; \text{ if } \tau_c > \tau_1 \text{ then } \tau_c = 5/2 a_2 T_s \quad (3.22)$$

$$\tau_{\rho_{\max}} = ((\rho_{\max} / \rho_0 - 1) / b_1 T_s^{0.22} U^{0.32})^{(1/b_2)} + \tau_0 \quad (3.23)$$

Step 3 Nondimensionalize the user defined times.

Step 4 Determine the density and the vapor pressure at various times specified by the user:

$$R = 1 + b_1 T_s^{0.22} U^{0.32} (\tau - \tau_0)^{b_2} \quad (3.24)$$

$$P = a_1 T_s^{0.66} \exp((\tau - \tau_0) (-a_2 T_s^{0.22})) \quad (3.25)$$

Note: If τ is greater than $\tau_{\rho_{\max}}$, assume ρ equals ρ_{\max} .
If τ is greater than τ_c , calculate P & τ equal to τ_c .

Step 5 If the nondimensionalized, user-specified time is less than 1, use equations (3.26) and (3.27) to determine the residual volume and the area of the slick. If τ is greater than τ_1 , use equations (3.28) and (3.29) to determine the residual volume and the area of the slick:

$$V = V_0 (1 - c_1 f_1 g_1 h_1 U P (\tau^{3/2} - \tau_0^{3/2}))^3 \quad (3.26)$$

$$A = c_2 f_2 g_2 h_2 V^{2/3} \tau^{1/2} \quad (3.27)$$

$$V = V_0 \left(V_1/V_0 - c_3 f_3 g_3 h_3^{UP} (\tau^{5/2} - \tau_1^{5/2}) \right) \quad (3.28)$$

$$A = c_4 f_4 g_4 \tau^{3/2} \quad (3.29)$$

where the various symbols are defined as:

$$\begin{aligned} c_1 &= 0.670 k_0 / (\nu_w^{1/6} g^{5/12} \rho_w) & c_2 &= 3.02 g^{1/2} / \nu_w^{1/6} \\ c_3 &= 3.217 k_0 / (\nu_w^{1/2} \rho_w^2 g^{5/4}) & c_4 &= 8.04 / (\nu_w^{1/2} \rho_w g^{3/4}) \\ f_1 &= V_0^{-1/12} & f_2 &= V_0^{1/12} \\ f_3 &= V_0^{-7/12} & f_4 &= V_0^{1/4} \\ g_1 &= 1 / \Delta (1 - \Delta)^{3/4} & g_2 &= 1 / (1 - \Delta)^{1/4} \\ g_3 &= \sigma / \Delta (1 - \Delta)^{5/4} & g_4 &= \sigma / (1 - \Delta)^{3/4} \\ h_1 &= (1 - \Delta R)^{1/3} / R & h_2 &= (1 - \Delta R)^{1/3} \\ h_3 &= 1/R \end{aligned}$$

and V_1 is the remaining volume at τ_1 calculated using equation (3.26).

Note: if τ is greater than τ_c , calculate V at τ equal to τ_c using equation (3.27) or (3.29).

Step 6 To determine the slick thickness divide the residual volume by the area of the slick.

$$h(\tau) = V(\tau) / A(\tau) \quad (3.30)$$

to obtain the evaporation flux use the equation:

$$k = k_0 UP \quad (3.31)$$

Step 7 Summarize results by tabulating the residual volume V , slick surface area A , slick thickness h , and average density of residual oil ρ , as a function of time. These results will be used as input to the droplet formation model discussed in Chapter 4.

3.5 Conclusions

The conclusions of the evaporation model are:

- The inputs to the model are the type of oil, initial volume spilled, wind velocity, and slick temperature.
- The outputs of the model are the volume remaining, the area and the thickness of the slick, the average density of the oil in the slick, and the evaporation flux.

4. DROPLET FORMATION MODEL

4.1 INTRODUCTION

In Chapter 3, we developed a simple model to predict the evaporation loss of oil from a slick. We indicated that evaporation is the primary means of mass transfer from the slick during the initial stages of its existence. Since the lighter components of the oil evaporate rapidly, the evaporative flux decreases with time. Further, the thickness of the slick decreases with time, and the interaction of the oil slick with ocean water begins to dominate the mass transfer process. At sufficiently large times after the spill, the loss of oil due to evaporation is expected to be small compared to the loss due to dispersion of oil in the form of fine droplets. In this chapter, we discuss the droplet formation models and present a simple formulation to predict the droplet size.

Our objective in selecting a model is based on developing a simple sequential algorithm to determine the sizes of droplets that are formed by the turbulence in the ocean. We have approached the problem in the following manner:

-We used the Raj (1977) model to determine the maximum size of the droplets.

-We used the model developed by Milgram et. al. (1978) to determine the smallest size of the droplets.

These two droplet formation models are discussed in detail in Section 4.2.

4.2 MODEL DEVELOPMENT

4.2.1 Determination of the Largest Droplet Diameter

Raj (1977) considered the floating oil slick subjected to wave action. The force acting on a droplet of oil tending to separate from the slick is primarily due to turbulent pressure fluctuations. The restoring forces are due to buoyancy and surface tension. A droplet is formed when the separating forces are greater than the restoring forces. This condition is given by:

$$p^* (\pi d^2 / 4) \approx 1/12 \pi d^3 \rho_w g (1 - \rho / \rho_w) + \pi \sigma d \quad (4.1)$$

suction force = buoyancy force + surface-tension force

Where the turbulent pressure fluctuation is given by:

$$p^* \approx 1/2 \rho_w \overline{u'^2} \quad (4.2)$$

The minimum turbulent intensity in water when a droplet is formed is given by:

$$\overline{u'^2} = \left(64/3 \frac{g\sigma}{\rho_w} (1 - \rho/\rho_w) \right)^{1/2} \quad (4.3)$$

The size of the drop formed at the above intensity is given by:

$$d_{\max} = \left(12\sigma/g(\rho_w - \rho) \right)^{1/2} \quad (4.4)$$

Using a second approach based on Kelvin-Helmholtz instability, Raj (1977) arrived at a critical diameter given by:

$$d_{\max} = \pi \left(\sigma/g(\rho_w - \rho) \right)^{1/2} \quad (4.5)$$

Since equations (4.4) and (4.5) yield approximately the same value for the droplet diameter, we used equation (4.4) in our prediction procedure. When the slick thickness is smaller than the droplet diameter predicted by equation (4.4), The maximum droplet diameter is assumed to be equal to the slick thickness.

4.2.2 Determination of the Smallest Diameter of the Droplets

Milgram et. al. (1978) used the Kolmogoroff-Hinze criterion for the splitting of droplets in the inertial subrange of turbulence. Under the influence of turbulence created by breaking waves, an oil slick will be broken up, or split, into many oil droplets. These droplets, in turn, may split into smaller droplets. This process will continue until the forces tending to split the oil droplets are balanced by other forces tending to maintain their integrity.

In the inertial subrange of turbulence, the dominant splitting force is due to dynamic pressures, and the restoring force is due to surface tension. The ratio of these two forces is the Weber number and is given:

$$We = \frac{\sigma}{\rho_w V_d^2 d} \quad (4.6)$$

Here V_d is the r.m.s. velocity difference, given a distance of d .

If the Weber number is equal to unity, and d lies in the inertial subrange, the splitting and resisting forces will balance and the splitting process will cease. The smallest droplet size in that case will be on the same order of magnitude as this value of d . If the oil is subjected to the turbulence of breaking waves for a prolonged period, all the droplets of size larger than d will be split, and d will represent the typical size of droplets.

One does not know a priori if the splitting of oil into droplets takes place in the inertial subrange. One can compute the Weber number at the turbulent microscale η to determine whether splitting takes place on such a small scale. The microscale Weber number is given:

$$We_{\eta} = 0.6 \frac{\sigma \omega^{1/4}}{\rho_g^{1/2} \nu_{eff}^{5/4}} \quad (4.7)$$

Here the effective viscosity is used to determine the effect of slick thickness on breaking waves ν_{eff} is defined:

$$\nu_{eff} = (1 - h/t_1) \nu_w + h/t_1 \nu_o \quad (4.8)$$

where t_1 is the thickness of the turbulent bore. An approximate estimate of t_1 is:

$$t_1 \approx 0.001 g/\omega^2 \quad (4.9)$$

The r.m.s. velocity difference V_d in the inertial subrange is given by:

$$V_d^2 = 10^{3/2} \frac{g^{4/3} d^{2/3}}{\omega^{2/3}} \quad (4.10)$$

With equation (4.7), the expression for the Weber number becomes:

$$We_{\eta} = 10^{-3/2} \sigma \omega^{2/3} / (\rho_w g^{4/3} d^{5/3}) \quad (4.11)$$

The minimum droplet size may be estimated for equation (4.8), once the critical Weber number at which the splitting ceases is known. Milgram et al. (1978) have chosen a Weber number of 1 to determine the minimum droplet size.

There are documented cases (such as water drop splitting in jet streams from fire sprinklers) where drop splitting occurs at a Weber number of about 10. Using a limiting Weber number of 10, the expression for minimum droplet size is:

$$d_o \approx 0.03 \frac{\sigma^{3/5} \omega^{2/5}}{\rho_w^{3/5} g^{4/5}} \quad (4.12)$$

If the microscale Weber number is less than 10, then the smallest droplet size will be the same as the microscale η . The droplet diameter is given by:

$$d_o \approx 0.6 \frac{\omega^{1/4} \nu_{eff}^{3/4}}{g^{1/2}} \quad (4.13)$$

If the thickness of the oil slick is small compared to the size of the turbulent bore, yet large compared to the droplet size it will not influence the results. When the thickness of the oil slick is small compared to d_o , the size of the smallest droplets will be reduced. The parameter governing the thin slick is still the Weber number, and equation (4.12) gives the length scale, d_o , at which the inertial forces and surface-tension forces balance. In this case, d_o represents the diameter of the smallest portions of the slick which are broken off to form oil droplets. Milgram et al. (1978) demonstrate that this "thin limit" minimum droplet size is:

$$d_{o,thin} = d_o^{2/3} h^{1/3} \quad (4.14)$$

Where h is the average thickness of the slick. Since $d_{o,thin}$ is smaller than d_o these droplets will not split further.

Details on the Weber number criteria and the effect of slick thickness on droplet formation are described in Appendix C.

4.2.3 Size Distribution of Droplets

There is no theoretical or experimental evidence to estimate the number distribution of droplets of various sizes. Using existing theory, one can determine the dimensions of the smallest and largest droplets which are formed in a given sea state. For mathematical simplicity, we shall assume that the number distribution of droplets is linear, with the number of smallest droplets at the maximum and the number of largest droplets at zero.

4.3 MODEL LIMITATIONS

In the preceding section we developed a simple model to estimate the maximum and minimum size of droplets that are formed in a given sea state. We accounted for the effect of the oil slick on the damping of breaking waves by assuming a weighted-average viscosity.

Viscosity, defined by equation (4.8), is based on the relative thickness of oil slick and the turbulent bore in the face of the breaking wave. The effect of this increased viscosity will be an increase in the microscale of turbulence, and a decrease in the microscale Weber number.

At present, there is no information available to validate the effect of slick thickness on the microscale of turbulence. As long as the Weber number based on that microscale is larger than the critical Weber number for droplet formation (which in this case is assumed to be 10), the slick thickness will not affect the size of typical droplets given by equation (4.12). If the microscale Weber number is significantly smaller than 10, the viscous effects are important and the Weber number is no longer the sole criterion for the splitting of droplets. For simplicity, we assumed that the size of droplets is the same as the microscale of turbulence when the Weber number is less than 10.

We assumed that the number of droplets varies linearly with droplet size. Physically, it is justifiable to assume that the maximum number of smallest droplets and minimum number of largest droplets occur during breaking wave-slick interaction. The number distribution of various sizes of droplets is unknown and the assumption of linearity is made for simplicity.

More experimental data may yield useful results pertaining to the damping of waves in the presence of oil and the number distribution of droplets of various sizes. Once such data is available, these models may be improved to correspond with a more realistic situation.

4.4 APPLICATION OF THE SIMPLE ALGORITHM

A simple algorithm to determine the diameters of the largest and smallest droplets formed by the action of breaking waves is presented here. The inputs to this algorithm are the physical properties of oil and water,

description of the sea state, the thickness of the slick, and the average density of oil in the slick. The last two quantities are output from the evaporation model described in Chapter 3.

Step 1. Determine the wave frequency:

$$\omega = 0.7 \text{ g/u} \quad (4.15)$$

The wind velocity and the significant wave height are related by the empirical expression given by Pierson and Moskowitz (1964) which is:

$$H_{1/3} = 0.283 (U^2/g) \quad (4.16)$$

Step 2. Determine the thickness of the turbulent bore:

$$t_1 = 0.001 \text{ g}/\omega^2 \quad (4.17)$$

Determine the effective viscosity:

$$\nu_{\text{eff}} = (1 - h/t_1) \nu_w + h/t_1 \nu_o \quad (4.18)$$

If $\nu_{\text{eff}} < \nu_w$, then assume $\nu_{\text{eff}} = \nu_w$.

If $\nu_{\text{eff}} > \nu_o$, then assume $\nu_{\text{eff}} = \nu_o$.

Step 3. Determine the microscale Weber number

$$We_\omega = 0.6 \frac{\sigma \omega^{1/4}}{\rho_w^{1/2} \nu_{\text{eff}}^{5/4}} \quad (4.19)$$

Step 4. Determine the size of the smallest droplets using:

$$\begin{aligned} \text{if } We_\omega \leq 10 \text{ then } d_o &= 0.6 \frac{\omega^{1/4} \nu_{\text{eff}}^{3/4}}{g^{1/2}} \\ \text{if } We_\omega > 10 \text{ then } d'_o &= 0.03 \frac{\sigma^{3/5} \omega^{2/5}}{\rho_w^{3/5} g^{4/5}} \end{aligned} \quad (4.20)$$

If $h > d'_o$ then $d = d'_o$; where h is the slick thickness.

If $h < d'_o$ then $d_o = h^{1/3} d_o^{2/3}$

Step 5. Determine the size of the largest droplet using:

$$d'_{\text{max}} = \left(12 \sigma / g (\rho_w - \rho) \right)^{1/2} \quad (4.21)$$

If $h > d'_{\text{max}}$ then $d_{\text{max}} = d'_{\text{max}}$; where h is the oil slick thickness.

If $h < d'_{\text{max}}$ then $d_{\text{max}} = h$.

Step 6. Assume a linear number distribution for droplets with a maximum of size d_o , determined by equation (4.20), and zero at d_{max} determined by equation (4.21).

Note: If the thickness of the slick is smaller than d_o , given by equation (4.20), then assume that all the droplets have a typical diameter given by d_o in equation (4.20).

Step 7. Summarize all the results in a table.

4.5 CONCLUSIONS

The conclusions of the droplet formation model are:

-The inputs to the model are the sea state (characterized by the significant wave height), slick thickness and the average density of oil in the slick (the last two are the output of the evaporation model discussed in Chapter 3).

-The outputs of the model are the diameters of the largest and the smallest droplets that are formed.

5. DROPLET DISTRIBUTION MODEL

5.1 Introduction

In the preceding chapter we presented a simple model to determine the maximum and minimum diameters of the droplets which are formed by the interaction of breaking waves with the oil slick. In this chapter we will present a mathematical model to predict:

- the maximum depth of dispersion of oil droplets
- volumetric fraction of the dispersed oil.

The input data to this model are the sea state conditions, the physical characteristics of the oil slick, the droplet dimensions, and the time since the spill.

The model is exercised for a broad spectrum of input data and output information and is compared to the Massachusetts Institute of Technology tests (Milgram, et. al., 1978). The accuracy of the model predictions is discussed. The proposed model is a set of analytical equations solved in a sequential way, given the aid of a pocket calculator or tables presented in this work. The droplet dispersion model is developed in Section 5.2. Section 5.3 then discusses the limitations of the model, and the step-by-step calculation procedure is developed in section 5.4.

5.2 Model Development

5.2.1 Assumptions

We have assumed that the reader of this chapter has an overview of the basic physical mechanics of globular dispersion. Discussions in the following sections are brief and oriented towards the theoretical approach employed.

Recent experimental results (Milgram, et. al., 1978) indicate that when a wave breaks in an oil slick, oil droplets are dispersed to depths significantly larger than the depth of the turbulent bore on the face of the wave, and these droplets reach their maximum depth well after the breaker has passed. It appears that the dispersed oil is not driven down so much by the direct action of the breaker, but rather is entrained in the wake of turbulence which lies behind the wave. After the droplets reach their maximum depth, they rise due to buoyancy forces. The ambient turbulence

encountered by the droplets, due not only to waves breaking, but also to other forces of oceanic turbulence, will affect the rate of rise in a random fashion.

The vertical dispersion of oil slicks by breaking waves is a complex process which has not been fully described mathematically. Liebovich (1975) proposed a model for predicting the probability density function for the position of an oil droplet, assuming it was originally dispersed to some depth by a breaking wave. Liebovich estimated the fraction of oil entrained in globules in the upper sea layer, but Milgram et. al. (1978) concluded that conceptual errors invalidate some of those results. Raj (1977) proposed a stochastic model to obtain the time history of the probability density distributions for the positions of the oil globules in water in order to estimate the time dependant mass of oil in the water column. Milgram et. al. conducted experimental research to determine the maximum depth to which oil droplets are entrained by the water of a breaking wave. They seperately verified certain assumptions made by Liebovich and Raj and proposed a methodology to mathematically predict the maximum and average depth to which oil droplets might disperse.

The analysis in the following sections relies on the work of Milgram and uses Liebovich's results to a lesser extent. The main assumptions made in developing the model are:

- The droplet dispersion is driven mainly by the turbulent wake which lies behind the breaker.
- The rate at which droplets are driven downward equals the difference between the wake growth rate and the terminal velocity of the oil droplets in calm water.
- Actual droplet velocities are the net velocity arising from the turbulent velocity fluctuations and the terminal rising velocity of the droplet.
- Sea state conditions can be described via the significant wave period and the Pierson-Moskowitz sea spectrum.
- Only a fraction of the wave length, λ , of a breaking wave is actually breaking. The fraction has been assumed to be 1/4, in the absence of conclusive experimental evidence.
- The number of droplets entrained as a function of droplet diameter is linear, with the maximum number of droplets exhibiting the minimum size, d_0 , and no droplets exceeding the maximum size, d_m .

5.2.2 Depth of Dispersion

Momentum of a Wake

Wave kinetic energy and momentum dominate the dynamics of the uppermost 10 meters of the ocean waters. As the wave system loses momentum flux, a corresponding increase in non-wave momentum takes place. The momentum is contained in the turbulent wake. The rate of loss of momentum flux per unit crest length (\dot{M}) is proportional to:

$$\dot{M} \approx \rho_w C_p U_w b \quad (5.1)$$

where ρ_w = density of sea water

C_p = phase speed of wave

U_w = maximum wake velocity

b = thickness of the wake.

Milgram, et. al. proposed these analytical expressions for \dot{M} and b :

$$\dot{M} = \frac{1}{32} \rho_w g H_{1/3}^2 \quad (5.2)$$

$$b = 1.14 (\dot{M} / \rho_w C_p)^{1/2} \quad (5.3)$$

Where $H_{1/3}$ is the significant wave height. The experimental results from Duncan (1979) further support the $t^{1/2}$ dependence of wave thickness.

Time Dependant Droplet Depth

Milgram, et. al. (1978) assumed the maximum rate at which oil droplets will be driven down to equal the difference between the wake growth (db/dt) and the terminal velocity W of the oil droplet in calm water. When making this assumption, the time dependant droplet depth equals:

$$z(t) = 1.14 (\dot{M} / \rho_w C_p)^{1/2} - Wt \quad (5.4)$$

the maximum depth which the droplets can reach equals

$$z_0 = 0.32 \frac{\dot{M} \bar{\omega}}{\rho_w g W} = 0.01 \frac{H_{1/3}^2 \bar{\omega}}{W} \quad (5.5)$$

the maximum depth is attained after time t_0 of downward flow:

$$t_0 = 0.32 \frac{\dot{M}}{W^2 \rho_w C_p} = \frac{z_0}{W} \quad (5.6)$$

This time equals the rising time of the droplet (z_0/W by definition). The characteristic separation time of an oil droplet equals:

$$t_c = 2 \frac{z_0}{W} \quad (5.7)$$

which represents the separation time from the slick.

Terminal Velocity

When droplets are released at a certain depth z_0 , they rise through the water at their terminal velocity. The terminal velocity is dependant on the buoyancy forces tending the move the droplet to the surface and the drag force resisting the movement. The drag force acting on a droplet is a function of the Reynolds number of the droplet.

For Reynolds numbers up to about 10, the flow around a droplet may be considered to be Stokesian flow. The drag coefficient in such a flow is inversely proportional to the Reynolds number. The terminal velocity is given by:

$$W = \frac{gd^2(1-\Delta)}{18\mu_w} \quad (5.8)$$

Here Δ is the density ratio ρ/ρ_w .

The drag coefficient becomes constant for Reynolds numbers greater than about 100. The value of the drag coefficient is approximately 0.5 and the terminal velocity is given by:

$$W = (8/3 gd(1-\Delta))^{1/2} \quad (5.9)$$

It is possible to determine a critical diameter at which the drag coefficient becomes approximately constant. This can be obtained by equating the Reynolds numbers for the two different situations described in equations (5.8) and (5.9), and solving for d . The droplet diameter is given as:

$$d_c^* = \frac{9.52\mu_w^{2/3}}{g^{1/3}(1-\Delta)^{1/3}} \quad (5.10)$$

The Reynolds number corresponding to the diameter d_c^* is approximately 50. For droplet diameters less than d_c^* , equation (5.8) is used to determine the terminal velocity. For droplet diameters greater than d_c^* , the terminal velocity is given in equation (5.9). These equations are graphically presented in Figure 5.1.

Relation to the Wave Length

The reason that waves break at sea is that they enter regions, or wave groups, where the energy density is too large for them to support. The excess in energy is generally not dissipated by a single wave, but rather by a series of waves. Since the wave group moves at half the wave velocity, each wave breaks one wave length further downwind (Donelan, et. al., 1972). When droplets are very deep, the wake region they are impacted from is due to a series of breaking waves, rather than a single breaker. If z_0 is not small compared to the size of the region within which waves break, the model can no longer reliably predict the depth of dispersion. In this case, Milgram et. al. (1978) approximated the maximum depth of the droplets as equal to the wave length, λ . In this situation, the characteristic (separation) time of the droplet can be stated by:

$$t_c = \frac{\lambda}{W} \left[\frac{z_0}{\lambda} \left\{ 1 - \left(1 - (\lambda/z_0)^2 \right)^{1/2} \right\} + 1 \right] \quad (5.11)$$

5.2.3 Dispersed Oil Volume

Knowledge regarding the sea state condition is important for estimating the oil volume dispersed. The latter is estimated per unit width of oil slick, and for each formed droplet size separately. The total oil volume dispersed at a specific time equals the sum of the volume estimates for the various droplet sizes.

Sea State Condition

The present analysis considers the sea state condition by means of the significant wave period, and the assumption of a Pierson-Moskowitz sea spectrum (Raj, 1977). Given this assumption, one can show that the number of wave breaking events (N) per unit time within the area of the oil slick is

$$N = Pr^* \frac{A^{1/2} \bar{\omega}}{2\pi \lambda} \quad (5.12)$$

where Pr^* = probability of the wave breaking

$A^{1/2}$ = characteristic size of the slick

$\bar{\omega}$ = zero crossing frequency of waves from the Pierson-Moskowitz spectrum.

Shuleikin (1967) assumed a Rayleigh distribution of waves and arrived at the following expression for the probability of exceeding a given wave height

$$Pr^* = \exp \left(-\pi/4 (H/H_a)^2 \right) \quad (5.13)$$

where H_a = the average height of waves. It is interesting to note that

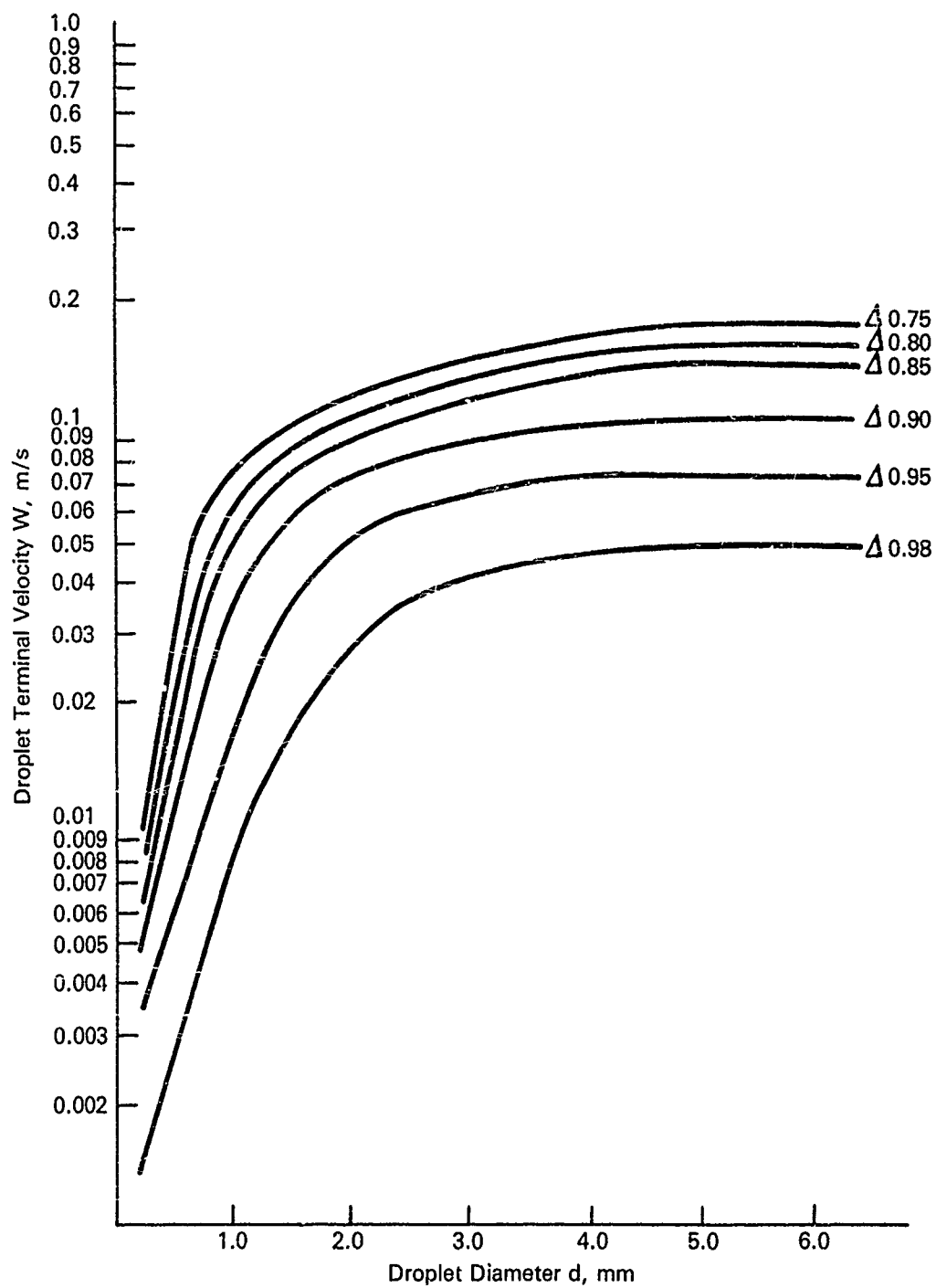


Figure 5.1 Variation of Droplet Terminal Velocity with Diameter (RAJ, 1977)

the probability of waves breaking given in equation (5.13) is independent of the significant wave height. This is primarily because higher waves also have longer wave lengths and the steepness of the wave is independent of sea state. This conclusion contradicts the empirical estimate of wave breaking events given by Van Dorn (1974). Wu (1979) reviewed the results of whitecap coverages of the ocean surface obtained by several investigators in both Atlantic and Pacific Oceans. Wu's (1979) results indicate that the variation of whitecap coverage with wind velocity is strongly related to the rate of energy supplied by the wind and is given by:

$$A_{wc} = 1.7 \times 10^{-6} u_{10}^{3.75} \quad (5.13a)$$

where A_{wc} = fraction of area covered by whitecaps
 u_{10} = wind velocity at a height of 10m above the ocean surface.

Only a fraction of the area covered by whitecaps is actually subject to breaking. This fraction is dependant on the sea state and can be significantly modified by the presence of oil. In our analysis we will assume that 10% of the whitecap region is subject to breaking. The probability of breaking is given by

$$Pr^* = 1.7 \times 10^{-7} u_{10}^{3.75} \quad (5.14)$$

Clearly, more information in the area of determining wave breaking probabilities will be useful.

Volume of Dispersed Oil Droplets

Liebovich (1975) derived the probability density function (PDF) for the position at time t of any droplet released at $z = z_0$ and $t = 0$ in homogeneous stationary turbulence. He found the distribution of turbulence to be Gaussian, with the variance of position approaching the value tK_T (where K_T is diffusivity), if the time of rise is large with respect to the integral time of the turbulence. Milgram et. al. (1979) concluded that although certain of Liebovich's results are accurate, they do not address the question of the rate of oil entrainment, and that the vertical distribution of small droplets may be described more simply by the wake growth similarity theory.

The probability that a droplet of diameter d , terminal velocity w , released at depth z_0 at time $t = 0$, is still dispersed at any time t is given by:

$$\int_0^{\infty} f(z,t) dz = \frac{1}{2} \operatorname{erfc} \left(\frac{Wt - z_0}{(2K_T t)^{1/2}} \right) \quad (5.15)$$

where erfc is the complimentary error function. The turbulence diffusivity was established by Ichiye (1967) to be:

$$K_T = 0.004 H^2 \quad (5.16)$$

The rate of entrainment of oil is given by:

$$\dot{V} = \frac{Nh \lambda_A^{1/2}}{4} = \frac{\operatorname{Pr}^* A \bar{\omega} h}{8\pi} \quad (5.17)$$

This represents the volume of oil entrained by breaking waves per unit time over the width of the slick. We have assumed an given characteristic wave length, and that the breaking region comprises 1/4 of that wave length.

Using equations (5.13), (5.15), and (5.17) and keeping track of the process of droplet formation, dispersion, and ultimate rise of oil droplets to recombine with the surface slick, we can find the total volume of oil dispersed in the water column at any time t (after the spill) and contained in droplets of diameters between d and $d + \Delta d$ as:

$$V_d(d,t) = \int_{t-t_0}^t \dot{V}(t') dt' + \frac{1}{2} \int_0^{t-t_0} \dot{V}(t') \operatorname{erfc} \left(\frac{W(t-t'-2t_0)}{(2K_T(t-t'-t_0))^{1/2}} \right) dt' \quad (5.18)$$

Total Dispersed Oil Volume

To determine the fraction of the entrained volume within a given size range, it is necessary to adopt an assumption regarding the droplet size distribution. There are no reliable observations or theoretical estimates of the actual size distribution.

For this model, one of the simplest plausible distributions has been adopted. It is assumed that the number density of oil droplets is at a maximum at d_0 and decreases linearly to zero at d_m , as shown in figure 5.2. This function, $g(d)$ is given by:

$$g(d) = a(d_m - d) \quad (5.19)$$

where a is some constant. This implies that within a range of diameters d to $d + \Delta d$ there are $g(d)$ droplets.

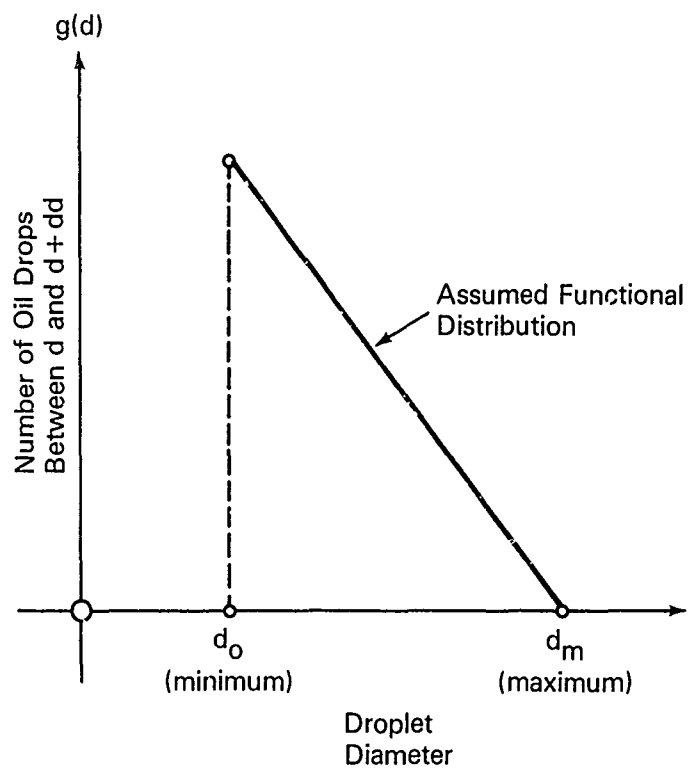


Figure 5.2 Number Distribution of Oil Droplets as a Function of Their Diameter

The volume of oil within a given size fraction d to $d + \Delta d$ is proportional to d^3 . The volume is given by:

$$V(d) = a (d_m - d) d^3 \quad (5.20)$$

This is shown in figure 5.3. We define the fraction of the total volume contained in droplets, in the size range d to $d + \Delta d$ as:

$$F_d = \frac{\int_d^{d+\Delta d} V(d) dd}{\int_{d_0}^{d_m} V(d) dd} \quad (5.21)$$

The denominator in equation (5.21) is given by

$$a \left[\frac{d_m^5}{20} - \frac{d_m d_0^4}{4} + \frac{d_0^5}{5} \right]$$

We further define:

$$W^* = \left(\frac{d_m^5}{20} - \frac{d_m d_0^4}{4} + \frac{d_0^5}{5} \right) \quad (5.22)$$

and set the denominator in equation (5.21) to unit volume. This leads to a definition of the value of the constant a as:

$$a = \frac{1 \text{ meter}^3}{W^*}$$

With this, the fractional volume in the diameter range d to $d + \Delta d$ may be redefined as:

$$F_d = \frac{1}{W^*} \left(\frac{d_m d^4}{4} - \frac{d^5}{5} \right) \Big|_d^{d+\Delta d} \quad (5.23)$$

Giving a total volume of oil dispersed as:

$$V_d(t) = \sum_{\text{over the range of droplet diameters}} F_d V_d(d) \quad (5.24)$$

where $V_d(d)$ is given by Equation (5.18).

5.3 Model Limitations

To avoid complicated analysis at incremental time steps, the model presented is based on the assumption that the droplet distribution function at any time reflects slick and dispersion conditions. The implication of this simplification is that the slick and environmental conditions are

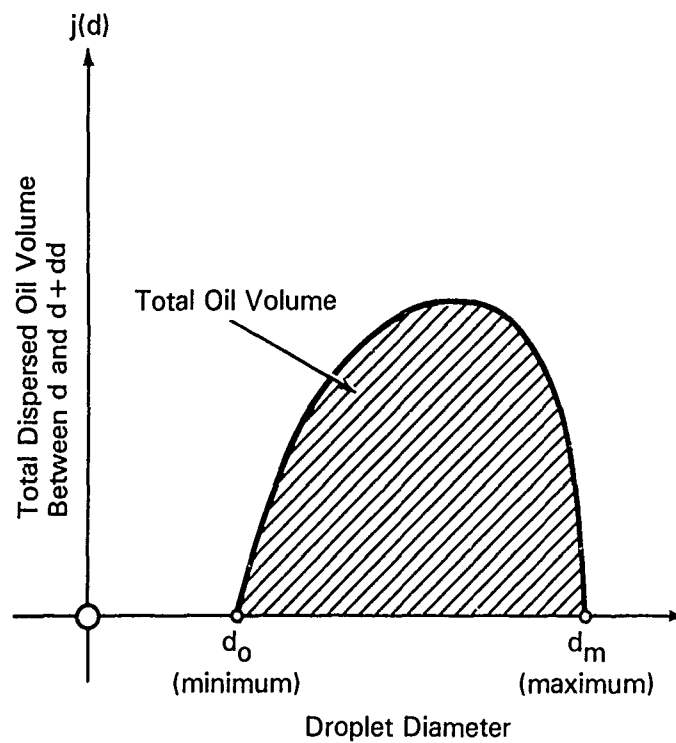


Figure 5.3 Distribution of Dispersed Mass as a Function of Droplet Diameter

changing so slowly that the droplet distribution at the time of analysis is not affected by droplets formed in the distant past.

The above assumption fails when slick thickness or oil density is changing rapidly, or when the sea state changes abruptly. Under these conditions, the user is urged to carefully consider the potential effects of such changes, and, if necessary, modify the integration of the complementary error function over time to simulate step-wise changes in the entrainment rate and diffusion coefficient. A recommended approach is:

- Calculate V_d at the time of a significant change in sea state;
- Estimate a new effective z_0 by determining the depth of the center of mass of the probability function; and
- use that depth as z_0 , at subsequent times, to track the distribution of these "old" droplets, applying a currently valid K_T . Droplets dispersed after that time follow the standard procedure with the "new" K_T and V .

Where past theoretical and observational studies have not yielded conclusive relationships, certain assumptions have been adopted in the development of the model. The two most critical assumptions are the linear variation of number of droplets vs. diameter, and the estimate that the breaking portion of the wave encompasses 1/4 of the wave length. As new information is developed, these assumptions may be replaced with more accurate relationships.

Because of multiple scaling laws, it has not been possible to rigorously scale the laboratory results of Milgram et. al. (1978) to ocean scales of interest. By applying rudimentary Froude number scaling, the model reproduces the order of magnitude of z_0 in Milgram's experiments. The proposed model has not been validated or even tuned to experimental or oceanic observations. This is a serious limitation which can only be eliminated through field experiments in which oil globule concentrations and size distributions were established as a function of depth under a wind-generated wave field.

For a more detailed discussion of the assumptions and limitations of the vertical distributions model, the interested reader is referred to Milgram et. al. (1978).

5.4 Application of the Simple Algorithm

In this section we present a simple step-by-step calculation procedure to determine the total volume of oil dispersed in the water column as a function of time. The inputs to this model are from the evaporation model and the droplet formation model.

Step 1 Calculate the following ocean parameters:

(if only wind speed is given) determine the significant wave height

$$H_{1/3} = 0.283 U^2/g \quad (5.25)$$

wave frequency and period

$$\omega = 0.7 g / U \quad (5.26)$$

$$T_1 = 2 \pi / \omega$$

zero crossing frequency of waves from the Pierson-Moskowitz spectrum

$$\bar{\omega} = 6.83 / T_1 \quad (5.27)$$

wave length

$$\lambda = 2 \pi g / \bar{\omega}^2 \quad (5.28)$$

Step 2 Calculate N, the number of breaking events per unit time

$$N = Pr^* \frac{A^{1/2} \bar{\omega}}{2 \pi \lambda} \quad (5.29)$$

$$\text{where } Pr^* = 1.7 \times 10^{-7} U^{3.75}$$

Step 3 Calculate the rate of entrainment of oil per unit time and unit width of the slick.

$$\dot{v} = \frac{Nh\lambda}{4} \quad (5.30)$$

Step 4 Divide the range of droplets into four groups. Calculate the mean diameter of each group using:

$$\begin{aligned} d_1 &= \frac{7d_0 + d_m}{8} \\ d_2 &= \frac{5d_0 + 3d_m}{8} \\ d_3 &= \frac{3d_0 + 5d_m}{8} \\ d_4 &= \frac{d_0 + 7d_m}{8} \end{aligned} \quad (5.31)$$

Determine W^* :

$$W^* = \frac{d_m^5}{20} - \frac{d_m d_0^4}{4} + \frac{d_0^5}{5} \quad (5.32)$$

Determine the following diameters:

$$\begin{aligned} d_a &= \frac{3d_0 + d_m}{4} \\ d_b &= \frac{d_0 + d_m}{2} \\ d_c &= \frac{d_0 + 3d_m}{4} \end{aligned} \quad (5.33)$$

Determine the weighting factors in each range

$$\begin{aligned} F_{d_1} &= \frac{1}{W^*} \left(\frac{d_m d_a^4}{4} - \frac{d_a^5}{5} - \frac{d_m d_0^4}{4} + \frac{d_0^5}{5} \right) \\ F_{d_2} &= \frac{1}{W^*} \left(\frac{d_m d_b^4}{4} - \frac{d_b^5}{5} - \frac{d_m d_a^4}{4} + \frac{d_a^5}{5} \right) \\ F_{d_3} &= \frac{1}{W^*} \left(\frac{d_m d_c^4}{4} - \frac{d_c^5}{5} - \frac{d_m d_b^4}{4} + \frac{d_b^5}{5} \right) \\ F_{d_4} &= \frac{1}{W^*} \left(\frac{d_m^5}{20} - \frac{d_m d_c^4}{4} + \frac{d_c^5}{5} \right) \end{aligned} \quad (5.34)$$

Step 5 Determine the critical diameter

$$d_c^* = \frac{9.52 \nu_w^{2/3}}{g^{1/3} (1 - \Delta)^{1/3}} \quad (5.35)$$

For droplet diameters less than the critical diameter, use equation (5.36) to calculate the terminal velocity. For droplets larger than the critical diameter, use equation (5.37).

$$W = \frac{gd^2(1 - \Delta)}{18 \nu_w} \quad \text{for } d \leq d_c^* \quad (5.36)$$

$$W = (8/3) gd (1 - \Delta)^{1/2} \quad \text{for } d > d_c^* \quad (5.37)$$

Step 6 Calculate the maximum depth of dispersion for each droplet diameter, using:

$$z_w = \frac{0.01 H^2 \bar{\omega}}{W} \quad (5.38)$$

$$z_g = \frac{\pi g}{2 \bar{U}^2} \quad (5.39)$$

The maximum depth of dispersion for each droplet diameter is then given by:

$$\left. \begin{aligned} z_0 &= z_w && \text{if } z_w \leq z_g \\ z_0 &= z_g && \text{if } z_w > z_g \end{aligned} \right\} \quad (5.40)$$

Step 7 Determine the turbulent diffusivity

$$K_T = 0.004 H^2 \quad (5.41)$$

Step 8 Evaluate the volume dispersed for each droplet diameter.

Use the following procedure to evaluate the integral in equation (5.18).

Divide t' into 8 parts. At $t'/8$, $3t'/8$, $5t'/8$, and $7t'/8$, evaluate

$$x = \frac{W(t - t' - 2t_0)}{(2K_T (t - t' - t_0))^{1/2}} \quad (5.43)$$

Calculate the error function using:

$$\left. \begin{aligned} \text{erfc}(x_{d,t'}) &= 1 + \text{erf}(x_{d,t'}) && \text{if } x_{d,t'} \leq 0 \\ \text{erfc}(x_{d,t'}) &= 1 - \text{erf}(x_{d,t'}) && \text{if } x_{d,t'} > 0 \end{aligned} \right\} \quad (5.44)$$

The value of the error function can be obtained from Mathematical Tables.

For arguments greater than 2, the error function may be assumed to be unity. The value of the integral is given by the sum of the four values of the complementary error functions calculated above.

$$I_d = \frac{t'}{4} \sum_{\substack{\text{over} \\ \text{time} \\ \text{steps}}} \text{erfc } x_{d,t'} \quad (5.45)$$

$$V_d(d) = \dot{V}_d t_0 + \frac{1}{2} \dot{V}_d I_d \quad (5.46)$$

Step 9 Determine the total volume of oil dispersed:

$$V_d(t) = F_{d_1} V_d(d_1) + F_{d_2} V_d(d_2) + F_{d_3} V_d(d_3) + F_{d_4} V_d(d_4) \quad (5.47)$$

5.5 Conclusions

A mathematical model describing the distribution of oil droplets dispersed in the upper ocean by breaking waves has been presented. The model is designed to permit droplet distributions to be estimated by following a simple step-by-step calculation procedure using a hand calculator. The required inputs are the time since the spill occurred, the

significant wave height, the significant period of the waves, the wind speed, and the viscosity of the oil. Other inputs are results from models described elsewhere in this report: oil density from the evaporation model, area of the slick from the surface oil distribution model, and the minimum and maximum droplet diameters from the droplet formation model.

The key outputs of this model are the maximum depth of dispersion and the total volume of dispersed oil in the water column. By subtracting this from the remaining volume resulting from the evaporation model, one obtains the volume of floating oil.

The computational procedure is not difficult and can be implemented on a hand calculator. The procedure is tedious because of the large number of computations involved. It is recommended that the procedure be programmed for several standard calculators and these programs be provided to eventual users.

The model has not been calibrated or verified because of the lack of relevant observations. The model has been used to derive the results presented in the Table of Dispersion Predictions.

6. SURFACE OIL DISTRIBUTION MODEL

6.1 INTRODUCTION

In previous chapters we developed simple models to predict the loss of oil due to evaporation from the oil slick and due to interaction of the breaking waves with the slick. We also pointed out that at sufficiently large times after the spill, the loss of oil due to evaporation is smaller compared to the loss due to dispersion of oil in the form of fine droplets. The amount of oil remaining on the water surface was determined by accounting for losses due to evaporation of the oil and the vertical dispersion of the oil in the form of globules in the water column. In this chapter, we address the spatial distribution of oil remaining on the surface of water.

The surface area of the coherent oil slick was given by the gravity-inertia, gravity-viscous, and viscous-surface tension formulae given in Chapter 3. The area of the slick increases with time and the thickness decreases. When the slick is thin enough, it is subject to wave action and is broken into slicklets. The slicklets continue to spread and are subject to horizontal diffusion. In this chapter, we have developed a model to predict the extent of growth of the non-coherent oil slick as a function of time. The model predicts the boundary of the floating oil slick and the percentage of the bounded area covered with oil.

6.2 ASSUMPTION ON THE PARAMETERS

Wave breaking ruptures the slick and disperses oil vertically over a limited area. When such action occurs near the edge of the slick, it is possible to separate a small slicklet from the main slick. As demonstrated by Raj (1977), separation of a slick into slicklets can only occur if the mean crest length of the breaking waves is of the same order of magnitude as the length or width of the slick. Non-shoaling breaking waves, or whitecaps, are known to exhibit relatively small crest lengths. Generally, they are much less than one wave length.

Raj's (1977) analysis indicates that non-shoaling breaking waves will not cause slicklet formation. It is apparent that one of the reasons for this result is the assumption of a rectangular shape of the slick. Raj's analysis is extended here to include irregularly shaped slicks.

For a rectangular slick, the length and width are the only pertinent scales to compare the mean crest length with. When a real slick spreads on the ocean it does not exhibit a regular, rectangular shape; nor does it form a smooth oval shape.

The real shape of an oil slick under the action of wind and waves is likely to be quite irregular. Basically, it is an oval shape with a distorted edge, which is affected by the turbulent character of both wind above and water below. Protuberances or fingers appearing at the outer edge may be variable in length and width. These fingers may be separated from the main slick by wave action to form slicklets. Slicklet formation is hypothesized to begin at the edges and gradually to proceed through the slick as fingers are separated. Although a variety of finger sizes will form, only those of comparable scale to the crest length of the breaking waves will be separated as a coherent slicklet. Larger fingers will not be detached and may gradually disappear as an identifiable shape. Small fingers will vertically disperse by breaking wave action, rather than separate to form slicklets. The characteristic slicklet size will be comparable to the mean crest length of breaking waves. In the droplet formation model and vertical distribution model we assumed, in lieu of specific observational or theoretical evidence, that the mean crest length is $1/4$ the wave length. This assumption is adopted here as well. The typical slicklet size is $1/4$ of the significant wave length ($H_{1/3}$).

The distribution of oil on the surface is dictated by gravitational spreading while the slick is thick. When the thickness is approximately a few millimeters, it will begin to be broken up and dispersed by waves. The thickness criterion for breaking waves is arbitrary. The actual critical thickness at which dispersion of oil by breaking waves becomes effective is probably dependent on the size of the spill, sea state, and the physical properties of the oil. A single critical thickness criterion has some support in the extrapolation of experimental results of Milgram et al. (1978).

Considering the foregoing discussion, the model for the surface distribution of oil is based on the assumption that the slick, under gravitation influence, spreads uniformly until its thickness decreases to a critical thickness, h_c . At that time, the slick is fractured into slicklets of characteristic size $\lambda/4$, and the slicklets are dispersed as

any other passive contaminant.

The rate of spreading by turbulent diffusion is dependent upon the intensity of turbulence and the length scale over which the turbulence is coherent. The assumed problem is described in a Lagrangian coordinate system where slicklets move with respect to the center of mass of the slick. In the diffusive spreading regime, oil is presumed to act like any other substance in water, and turbulent diffusion aspects of the model are insensitive to the physical properties of the oil. We assume that the oil distribution during the gravity spreading regime is of uniform thickness and that the spread is isotropic. Spreading in the turbulent diffusion regime approaches a Gaussian distribution of oil volume per unit surface area (Obuko, 1972).

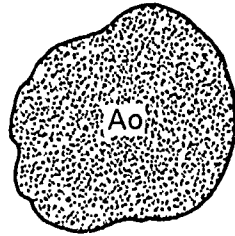
6.3 MODEL DEVELOPMENT

6.3.1 Interface with Evaporation Model

The volume $V(t)$ and the radius $r(t)$ of the unbroken slick were given by Equations (3.5) through (3.12) in the description of the evaporation model. The thickness, $h(t)$, is calculated knowing the volume of oil and the slick radius remaining at time t . It is necessary to exercise the evaporation model prior to the surface oil distribution model and to establish the time, t_g , at which the slick thickness diminishes to the critical thickness, h_c . At this time the distribution of oil has a top hat profile, i.e., the volume of oil per unit surface area is uniform for $r < r(t)$ and is zero for $r > r(t)$. The horizontal turbulent diffusion process is responsible for determining the area of ocean surface which is contaminated by oil, requiring cleanup. The area actually covered by oil can be estimated from $r(t)$ by Equations (3.11) and (3.12) of the evaporation model. (This approximation is not technically valid because under surface tension the small slicklets will not spread at the same rate as the large slick.) The total surface area contaminated by oil, A_s , and the surface of floating oil, A_o , are illustrated in Figure 6.1.

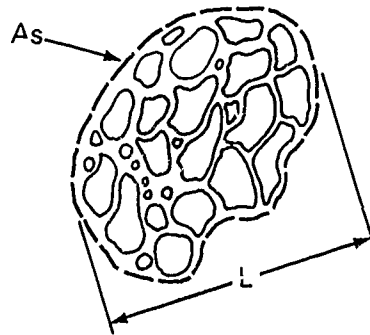
6.3.2 Initial Horizontal Diffusion of the Slicklet

The problem of horizontal turbulent dispersion of an initially finite-sized cloud in the ocean has been investigated by Csanady (1973). His review of the literature and discussion indicates that although the physics

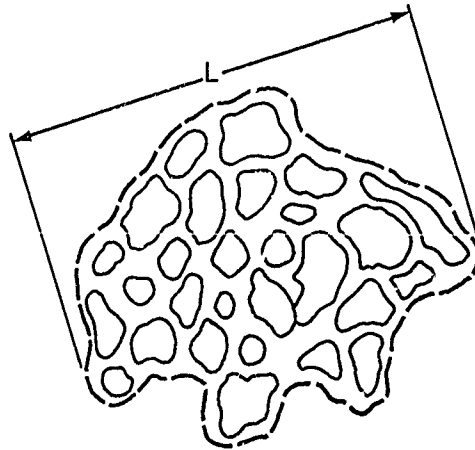


A_o — Is The Area Covered by Oil
 A_s — Is The Total Contaminated Area Requiring Cleanup

a. At Any Time, Prior to Slicklet Formation; Slick Thicker than h_b



b. At a Time, Just After Slicklet Formation



c. At a Later Time After Slicklet Dispersion

Figure 6.1 Schematic of Surface Distribution Model

of the problem is understood, a rigorous mathematical expression is not available because of the complexities involved in describing the effects of larger eddies on a finite-size cloud.

The dispersion is described in a frame of reference moving with the center of gravity of the cloud. The speed of the moving frame is approximately that of the mean current. Velocity fluctuations relative to this frame of reference are responsible for dispersing the cloud. Frequently called Taylor's theorem, the basic dispersion equation is:

$$\frac{d\sigma^2}{dt} = 2 \int_0^t \langle U(t)U(t') \rangle dt' \quad (6.1)$$

where σ^2 = the variance or second moment of distribution of contaminant around the center of gravity of the slick;

u = the fluctuating Lagrangian velocity relative to the center of gravity of a particle at time t and t' ;

$\langle \rangle$ = an ensemble average over all the oil in the slick.

By definition of the Lagrangian autocorrelation function, $R(t')$:

$$\frac{d\sigma^2}{dt} = 2 \langle U^2(t) \rangle \int_0^t R(t') dt' \quad (6.2)$$

The autocorrelation function, a decreasing function of t' , can be established by measurement, but there is no general expression. Figure 6.2 indicates schematically the expected shape of $R(t')$ and gives a linear approximation of that function. Using the linear approximation, we obtain:

$$\frac{d\sigma^2}{dt} \approx \langle U^2(t) \rangle t_c \quad \text{for } t > t_c \quad (6.3)$$

where t_c is assumed to be a constant. This assumption is supported by Smith and Hay (1961). Integrating Equation (6.3), we obtain:

$$\sigma^2(t) = (\text{a constant}) + \langle U^2(t) \rangle t_c t \quad (6.4)$$

At time $t = t_g$, t_g being the time at which the slicklets are formed, the variance should correspond to the variance of the coherent slick. Further, if there is no turbulence in the ocean, i.e., $u^2(t) = 0$, the increase in variance should be the same as the increase in the variance of the coherent slick. We now have

$$\sigma^2(t) = \sigma_0^2(t) + \langle U^2(t) \rangle t_c (t - t_g) \quad (6.5)$$

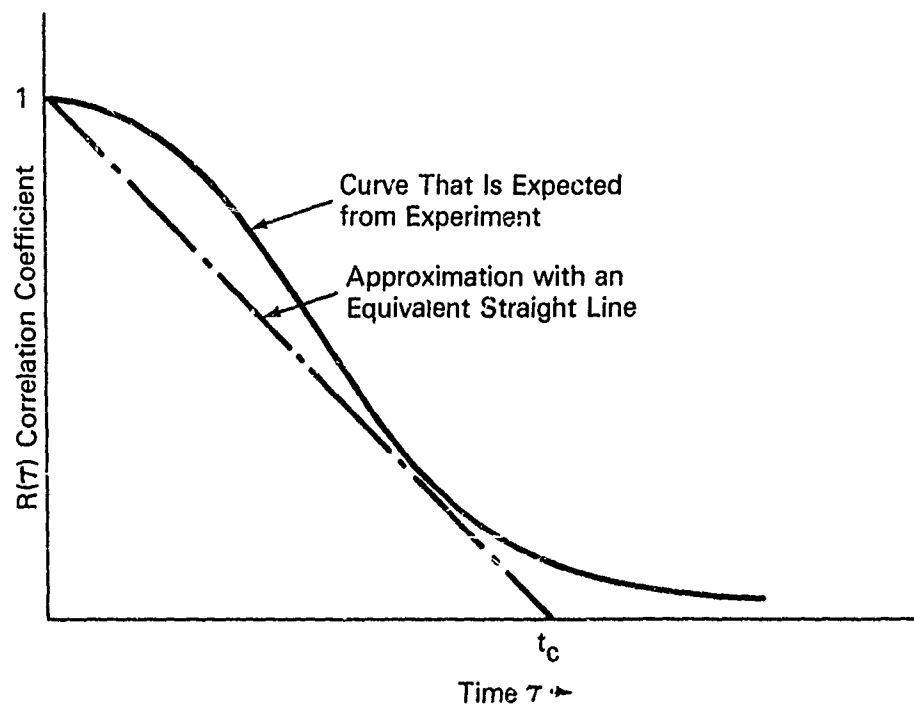


Figure 6.2 Schematic Diagram Showing the Expected Variation of Coefficient of Correlation Between Turbulent Velocity at One Instant and Another

where $\sigma_0^2(t)$ = the variance of the coherent slick:

$$\sigma_0^2(t) = r^2(t)/3 \quad (6.6)$$

It should be noted that the rate of spread of the slicklets will be significantly less than the rate of spread of the coherent slick. The variance given by Equation (6.5) will always be greater than the actual variance of the incoherent slick and represents a maximum-value estimate of the total contaminated area.

The initial slick-averaged velocity covariance, $U^2(t)$, will depend on the size of the slick and turbulence intensity. The turbulence intensity can be expressed as

$$i^2 = aU_c^2 + i_0^2 \quad (6.7)$$

where i_0 is the background turbulence intensity and U_c is the mean current speed. In oceanic conditions, observations to determine the value of the constant 'a' indicate a wide scatter from 0.1 to more than 1. Values of 'a' greater than unity indicate that the fluctuating components of velocity are of greater magnitude than the mean current. This is possible in the open ocean. An average value of $a = 0.5$ is assumed in the present analysis. There is no experimental data on the intensity of background turbulence in the ocean in absence of a current. The background intensity is assumed to be zero in the present analysis.

The value of $u^2(t)$ should approach the value of i^2 as the size of the slick increases. The slick-average velocity fluctuation covariance, relative to the center of gravity of the slick, cannot exceed the intensity of the turbulence spectrum. Slick size is expected to be positively correlated with $u^2(t)$. The velocity of a slicklet relative to the center of gravity of the slick is bound to increase as the slicklet's distance from the center increases because of the interaction with larger eddies. An initially large slick has a greater mean separation distance, slicklet center to slick center. The functional dependence of $u^2(t)$ with slick size is unknown. It is difficult to conceive of an experimental design which would allow one to measure this dependence. It is clear that the appropriate function should approach i^2 asymptotically as r , the slick radius, approaches L , the length scale of the largest eddies. We assume the following functional relationship for the velocity covariance.

$$\begin{aligned} \langle U^2(t) \rangle &= 0.5 U_c^2 \left(\frac{r(t)}{L} \right)^{1/2} && \text{for } r \leq L \\ &= 0.5 U_c^2 && \text{for } r > L \end{aligned} \quad (6.8)$$

The typical value of L in the ocean is on the order of 10 to 100 km.

The Lagrangian correlation time t_c will depend of the size of slick (characterized by its radius, r) and the fluctuating velocity of turbulence. An approximate value for t_c is:

$$t_c = r(t)/3i \quad (6.9)$$

Substituting Equations (6.8) and (6.9) in Equation (6.5), we obtain this expression to describe the initial stages of horizontal dispersion.

$$\sigma^2(t) = \frac{r^2(t)}{3} + 0.23 U_c r^{3/2}(t) (t - t_g) L^{-1/2} \quad (6.10)$$

By introducing the two assumed forms of covariance, the Lagrangian correlation function $R(t)$ and the turbulence intensity, the resulting expression has little value as a fundamental characteristic of the dispersion process. The extent of dispersion given by Equation (6.10) exhibits the following essential behavior of the process:

-The extent of dispersion increases with the current velocity. When the current velocity is zero, the variance of dispersion approaches the variance of spreading.

-The increase in the size of the slick also increases the variance of dispersion. This functional relationship, by Equation 6.10 is $r^{1.5}$.

In fact, the coefficient $U_c r^{1.5} L^{-1/2}$ can be thought of as a diffusion coefficient. The measurements by Obuko (1971) show that the increase in apparent diffusivity caused by an increase in the length scale can be approximated by:

$$\text{diffusivity} \sim (\text{length scale})^{1.1}$$

Within an order of magnitude, results from our expression agree with Obuko's measurements.

-An increase in eddy size decreases the variance of the dispersion.

As Csanady discusses, this behavior is expected during the early growth regime of a finite-size cloud having an initially uniform concentration distribution. As time progresses, the contaminant will tend toward a Gaussian distribution. Once the Gaussian distribution is attained, subsequent slick growth will be indistinguishable from the dispersion of an instantaneous point source.

6.3.3 Transition Time to Gaussian Distribution

The transition time, from top hat profile to a Gaussian profile, can be estimated using the experimental results of Obuko (1971). The variance of the coherent slick, σ_g^2 , at time t_g , is calculated using the formulae described in the evaporation model. An estimate of the time for transition from top hat to Gaussian, t_G , is made using Figure 6.3. The ordinate of Figure 6.3 is entered using the variance σ_g^2 and the abscissa is taken as the transition time, t_G . For times between t_g and t_G , Equation (6.10) describes the variance of dispersion. For times greater than t_G , a Gaussian dispersion formula is used to determine the extent of spread. Details of the Gaussian dispersion formula are given in the following section. The value of t_G given by this procedure will serve only as a first approximation. The actual value of the Gaussian transition time is determined on an interactive basis. Details of this procedure are given in Section 6.5.

6.3.4 Gaussian Dispersion Formula

Obuko (1971) studied the diffusion of passive contaminants in the upper mixed layer of the sea. The experimental data covered a time scale of diffusion ranging from 2 hours to one month and a length scale from 30m to 100 km. Using this experimental data, Obuko arrived at some empirical relationships for diffusion of instantaneously released contaminant. The "diffusion diagrams" of Obuko provide a practical means to predict the rate of horizontal spread of a passive substance.

In Figure 6.3 we show the variance of an instantaneous release of a contaminant as a function of time after release. The data points are omitted for sake of clarity. Obuko arrived at the following approximate relationship for the variance of horizontal diffusion as a function of time.

$$\sigma^2 \sim 5 \times 10^{-6} t^{2.3} \quad (6.11)$$

At time $t = t_G$, the variance of the spread is given by Equation (6.10).

For times $t > t_G$, the following is used to determine the extent of spread.

$$\sigma^2(t) = \frac{r_G^2(t)}{3} + 0.23 U_c r_G^{3/2} (t - t_g) L^{-1/2} + 5 \times 10^{-6} (t^{2.3} - t_g^{2.3}) \quad (6.12)$$

where r_G is the radius of the slick at time $t = t_G$.

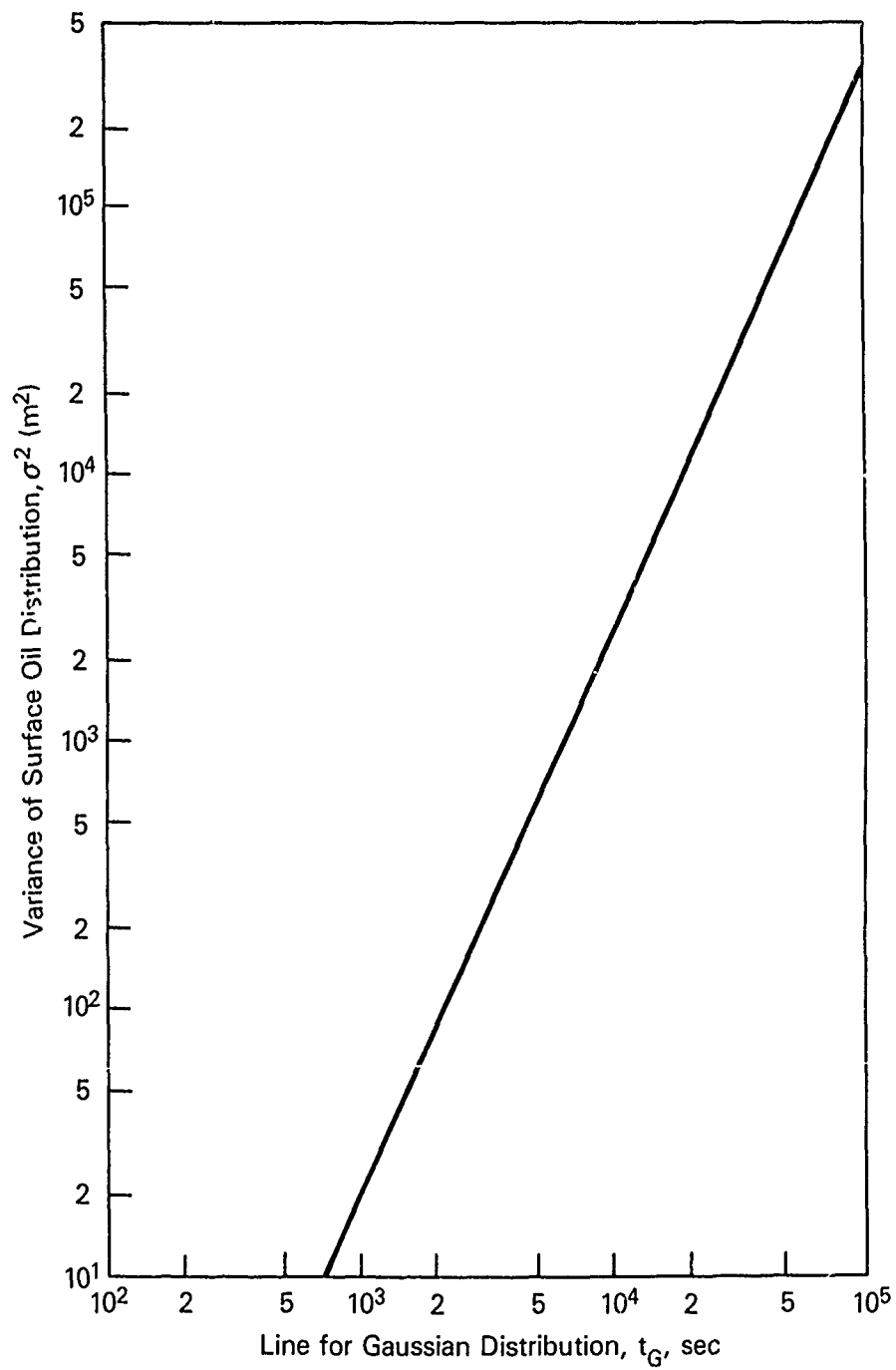


Figure 6.3 Growth of Oil Slick Under Influence of Horizontal Diffusion

To determine the area of the ocean surface contaminated by oil we adopt the approximation that all oil is contained within 2 of the center of mass. This approximation gives slick area as:

$$A_s = 4\pi\sigma^2 \quad (6.13)$$

The area of the floating oil is assumed to be A_0 , as developed by the evaporation model. The fraction of the bounded area that is covered by oil is:

$$f = A_0 / A_s \quad (6.14)$$

6.4 MODEL LIMITATIONS

The most serious model limitation is the lack of validation by comparison with observations for large spill volumes and long time periods. This data may be obtained from historical spill reports or from detailed observations at spills of opportunity. Although the model is developed for instantaneous releases, observations from continuous releases, such as the recent blow-out in the Gulf of Mexico, is analogous and would be valuable in model tuning and validation. The type of data required are the current velocity, time since spill (or time of travel for continuous slick), and the horizontal length scales of the slick. For a finite slick, the slick area would be acceptable; for a continuous slick, the slick-width transverse to the flow would be acceptable.

It is also necessary to establish a criterion for the formation of slicklets. The times t_g and t_G are sensitive to the thickness of the slick where the slicklets begin to form. In our calculation procedure we have used a critical thickness of 1 mm. The final area of dispersion calculated using this criterion corresponds closely to the estimated maximum areas of oil spills of different initial volumes given by Hoult (1972), which is:

$$\text{Maximum area (m}^2\text{)} = 10^5 \times (\text{initial volume, m}^3\text{)}^{0.75}$$

The thickness criterion should be a function of sea state and properties of oil. Clearly, more theoretical and experimental studies should be conducted to determine the critical thickness criterion for the slicklet formation.

At a more fundamental level, it would be advantageous to measure the sub-ensemble average of Lagrangian velocity fluctuations with respect to the center of gravity of the slick, or $u^2(t)$, and its variation with slick size.

An alternative to this type of fundamental measure of turbulence properties, which may be very difficult to obtain, would be to conduct experiments on the initial dispersion of a finite patch of drifters of uniform initial distribution. Obtaining the rate of change of the variance of the distribution with respect to time for patches of various initial sizes would supercede the observations of $u^2(t)$ mentioned above.

The concept of slicklet formation presented here is admittedly crude. This results not only from inadequacies of our understanding of the problem, but also from the constraints of this study that the algorithm presented must be sufficiently simple to be implemented on a hand calculator. Additional theoretical and observational research in this area is warranted.

6.5 APPLICATION OF THE SIMPLE ALGORITHM

A simple algorithm to determine the extent of dispersed area is presented here. The input to this algorithm are the radius and thickness of the slick from the evaporation model.

Step 1

Using user input data, determine:

$$\left. \begin{aligned} U_c &= 0.035 u \\ L^* &= 0.4 d_s \\ L &= 1 \times 10^5 \text{ or } L = L^*, \text{ whichever is smaller of the two} \end{aligned} \right\} (6.15)$$

Step 2

Determine, using the evaporation model, the time t_g when the thickness of the slick is 1 mm. Let r_g be the radius of the slick at this time.

$$\sigma_g^2 = r_g^2 / 3 \quad (6.16)$$

Using Figure 6.3, determine the time for transition to Gaussian, t_G .

Step 3

For time $t_g < t < t_G$, use Equation (6.17) to determine the variance of dispersion. For $t > t_G$, calculate σ^2 using Equations (6.17) and (6.18). If σ^2 given by Equation (6.17) is larger than the σ^2 given by Equation (6.18), choose the larger value and increase the value of t_G by the time step size. Continue this process until the value of σ^2 given by Equation (6.18) is larger than the one given by Equation (6.17). This value of time is the actual time for transition to Gaussian distribution.

Evaluate r_G at this time t_G .

$$\sigma^2(t) = \frac{r^2(t)}{3} + 0.23 U_c r_G^{3/2}(t) L^{-1/2} (t - t_g) \quad (6.17)$$

$$\sigma^2(t) = \frac{r^2(t)}{3} + 0.23 U_c r_G^{3/2}(t - t_g) L^{-1/2} + 5 \times 10^{-6} (t^{2.3} - t_g^{2.3}) \quad (6.18)$$

where r_G is the radius of the slick at time t_G .

Step 4

Determine the dispersed area

$$A_s = 4\pi\sigma^2 \quad (6.19)$$

Step 5

Compute the ratio of actual area of the slick to dispersed area of the slick.

6.6 CONCLUSIONS

From the analysis performed in this chapter the following conclusions can be drawn:

- Oil spill dispersion on the ocean's surface can be adequately described by a two-dimensional model analogous to the three dimensional turbulent diffusion model used for calculating the particle concentrations in a puff dispersing in the atmosphere. The empirical relationships describing turbulent diffusion were obtained from Obuko's (1971) results.
- While the model describes the behavior of the slicklet group after the patches are formed, we have been unable to obtain any criteria for determining the exact conditions under which slicklet formation begins. The breaking wave induced slicklet information model is utilized.

7. TABLE OF DISPERSION PREDICTIONS

7.1 Introduction

The objective of this chapter is to illustrate in detail the calculation procedure for determining the oil dispersion parameters for a specified spill quantity and environmental conditions.

The models presented in Chapters 3, 4, 5, and 6 deal with different aspects of oil slick behavior in the open ocean. In this chapter, these models are utilized and the sequential calculations are illustrated. The purpose of the illustrative example is to indicate how the outputs from each model are utilized in the succeeding calculations.

The step-by-step illustrative calculations are performed for a hypothetical instantaneous spill of 10,000 cubic meters of light crude oil on a sea with a significant wave height of 1 meter. The procedure indicates the input values needed, the equation on which the particular calculation is based, and the output results.

Also presented in this are the results of calculations for three other types of oil: heavy crude, fuel oil number two, and fuel oil number six. The important results are presented in tables and graphs. The results from each contributing model are presented in separate tables. Graphical displays are used to show the variation of the volume of oil floating and the slick area with time. In addition, the time required to reach 50% and 90% dispersion into the water are presented as functions of sea state.

Calculations presented are based on a fully developed sea state, and the assumption of a linear droplet size distribution.

The sensitivity of the results to these assumptions are addressed in the final sets of graphs where comparisons are made between two sets of parameters: the results obtained from a fully developed sea state and a much choppier sea where the waves are steeper, and the results obtained from the assumed linear droplet size distribution compared to the assumption that all the droplets were of the minimum size.

The calculations presented in the step-by-step illustrations are worked out by using only a scientific calculator. The calculations presented in the tables and graphs at the end of the chapter were obtained from the computer code discussed in Appendix E.

The illustration is formatted to serve as a self-sustained work sheet: the left column shows the results from the example calculation, while in the right column the results are left out to permit calculations by the user. These are shown in the right-hand pages of the report; the left-hand pages give the corresponding formulas supporting the calculations.

TABLE 3.1

Constants to be Used in Equations (3.24) and (3.25)

<u>Type of Oil</u>	<u>a₁</u>	<u>a₂</u>	<u>b₁</u>	<u>b₂</u>
Light Crude	350	9.67×10^{-5}	4.2×10^{-5}	0.62
Heavy Crude	27	2.47×10^{-5}	3.5×10^{-7}	1.05
Fuel Oil #2	4.6	1.56×10^{-6}	no change in density	
Fuel oil #6		no evaporation	no change in density	

$$\Delta = \rho_0 / \rho_w \quad (3.16)$$

$$G = g(1 - \Delta) \quad (3.17)$$

$$T = v_0^{1/6} G^{-1/2} \quad (3.18)$$

7.2 STEP-BY-STEP CALCULATION PROCEDURE ILLUSTRATION

7.2.1 Problem Statement

Given: Light crude of 10,000 cubic meters volume is spilled instantaneously onto the sea. The fully developed sea state corresponds to a significant wave height of 1 meter.

To find: the fate of the oil at different times after the spill, by evaluating the various dispersion parameters.

7.2.2. Calculations from the Evaporation and Spreading Model

User Supplied Data

Oil Type: Light Crude
 Initial Volume: 10,000 m³
 Wind Speed: 5 meters/second
 Slick Temperature: 25°C

User Supplied Data

Oil Type:
 Initial Volume: m³
 Wind Speed: m/s
 Slick Temperature °C

Obtain the following properties of the oil:

Initial Density: 8.68.6 kg/m³
 Surface Tension: 0.03 N/m
 Kinematic Viscosity: 8 x 10⁻⁶ m²/s

Initial Density: kg/m³
 Surface Tension: N/m
 Kinematic Viscosity: m²/s

Determine the following: volume, area, and thickness of the slick and the average density at 2, 4, and 8 hours after the spill.

Step 1 Assume the following properties for water:

Density = 1000 kg/m³

Kinematic Viscosity = 1 x 10⁻⁶ m²/s (1 centistoke)

also assume:

Gravity = 9.81 m/s²

Evaporation Constant = k₀ = 1 x 10⁻⁸ s²/m²

Calculate the following:

= 0.8686 (equation 3.16)

=

G = 1.29 m/s² (3.17)

G =

m/s²

T = 4.09 s (3.18)

T =

s

$$\tau_0 = 0.546 (V_0 G / \nu_w^2)^{1/6} \quad (3.19)$$

$$\tau_1 = 0.375 (\rho_w / \sigma) G^{5/6} \nu_w^{1/3} V_0^{1/2} \quad (3.20)$$

$$\tau_c = 3/2 a_2 T_s; \text{ if } \tau_c > \tau_1 \text{ then } \tau_c = 5/2 a_2 T_s \quad (3.22)$$

$$\tau_{p_{\max}} = \left((\rho_{\max} / \rho_0 - 1) / b_1 T_s^{0.22} U^{0.32} \right)^{(1/b_2)} + \tau_0 \quad (3.23)$$

$$R = 1 + b_1 T_s^{0.22} U^{0.32} (\tau - \tau_0)^{b_2} \quad (3.24)$$

$$P = a_1 T_s^{0.66} \exp((\tau - \tau_0) (-a_2 T_s^{0.22})) \quad (3.25)$$

Note: If τ is greater than $\tau_{p_{\max}}$, assume ρ equals ρ_{\max} .
 If τ is greater than τ_c , calculate P at τ equal to τ_c .

$$c_1 = 0.670 k_0 / (\nu_w^{1/6} g^{5/12} \rho_w) \quad c_2 = 3.02 g^{1/2} / \nu_w^{1/6}$$

$$f_1 = V_0^{-1/12}$$

Obtain the following constants for the oil from Table 3.1 or another source:

$$a_1 = 350$$

$$a_2 = 9.67 \times 10^{-5}$$

$$b_1 = 4.17 \times 10^{-5}$$

$$b_2 = 0.62$$

Step 2 Determine τ_0 and τ_1 .

$$\tau_0 = 264 \quad (3.19)$$

$$\tau_1 = 15455 \quad (3.20)$$

Determine τ_c and $\tau_{l_{max}}$.

$$\tau_c = 7640 \quad (3.22)$$

$$\tau_{l_{max}} = 46778 \quad (3.23)$$

Step 3 Determine $\tau = t/T$

t, hrs	τ
2	1760
4	3521
8	7042

Step 4 Use equations (3.24) and (3.25) to determine R and P

τ	R	P
1760	1.0132	2184
3521	1.0213	1545
7042	1.0336	774

Step 5 Determine the following:

$$c_1 = 2.58 \times 10^{-11}$$

$$c_2 = 36.5$$

$$f_1 = 0.46$$

$$a_1 =$$

$$a_2 =$$

$$b_1 =$$

$$b_2 =$$

$$\tau_0 =$$

$$\tau_1 =$$

$$\tau_c =$$

$$\tau_{l_{max}} =$$

t, hrs	τ

τ	R	P

$$c_1 =$$

$$c_2 =$$

$$f_1 =$$

$$g_1 = 1 / \Delta (1 - \Delta)^{3/4}$$

$$f_2 = v_0^{1/12}$$

$$g_2 = 1 / (1 - \Delta)^{1/4}$$

$$h_1 = (1 - \Delta_R)^{1/3} / R$$

$$h_2 = (1 - \Delta_R)^{1/3}$$

$$v = v_0 (1 - c_1 f_1 g_1 h_1 U^P (\tau^{3/2} - \tau_0^{3/2}))^3 \quad (3.26)$$

$$A = c_2 f_2 g_2 h_2 v^{2/3} \tau^{1/2} \quad (3.27)$$

$$h(\tau) = v(\tau) / A(\tau) \quad (3.30)$$

$$k = k_0 U^P \quad (3.31)$$

$$f_2 = 2.18$$

$$g_1 = 5.28$$

$$g_2 = 1.66$$

$$f_2 =$$

$$g_1 =$$

$$g_2 =$$

τ	h_1	h_2
1760	0.487	0.493
3521	0.473	0.483
7042	0.452	0.468

τ	h_1	h_2

Determine the slick volume and area using equations (3.26) and (3.27)

τ	V	A
1760	9321	1.21×10^6
3521	8648	1.59×10^6
7042	8192	2.11×10^6

τ	V	A

Step 6 Determine the slick thickness and evaporation flux

τ	h (m)	k (kg/m ² s)
1760	7.7×10^{-3}	1.09×10^{-4}
3521	5.4×10^{-3}	7.7×10^{-5}
7042	3.9×10^{-3}	3.9×10^{-5}

τ	h (m)	k (kg/m ² s)

Step 7 Prepare a summary Table of Results, similar to Table 7.1.

TABLE 7.1
SUMMARY OF EVAPORATION MODEL RESULTS

Time (hrs)	Residual Volume (m ³)	Slick Area (m ²)	Slick Thickness (m)	Average Density (kg/m ³)	Evaporation Flux (kg/m ² s)
0	10,000	-	-	868.6	-
0.3	10,000	5.0 x 10 ⁵	2 x 10 ⁻²	868.6	1.46 x 10 ⁻⁴
2	9,321	1.21 x 10 ⁶	7.7 x 10 ⁻³	880.1	1.09 x 10 ⁻⁴
4	8,648	1.59 x 10 ⁶	5.4 x 10 ⁻³	887.1	7.7 x 10 ⁻⁵
8	8,192	2.11 x 10 ⁶	3.9 x 10 ⁻³	897.3	3.9 x 10 ⁻⁵

$$\omega = 0.7 \text{ g/u} \quad (4.15)$$

$$t_1 = 0.001 \text{ g}/\omega^2 \quad (4.17)$$

$$v_{\text{eff}} = (1 - h/t_1)v_w + h/t_1 v_o \quad (4.18)$$

If $v_{\text{eff}} < v_w$, then assume $v_{\text{eff}} = v_w$.

If $v_{\text{eff}} > v_o$, then assume $v_{\text{eff}} = v_o$.

$$We_\eta = 0.6 \frac{\sigma \omega^{1/4}}{\rho_g^{1/2} v_{\text{eff}}^{5/4}} \quad (4.19)$$

$$\text{if } We_\eta \leq 10 \text{ then } d'_o = 0.6 \frac{\omega^{1/4} v_{\text{eff}}^{3/4}}{g^{1/2}}$$

$$\text{if } We_\eta > 10 \text{ then } d'_o = 0.03 \frac{\sigma^{3/5} \omega^{2/5}}{\rho_w^{3/5} g^{4/5}} \quad (4.20)$$

If $h > d'_o$ then $d = d'_o$; where h is the slick thickness.

If $h < d'_o$ then $d_o = h^{1/3} d_o^{2/3}$

7.2.3 Calculations from the Droplet Formation Model

The example given here is a continuation of the problem discussed in Section 3.5. The relevant results obtained there are:

t (hrs)	density (kg/m ³)	h (m)
2	879.9	7 x 10 ⁻³
4	888.6	5 x 10 ⁻³
8	893.9	3.8 x 10 ⁻³

Step 1 Find

$$\omega = 1.37 \text{ s}^{-1} \text{ (equation 4.15)}$$

Step 2 find t_1

$$t_1 = 5.23 \times 10^{-3} \text{ m} \text{ (4.17)}$$

Find the effective viscosity using equation (4.18)

t (hrs)	ν_{eff}
2	1.04 x 10 ⁻⁵
4	7.7 x 10 ⁻⁶
8	6.1 x 10 ⁻⁶

Step 3 Calculate We_h using equation (4.19)

t (hrs)	We_h
2	12.0
4	17.3
8	23

Step 4 Calculate the diameters of the smallest drops using equations (4.20)

t (hrs)	d_0 (m)
2	11.4 x 10 ⁻⁶

t (hrs)	density (kg/m ³)	h (m)

$$\omega = \text{ s}^{-1}$$

$$t_1 = \text{ m}$$

t (hrs)	ν_{eff}

t (hrs)	We_h

t (hrs)	d_0 (m)

$$d'_{\max} = \left(12\sigma/g(\rho_w - \rho) \right)^{1/2} \quad (4.21)$$

If $h > d'_{\max}$ then $d_{\max} = d'_{\max}$; where h is the oil slick thickness.

If $h < d'_{\max}$ then $d_{\max} = h$.

4 11.4×10^{-6}

8 11.3×10^{-6}

Step 5 Calculate the diameters of the largest drops using equation (4.21)

t (hrs)	d'_{\max} (m)	t (hrs)	d'_{\max} (m)
2	7×10^{-3}		
4	5×10^{-3}		
8	3.8×10^{-3}		

Step 6 does not apply to these hand calculations)

Step 7 Prepare a summary Table of Results, similar to Table 7.2

TABLE 7.2
DROPLET SIZE DISTRIBUTION

time (hrs)	smallest droplet	largest droplet
	diameter, d_0 (m)	diameter, d_{\max} (m)
2	11.4×10^{-6}	7×10^{-3}
4	11.4×10^{-6}	5×10^{-3}
8	11.3×10^{-6}	3.8×10^{-3}

TABLE 7.3

TABLE OF ERROR FUNCTIONS

x	$\text{erf } x$						
0.00	0.00000 00000	0.50	0.52049 98778	1.00	0.84270 07929	1.50	0.96610 51465
0.01	0.01128 34156	0.51	0.52324 36198	1.01	0.84681 04962	1.51	0.96727 67481
0.02	0.02256 45747	0.52	0.52789 86305	1.02	0.85083 80177	1.52	0.96841 34969
0.03	0.03384 12223	0.53	0.54646 40969	1.03	0.85478 42115	1.53	0.96951 62091
0.04	0.04511 11061	0.54	0.55493 92505	1.04	0.85864 99465	1.54	0.97058 56899
0.05	0.05637 19778	0.55	0.56332 33663	1.05	0.86243 61061	1.55	0.97162 27333
0.06	0.06762 15944	0.56	0.57161 57638	1.06	0.86614 35866	1.56	0.97262 81220
0.07	0.07885 77198	0.57	0.57981 58062	1.07	0.86977 32972	1.57	0.97360 26275
0.08	0.09007 81258	0.58	0.58792 29004	1.08	0.87332 61584	1.58	0.97454 70093
0.09	0.10128 05939	0.59	0.59593 64972	1.09	0.87680 31019	1.59	0.97546 20158
0.10	0.11246 29160	0.60	0.60385 60908	1.10	0.88020 50696	1.60	0.97634 83633
0.11	0.12362 28962	0.61	0.61168 12189	1.11	0.88353 30124	1.61	0.97720 68366
0.12	0.13475 83518	0.62	0.61941 14619	1.12	0.88678 78902	1.62	0.97803 80804
0.13	0.14586 71148	0.63	0.62704 64433	1.13	0.88997 06704	1.63	0.97884 28397
0.14	0.15694 70331	0.64	0.63458 58291	1.14	0.89308 23276	1.64	0.97962 17795
0.15	0.16799 59714	0.65	0.64202 93274	1.15	0.89612 38429	1.65	0.98037 55850
0.16	0.17901 18132	0.66	0.64937 66880	1.16	0.89909 62029	1.66	0.98110 49213
0.17	0.18999 24612	0.67	0.65662 77023	1.17	0.90200 03990	1.67	0.98181 04416
0.18	0.20093 58390	0.68	0.66378 22027	1.18	0.90483 74269	1.68	0.98249 27870
0.19	0.21183 98922	0.69	0.67084 00622	1.19	0.90760 82850	1.69	0.98315 25869
0.20	0.22270 25892	0.70	0.67780 11938	1.20	0.91031 39732	1.70	0.98379 04586
0.21	0.23352 19230	0.71	0.68466 55502	1.21	0.91295 55080	1.71	0.98440 70075
0.22	0.24429 59116	0.72	0.69143 31231	1.22	0.91553 38810	1.72	0.98500 28274
0.23	0.25502 25996	0.73	0.69810 39429	1.23	0.91805 01041	1.73	0.98557 84998
0.24	0.26570 00590	0.74	0.70467 80779	1.24	0.92050 51843	1.74	0.98613 45950
0.25	0.27632 63907	0.75	0.71115 56337	1.25	0.92290 01283	1.75	0.98667 16712
0.26	0.28689 97232	0.76	0.71753 67528	1.26	0.92523 59418	1.76	0.98719 02752
0.27	0.29741 82185	0.77	0.72382 16140	1.27	0.92751 36293	1.77	0.98769 09422
0.28	0.30788 00680	0.78	0.73001 04313	1.28	0.92973 41930	1.78	0.98817 41959
0.29	0.31828 34959	0.79	0.73610 34538	1.29	0.93189 86327	1.79	0.98864 05487
0.30	0.32862 67535	0.80	0.74219 09647	1.30	0.93400 79449	1.80	0.98909 05016
0.31	0.33890 81503	0.81	0.74800 32806	1.31	0.93606 31228	1.81	0.98952 45446
0.32	0.34912 59948	0.82	0.75381 07509	1.32	0.93806 51551	1.82	0.98994 31565
0.33	0.35927 80000	0.83	0.75952 37569	1.33	0.94001 50262	1.83	0.99034 68051
0.34	0.36936 45293	0.84	0.76514 27115	1.34	0.94191 37153	1.84	0.99073 59476
0.35	0.37938 20536	0.85	0.77066 80576	1.35	0.94376 21961	1.85	0.99111 10301
0.36	0.38932 97011	0.86	0.77610 02683	1.36	0.94556 14366	1.86	0.99147 24883
0.37	0.39920 59840	0.87	0.78143 98455	1.37	0.94731 23980	1.87	0.99182 07476
0.38	0.40900 94534	0.88	0.78668 73192	1.38	0.94901 60353	1.88	0.99215 62228
0.39	0.41873 87001	0.89	0.79184 32468	1.39	0.95067 32958	1.89	0.99247 93184
0.40	0.42839 23550	0.90	0.79690 82124	1.40	0.95228 51196	1.90	0.99279 04292
0.41	0.43796 90902	0.91	0.80188 28258	1.41	0.95385 24394	1.91	0.99308 99398
0.42	0.44746 76104	0.92	0.80676 77215	1.42	0.95537 61786	1.92	0.99337 82251
0.43	0.45688 66945	0.93	0.81156 35586	1.43	0.95685 72531	1.93	0.99365 56502
0.44	0.46622 51153	0.94	0.81627 10190	1.44	0.95829 65696	1.94	0.99392 25709
0.45	0.47548 17198	0.95	0.82089 08073	1.45	0.95969 50256	1.95	0.99417 93336
0.46	0.48465 53900	0.96	0.82542 36496	1.46	0.96105 35095	1.96	0.99442 62755
0.47	0.49374 50509	0.97	0.82987 02930	1.47	0.96237 28999	1.97	0.99466 37246
0.48	0.50274 96707	0.98	0.83423 15043	1.48	0.96365 40654	1.98	0.99489 20004
0.49	0.51166 82512	0.99	0.83850 80696	1.49	0.96489 78648	1.99	0.99511 14132
0.50	0.52049 98778	1.00	0.84270 07929	1.50	0.96610 51465	2.00	0.99532 22650

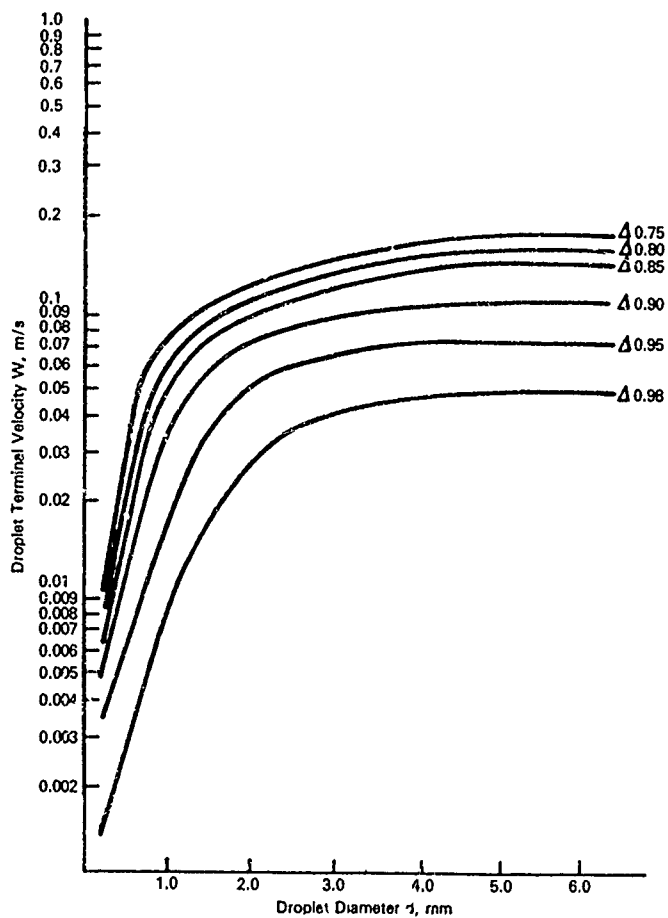


Figure 5.1 Variation of Droplet Terminal Velocity with Diameter (RAJ, 1977)

$$\omega = 0.7 g / U \quad (5.26)$$

$$T_1 = 2 \pi / \omega$$

$$\bar{\omega} = 6.83 / T_1 \quad (5.27)$$

$$\lambda = 2 \pi g / \bar{\omega}^2 \quad (5.28)$$

$$N = Pr^* \frac{A^{1/2} \bar{\omega}}{2 \pi \lambda} \quad (5.29)$$

where $Pr^* = 1.7 \times 10^{-7} U^{3.75}$

$$\dot{v} = \frac{Nh\lambda}{4} \quad (5.30)$$

7.2.4 Calculations from the Droplet Distribution Model

Summary of data:

time after spill = 7200 seconds

$t =$ s

significant wave height = 1 meter

$H_{1/3} =$ m

wind velocity = 5.0 meters per second

$U =$ m/s

from evaporation model:

$$\rho = 880.1 \text{ kg/m}^3$$

$\rho =$ kg/m³

$$h = 7.7 \times 10^{-3} \text{ m}$$

$h =$ m

$$A = 1.21 \times 10^6 \text{ m}^2$$

$A =$ m²

$$V = 9321 \text{ m}^3$$

$V =$ m³

$$\Delta = 0.88$$

$\Delta =$

from droplet formation model:

$$d_0 = 1.1 \times 10^{-5} \text{ m}$$

$d_0 =$ m

$$d_{\max} = 7.7 \times 10^{-3} \text{ m}$$

$d_{\max} =$ m

Step 1 Use equations (5.26), (5.27), and (5.28) to find:

$$\omega = 1.37 \text{ s}^{-1}$$

$\omega =$ s⁻¹

$$T_1 = 4.58 \text{ s}$$

$T_1 =$ s

$$\bar{\omega} = 1.49 \text{ s}^{-1}$$

$\bar{\omega} =$ s⁻¹

$$\lambda = 2.78 \text{ m}$$

$\lambda =$ m

Step 2 Use equation (5.29),

$$N = 3.7 \times 10^{-3} \text{ s}^{-1}$$

$N =$ s⁻¹

Step 3 Use equation (5.30) to calculate \dot{V}

$$\dot{V} = 2 \times 10^{-4} \text{ m}^3/\text{ms}$$

$\dot{V} =$ m³/ms

Step 4 Use equation (5.31) to find the four values of d_i

$$d_1 = 9.7 \times 10^{-4} \text{ m}$$

$d_1 =$ m

$$d_2 = 2.9 \times 10^{-3} \text{ m}$$

$d_2 =$ m

$$\begin{aligned}
 d_1 &= \frac{7d_0 + d_m}{8} \\
 d_2 &= \frac{5d_0 + 3d_m}{8} \\
 d_3 &= \frac{3d_0 + 5d_m}{8} \\
 d_4 &= \frac{d_0 + 7d_m}{8}
 \end{aligned}
 \tag{5.31}$$

$$W^* = \frac{d_m^5}{20} - \frac{d_m d_0^4}{4} + \frac{d_0^5}{5}
 \tag{5.32}$$

$$\begin{aligned}
 d_a &= \frac{3d_0 + d_m}{4} \\
 d_b &= \frac{d_0 + d_m}{2} \\
 d_c &= \frac{d_0 + 3d_m}{4}
 \end{aligned}
 \tag{5.33}$$

$$\begin{aligned}
 F_{d_1} &= \frac{1}{W^*} \left(\frac{d_m d_a^4}{4} - \frac{d_a^5}{5} - \frac{d_m d_0^4}{4} + \frac{d_0^5}{5} \right) \\
 F_{d_2} &= \frac{1}{W^*} \left(\frac{d_m d_b^4}{4} - \frac{d_b^5}{5} - \frac{d_m d_a^4}{4} + \frac{d_a^5}{5} \right) \\
 F_{d_3} &= \frac{1}{W^*} \left(\frac{d_m d_c^4}{4} - \frac{d_c^5}{5} - \frac{d_m d_b^4}{4} + \frac{d_b^5}{5} \right) \\
 F_{d_4} &= \frac{1}{W^*} \left(\frac{d_m^5}{20} - \frac{d_m d_c^4}{4} + \frac{d_c^5}{5} \right)
 \end{aligned}
 \tag{5.34}$$

$$d_c^* = \frac{9.52 \nu_w^{2/3}}{g^{1/3} (1 - \Delta)^{1/3}}
 \tag{5.35}$$

For droplet diameters less than the critical diameter, use equation (5.36) to calculate the terminal velocity. For droplets larger than the critical diameter, use equation (5.37).

$$W = \frac{gd^2(1 - \Delta)}{18} \quad \text{for } d \leq d_c^*
 \tag{5.36}$$

$$W = (8/3 gd(1 - \Delta))^{1/2} \quad \text{for } d > d_c^*
 \tag{5.37}$$

$$d_3 = 4.8 \times 10^{-3} \text{ m}$$

$$d_4 = 6.7 \times 10^{-3} \text{ m}$$

Determine W^* using equation (5.32)

$$W^* = 1.4 \times 10^{-12} \text{ m}^5$$

Determine d_a, d_b, d_c , using equation (5.33)

$$d_a = 1.9 \times 10^{-3} \text{ m}$$

$$d_b = 3.9 \times 10^{-3} \text{ m}$$

$$d_c = 5.8 \times 10^{-3} \text{ m}$$

Determine the four values of F_{d_i} using equation (5.34)

$$F_{d_1} = 0.017$$

$$F_{d_2} = 0.175$$

$$F_{d_3} = 0.447$$

$$F_{d_4} = 0.364$$

$$\sum F_{d_i} = 1$$

Step 5 Determine d_c^* using equation (5.35)

$$d_c^* = 9 \times 10^{-4}$$

Since all diameters are above d_c^* , use equation (5.37) to determine terminal velocities. (For convenience, one can use Figure 5.1 on page 7-18 to determine the terminal velocity.)

$$W_1 = 5.5 \times 10^{-2} \text{ m/s}$$

$$W_2 = 9.5 \times 10^{-2} \text{ m/s}$$

$$W_3 = 1.2 \times 10^{-1} \text{ m/s}$$

$$W_4 = 1.5 \times 10^{-1} \text{ m/s}$$

$$d_3 = \text{m}$$

$$d_4 = \text{m}$$

$$W^* = \text{m}^5$$

$$d_a = \text{m}$$

$$d_b = \text{m}$$

$$d_c = \text{m}$$

$$F_{d_1} =$$

$$F_{d_2} =$$

$$F_{d_3} =$$

$$F_{d_4} =$$

$$\sum F_{d_i} = 1$$

$$d_c^* =$$

$$W_1 = \text{m/s}$$

$$W_2 = \text{m/s}$$

$$W_3 = \text{m/s}$$

$$W_4 = \text{m/s}$$

$$z_g = \frac{\pi q}{2 \bar{\omega}^2} \quad (5.39)$$

$$z_w = \frac{0.01 H^2 \bar{\omega}}{W} \quad (5.38)$$

$$\left. \begin{aligned} z_0 &= z_w && \text{if } z_w \leq z_g \\ z_0 &= z_g && \text{if } z_w > z_g \end{aligned} \right\} (5.40)$$

$$K_T = 0.004 H^2 \quad (5.41)$$

$$\left. \begin{aligned} \text{erfc}(X_{d,t'}) &= 1 + \text{erf}(X_{d,t'}) && \text{if } X_{d,t'} \leq 0 \\ \text{erfc}(X_{d,t'}) &= 1 - \text{erf}(X_{d,t'}) && \text{if } X_{d,t'} > 0 \end{aligned} \right\} (5.44)$$

$$I_d = \frac{t'}{4} \sum_{\substack{\text{over} \\ \text{time} \\ \text{steps}}} \text{erfc } X_{d,t'} \quad (5.45)$$

$$v_d(d) = \dot{v}_d t_0 + \frac{1}{2} \dot{v}_d I_d \quad (5.46)$$

$$v_d(t) = F_{d_1} v_d(d_1) + F_{d_2} v_d(d_2) + F_{d_3} v_d(d_3) + F_{d_4} v_d(d_4) \quad (5.47)$$

Step 6 Calculate z_w and z_g using equations (5.38) and (5.39)

$z_g = 27.8 \text{ m}$	$z_g =$	m
$z_{w1} = 0.27 \text{ m}$	$z_{w1} =$	m
$z_{w2} = 0.16 \text{ m}$	$z_{w2} =$	m
$z_{w3} = 0.12 \text{ m}$	$z_{w3} =$	m
$z_{w4} = 0.10 \text{ m}$	$z_{w4} =$	m

Using equations (5.40) we obtain

$z_{01} = 0.27 \text{ m}$	$z_{01} =$	m
$z_{02} = 0.16 \text{ m}$	$z_{02} =$	m
$z_{03} = 0.12 \text{ m}$	$z_{03} =$	m
$z_{04} = 0.10 \text{ m}$	$z_{04} =$	m

Step 7 Determine K_T using equation (5.41)

$K_T = 5.96 \times 10^{-3} \text{ m}^2/\text{s}$	$K_T =$	m^2/s
--	---------	-----------------------

Step 8 From equations (5.44) and (5.45), find $I(d)$ and $V_d(d)$

All $X_{d,t}$ are greater than 2.

$I(d) = 0$	$I(d) =$
------------	----------

From equation (5.46),

$V_d(d) = 0$	$V_d(d) =$
--------------	------------

Step 9 From equation (5.47)

$V_d(t) = 0$	$V_d(t) =$
--------------	------------

This implies that there is no oil lost in the form of oil droplets at $t = 72000 \text{ s}$.

$$U_c = 0.035 u$$

$$L^* = 0.4 d_s$$

$$L = 1 \times 10^5 \text{ or } L = L^*, \text{ whichever is smaller of the two}$$

(6.15)

$$\sigma_g^2 = r_g^2 / 3$$

(6.16)

7.2.5 Calculations from the Surface Oil Distribution Model

Summary of data:

wind speed = 5.9 m/s

U = m/s

distance to shore = 10^7 m

$d_s =$ m

time after spill = 8 hours (2880 s)

t = s

Step 1 Using equation (6.15), find:

$U_c = 0.21$ m/s

$U_c =$ m/s

$L^* = 4 \times 10^6$ m

$L^* =$ m

$L = 10^5$ m

L = m

Step 2 Using evaporation model data, determine the thickness of the slick

(this is given in Table 7.1)

$h = 3.9 \times 10^{-3}$ m

h = m

Since slick thickness is greater than

1×10^{-3} m, the horizontal

dispersion model is not applicable.

If the thickness is less than

1×10^{-3} m, use equation (6.16)

to determine the region, r_g ,

$r_g =$

of the slick at this thickness

and the variance σ_g^2 .

$\sigma_g^2 =$

Using Figure 6.3, find a first

estimate for t_G

$t_G =$

$$\sigma^2(t) = \frac{r^2(t)}{3} + 0.23 U_c r^{3/2}(t) L^{-1/2} U_c (t - t_g) \quad (6.17)$$

$$\sigma^2(t) = \frac{r^2(t)}{3} + 0.23 U_c r_G^{3/2} (t - t_g) L^{-1/2} + 5 \times 10^{-6} (t^{2.3} - t_g^{2.3}) \quad (6.18)$$

$$A_s = 4\pi\sigma^2 \quad (6.19)$$

Step 3 Using an iterative solution based on these estimates, find the actual t_G . For t less than t_G , use equations (6.17) and (6.18) and chose the larger value of t^2 . If (6.17) yields the larger value, increase t_G by the stepsize and repeat the calculation until both equations yield the same result. This value is the actual t_G and can be used to calculate the radius r_G at this time. If (6.18) yields the larger value, decrease t_G by the stepsize and repeat the process.

Step 4 Determine the dispersed area using equation (6.19)

Step 5 Determine the ratio of area under oil to area affected by oil.

TABLE 7.4

SUMMARY OF RESULTS FOR LIGHT CRUDE SPILL IN VARIOUS STATES
EVAPORATION MODEL RESULTS

1/3 Significant Wave Height = 1m

<u>Time (hrs)</u>	<u>Volume of Oil Remaining (m³)</u>	<u>Slick Area (m²)</u>	<u>Slick Thickness (m)</u>	<u>Average Density (kg/m³)</u>	<u>Evaporation Flux (kg/m²s)</u>
0	10000	-	-	868.8	-
2	9205	1.2 x 10 ⁶	7.8 x 10 ⁻³	882.5	6.7 x 10 ⁻⁵
4	8799	1.6 x 10 ⁶	5.6 x 10 ⁻³	889.5	2.0 x 10 ⁻⁵
8	8411	2.1 x 10 ⁶	3.9 x 10 ⁻³	894.7	1.1 x 10 ⁻⁵
16	7721	3.3 x 10 ⁶	2.3 x 10 ⁻³	904.3	6.2 x 10 ⁻⁶
32	6996	9.4 x 10 ⁶	7.4 x 10 ⁻⁴	915.7	3.1 x 10 ⁻⁷
64	6168	2.7 x 10 ⁷	2.3 x 10 ⁻⁴	919.9	1.6 x 10 ⁻⁷
101	4336	5.3 x 10 ⁷	8.2 x 10 ⁻⁵	930.0	9.3 x 10 ⁻⁸

After 101 hours, the area vs. volume stopping criterion (area > 10⁵ x (volume)^{.75}) is reached: the slick breaks up.

TABLE 7.4 (continued)

SUMMARY OF RESULTS FOR LIGHT CRUDE SPILL IN VARIOUS STATES
DROPLET FORMATION MODEL RESULTS

1/3 Significant Wave Height = 1m

<u>Time (hrs)</u>	<u>Diameter of the Smallest Drop (m)</u>	<u>Diameter of the Maximum Drop (m)</u>
2	9.9×10^{-6}	7.8×10^{-3}
4	9.9×10^{-6}	5.6×10^{-3}
8	9.9×10^{-6}	3.9×10^{-3}
16	9.9×10^{-6}	2.3×10^{-3}
32	9.9×10^{-6}	7.4×10^{-4}
64	9.9×10^{-6}	2.3×10^{-4}
101	9.9×10^{-6}	8.3×10^{-5}

TABLE 7.4 (continued)

SUMMARY OF RESULTS FOR LIGHT CRUDE SPILL IN VARIOUS STATES
DROPLET DISTRIBUTION MODEL RESULTS

1/3 Significant Wave Height = 1m

<u>Time</u> <u>(hrs)</u>	<u>Volume of</u> <u>Oil</u> <u>Dispersed</u> <u>in Water, \bar{V}_d</u> <u>(m³)</u>	<u>Total Volume</u> <u>of Oil</u> <u>Remaining</u> <u>in the</u> <u>System, \bar{V}</u> <u>(m³)</u>	<u>Volume of</u> <u>Oil</u> <u>Floating</u> <u>on Water, V_r</u> <u>($V_r = \bar{V} - V_d$)</u> <u>(m³)</u>
2	0	9205	9205
4	0	8799	8799
8	0	8411	8411
16	0	7721	7721
32	11	7008	6996
64	448	6616	6168
101	1557	5893	4336

TABLE 7.4 (continued)

SUMMARY OF RESULTS FOR LIGHT CRUDE SPILL IN VARIOUS STATES
SURFACE OIL DISTRIBUTION MODEL RESULTS

1/3 Significant Wave Height = 1m

<u>Time (hrs)</u>	<u>Total of Oil Patches A_O (m²)</u>	<u>Total Polluted Sea Surface Area A_S (m²)</u>	<u>A_O/A_S</u>
2	1.2 x 10 ⁶	1.2 x 10 ⁶	1.0
4	1.6 x 10 ⁶	1.6 x 10 ⁶	1.0
8	2.1 x 10 ⁶	2.1 x 10 ⁶	1.0
16	3.3 x 10 ⁶	3.3 x 10 ⁶	1.0
32	9.4 x 10 ⁶	2.7 x 10 ⁷	.34
64	2.7 x 10 ⁷	2.8 x 10 ⁸	.10
101	5.3 x 10 ⁷	8.7 x 10 ⁸	.06

TABLE 7.5

SUMMARY OF RESULTS FOR LIGHT CRUDE SPILL IN VARIOUS STATES
EVAPORATION MODEL RESULTS

1/3 Significant Wave Height = 3m

Time (hrs)	Volume of Oil Remaining (m ³)	Slick Area (m ²)	Slick Thickness (m)	Average Density (kg/m ³)	Evaporation Flux (kg/m ² s)
0	10000	-	-	868.8	-
2	8973	1.1 x 10 ⁶	7.8 x 10 ⁻³	886.6	6.5 x 10 ⁻⁵
4	8616	1.6 x 10 ⁶	5.6 x 10 ⁻³	890.9	2.5 x 10 ⁻⁵
3	8086	2.1 x 10 ⁶	3.9 x 10 ⁻³	899.0	1.5 x 10 ⁻⁵
16	7325	3.3 x 10 ⁶	2.2 x 10 ⁻³	910.4	5.1 x 10 ⁻⁶
32	6663	9.4 x 10 ⁶	7.1 x 10 ⁻⁴	916.6	3.2 x 10 ⁻⁷
64	2309	2.7 x 10 ⁷	8.7 x 10 ⁻⁵	927.1	2.0 x 10 ⁻⁷
68	1941	2.9 x 10 ⁷	6.6 x 10 ⁻⁵	929.9	1.6 x 10 ⁻⁷

After 68 hours the area vs. volume stopping criterion (area > 10⁵ x (volume)^{.75}) is reached: the slick breaks up.

TABLE 7.5 (continued)

SUMMARY OF RESULTS FOR LIGHT CRUDE SPILL IN VARIOUS STATES
** DROPLET FORMATION MODEL RESULTS

1/3 Significant Wave Height = 3m

<u>Time (hrs)</u>	<u>Diameter of the Smallest Drop (m)</u>	<u>Diameter of the Maximum Drop (m)</u>
2	8.0×10^{-6}	7.8×10^{-3}
4	8.0×10^{-6}	5.6×10^{-3}
8	8.0×10^{-6}	3.9×10^{-3}
16	8.0×10^{-6}	2.2×10^{-3}
32	8.0×10^{-6}	7.1×10^{-4}
64	8.0×10^{-6}	9.0×10^{-5}
68	8.0×10^{-6}	6.9×10^{-5}

TABLE 7.5 (continued)

SUMMARY OF RESULTS FOR LIGHT CRUDE SPILL IN VARIOUS STATES

DROPLET DISTRIBUTION MODEL RESULTS

1/3 Significant Wave Height = 3m

<u>Time (hrs)</u>	<u>Volume of Oil Dispersed in Water, \bar{V}_d (m³)</u>	<u>Total Volume of Oil Remaining in the System, \bar{V} (m³)</u>	<u>Volume of Oil Floating on Water, V_r ($V_r = \bar{V} - V_d$) (m³)</u>
2	0	8973	8973
4	0	8616	8616
8	0	8086	8086
16	8	7333	7325
32	272	6935	6663
64	4040	6349	2309
68	4331	6272	1941

TABLE 7.5 (continued)

SUMMARY OF RESULTS FOR LIGHT CRUDE SPILL IN VARIOUS STATES

SURFACE OIL DISTRIBUTION MODEL RESULTS

1/3 Significant Wave Height = 3m

Time (hrs)	Total of Oil Patches A_O (m ²)	Total Polluted Sea Surface Area A_S (m ²)	A_O/A_S
2	1.1×10^6	1.1×10^6	1.0
4	1.6×10^6	1.6×10^6	1.0
8	2.1×10^6	2.1×10^6	1.0
16	3.3×10^6	3.3×10^6	1.0
32	9.4×10^6	2.7×10^7	.34
64	2.7×10^7	2.8×10^8	.10
68	2.9×10^7	3.2×10^8	.09

TABLE 7.6

SUMMARY OF RESULTS FOR LIGHT CRUDE SPILL IN VARIOUS STATES
EVAPORATION MODEL RESULTS

1/3 Significant Wave Height = 5m

<u>Time (hrs)</u>	<u>Volume of Oil Remaining (m³)</u>	<u>Slick Area (m²)</u>	<u>Slick Thickness (m)</u>	<u>Average Density (kg/m³)</u>	<u>Evaporation Flux (kg/m²s)</u>
0	10000	-	-	868.8	-
2	8882	1.1×10^6	7.8×10^{-3}	888.2	6.0×10^{-5}
4	8519	1.5×10^6	5.6×10^{-3}	893.3	2.6×10^{-5}
8	7904	2.0×10^6	3.9×10^{-3}	901.5	1.7×10^{-5}
16	7171	3.3×10^6	2.2×10^{-3}	912.7	3.9×10^{-6}
32	5435	9.4×10^6	5.8×10^{-4}	917.1	4.1×10^{-7}
52	1135	2.0×10^7	5.8×10^{-5}	929.0	2.2×10^{-7}

TABLE 7.6 (continued)

SUMMARY OF RESULTS FOR LIGHT CRUDE SPILL IN VARIOUS STATES
DROPLET FORMATION MODEL RESULTS

1/3 Significant Wave Height = 5m

<u>Time</u> <u>(hrs)</u>	<u>Diameter of the</u> <u>Smallest Drop</u> <u>(m)</u>	<u>Diameter of the</u> <u>Maximum Drop</u> <u>(m)</u>
2	7.2×10^{-6}	7.8×10^{-3}
4	7.2×10^{-6}	5.6×10^{-3}
8	7.2×10^{-6}	3.9×10^{-3}
16	7.2×10^{-6}	2.2×10^{-3}
32	7.2×10^{-6}	5.9×10^{-4}
52	7.2×10^{-6}	6.0×10^{-5}

TABLE 7.6 (continued)

SUMMARY OF RESULTS FOR LIGHT CRUDE SPILL IN VARIOUS STATES
DROPLET DISTRIBUTION MODEL RESULTS

1/3 Significant Wave Height = 5m

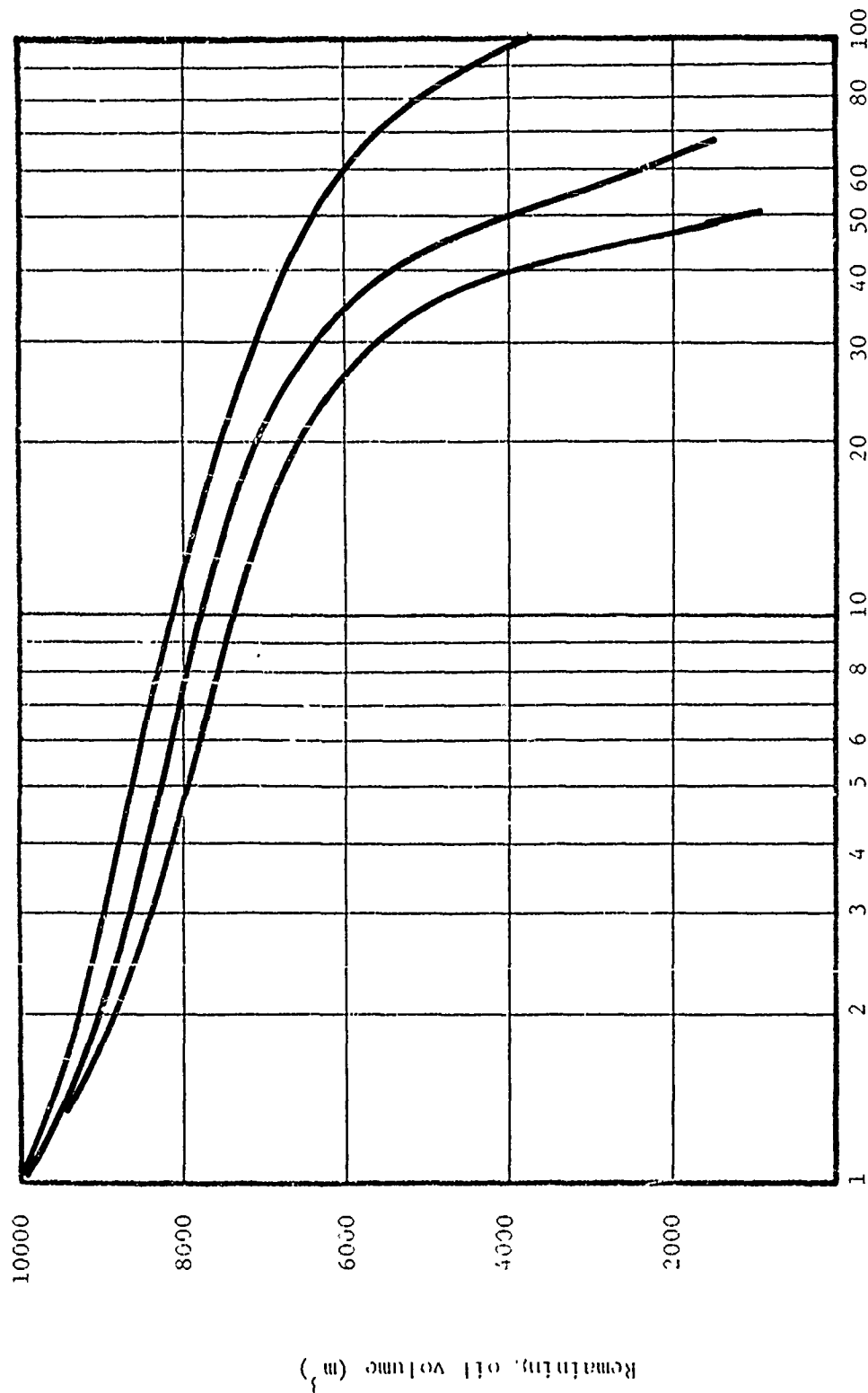
<u>Time (hrs)</u>	<u>Volume of Oil Dispersed in Water, \bar{V}_d (m³)</u>	<u>Total Volume of Oil Remaining in the System, \bar{V} (m³)</u>	<u>Volume of Oil Floating on Water, V_r ($V_r = \bar{V} - V_d$) (m³)</u>
2	0	8882	8882
4	0	8519	8519
8	3	7907	7904
16	24	7195	7171
32	1452	6887	5435
52	5382	6517	1135

TABLE 7.6 (continued)

SUMMARY OF RESULTS FOR LIGHT CRUDE SPILL IN VARIOUS STATES
SURFACE OIL DISTRIBUTION MODEL RESULTS

1/3 Significant Wave Height = 5m

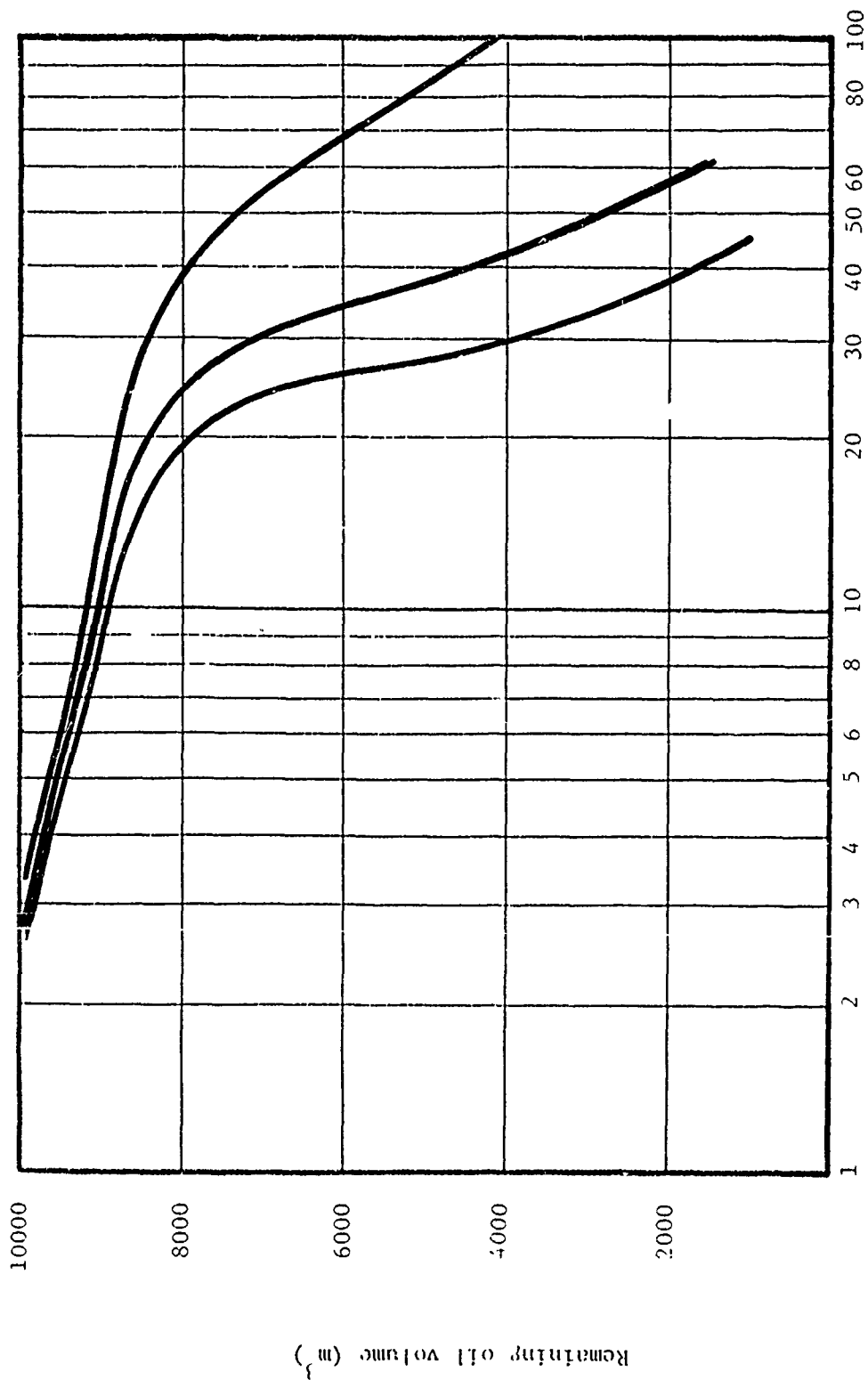
<u>Time (hrs)</u>	<u>Total of Oil Patches A_O (m²)</u>	<u>Total Polluted Sea Surface Area A_S (m²)</u>	<u>A_O/A_S</u>
2	1.1×10^6	1.1×10^6	1.0
4	1.5×10^6	1.5×10^6	1.0
8	2.0×10^6	2.0×10^6	1.0
16	3.3×10^6	3.3×10^6	1.0
32	9.4×10^6	3.2×10^7	.30
52	2.0×10^7	1.6×10^8	.12



Time after spill (hours)

Figure 7.1

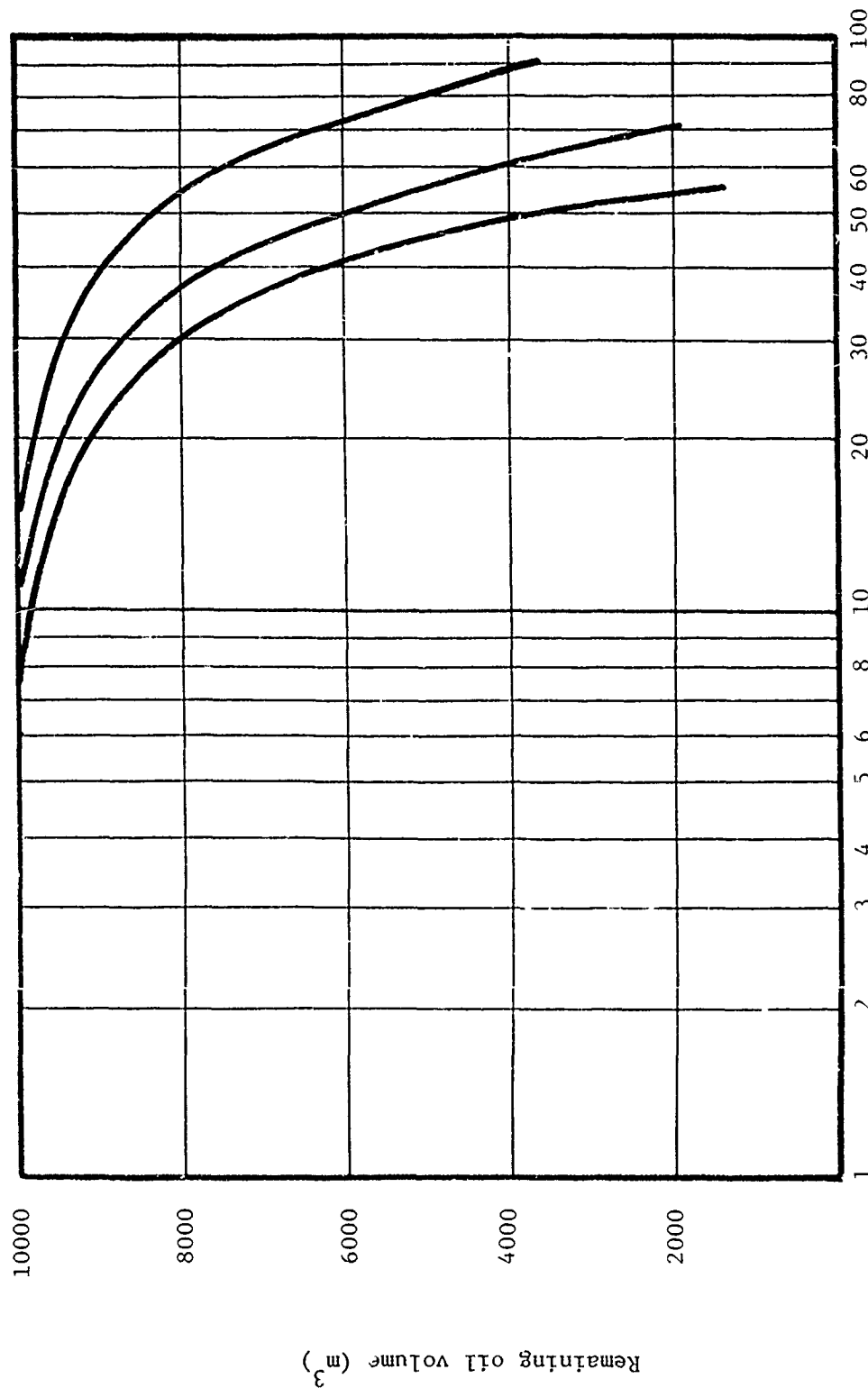
VOLUME OF LIGHT CRUDE OIL REMAINING ON THE SURFACE AS A FUNCTION OF TIME AFTER SPILL



Time after spill (hours)

Figure 7.2

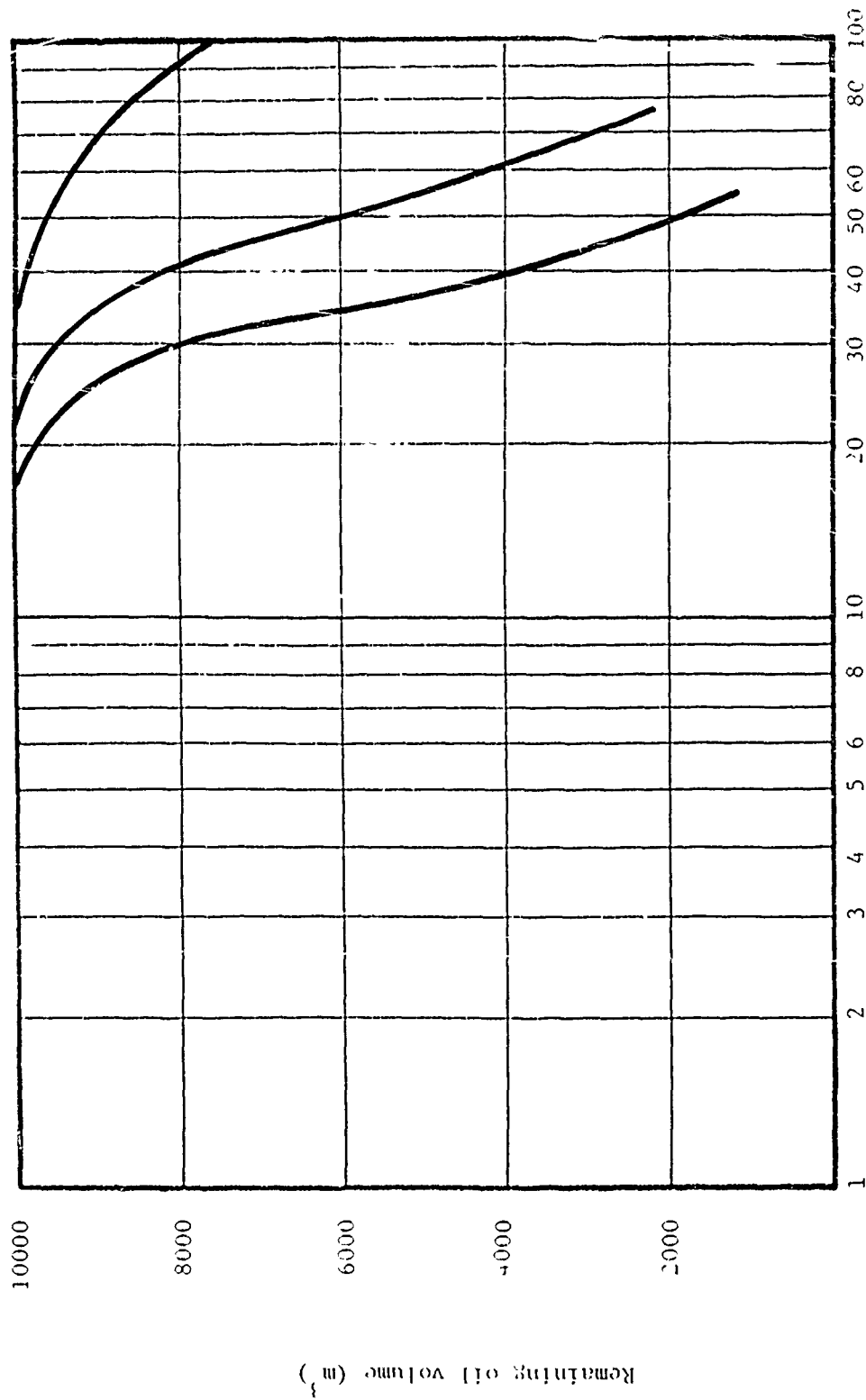
VOLUME OF HEAVY CRUDE OIL REMAINING ON THE SURFACE AS A FUNCTION OF TIME AFTER SPILL



Time after spill (hours)

Figure 7.3

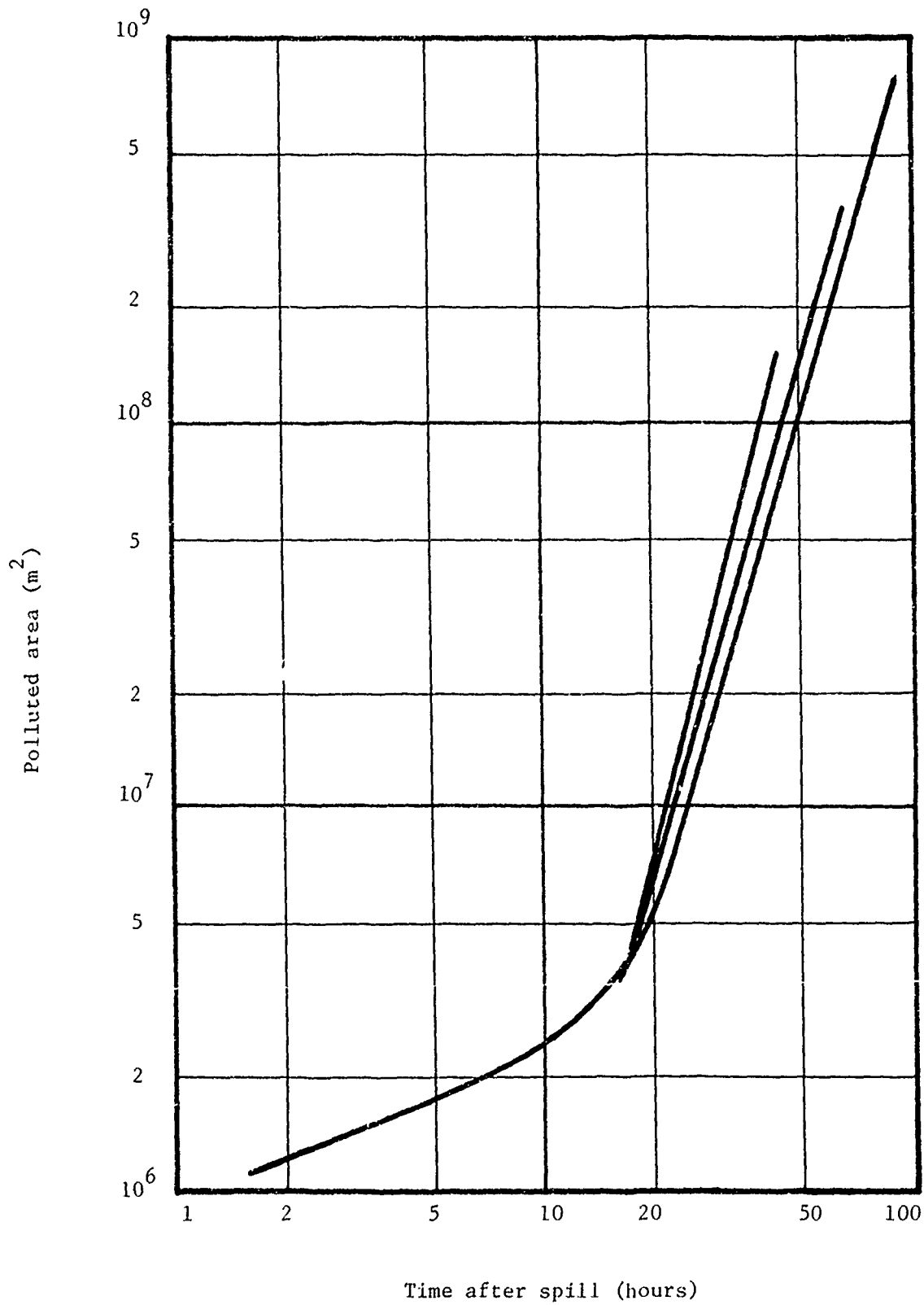
VOLUME OF FUEL OIL #2 REMAINING OF THE SURFACE AS A FUNCTION OF TIME AFTER SPILL



Time after spill (hours)

Figure 7.4

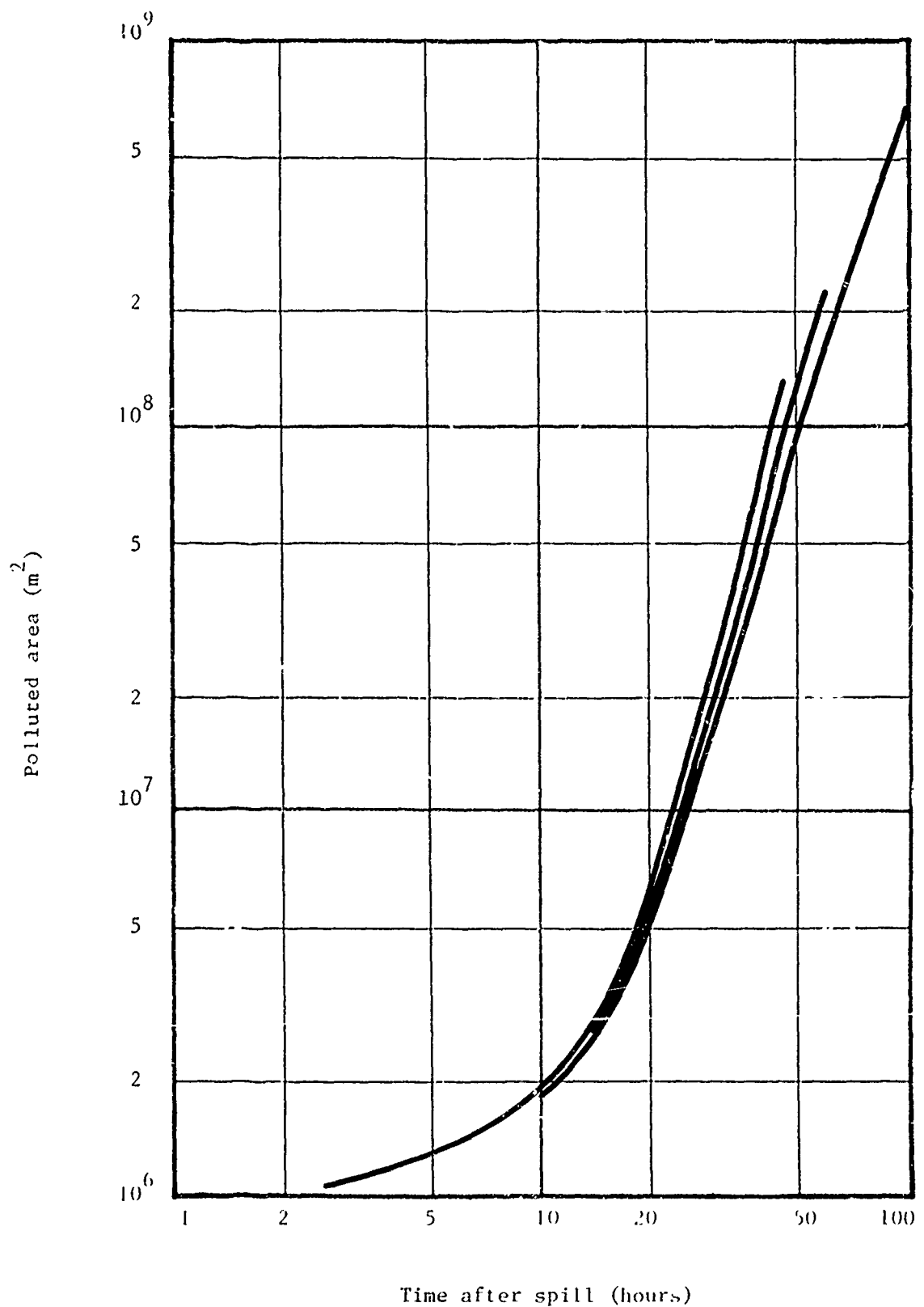
VOLUME OF FUEL OIL #6 REMAINING OF THE SURFACE AS A FUNCTION OF TIME AFTER SPILL



Time after spill (hours)

Figure 7.5

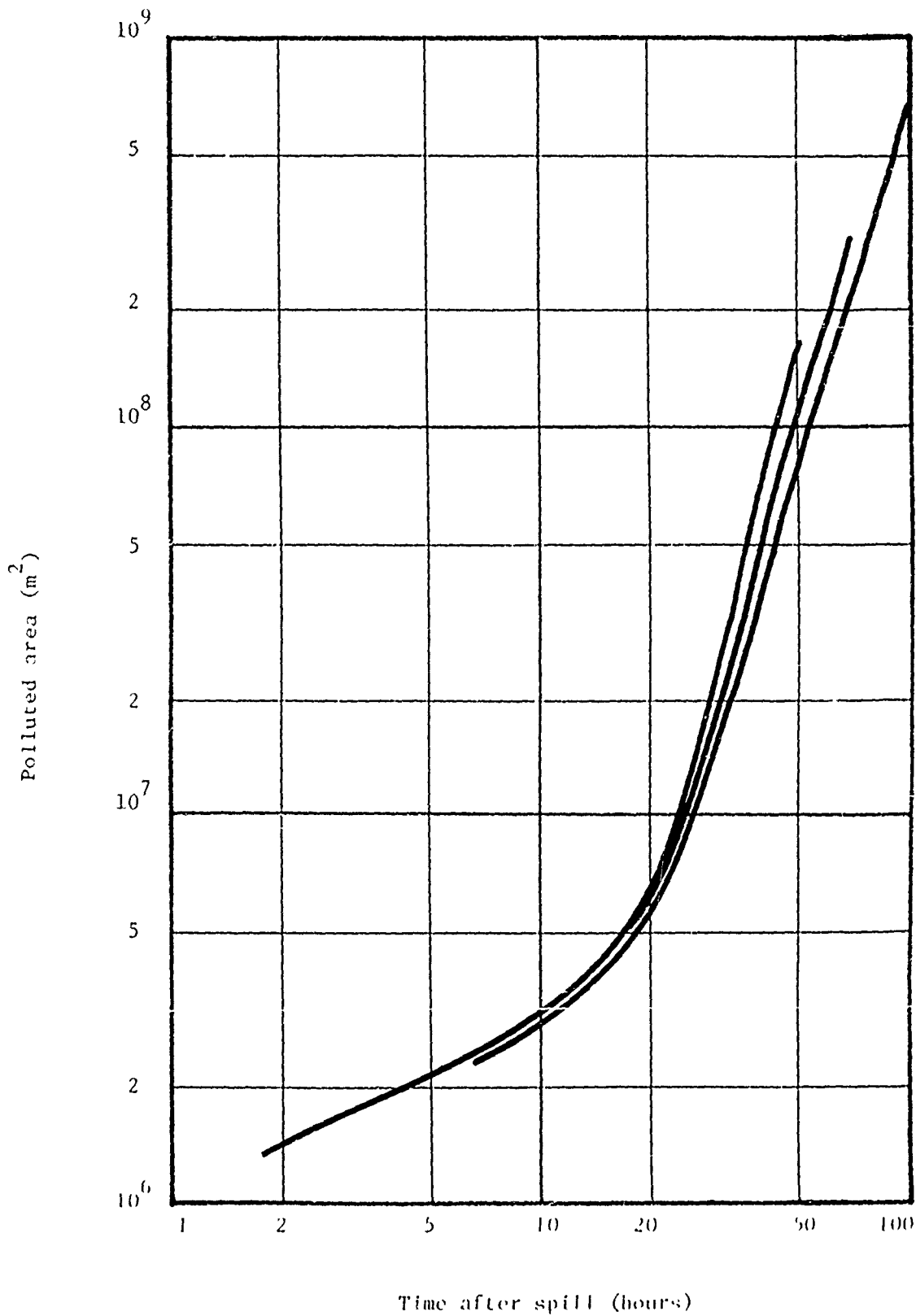
SURFACE AREA OF A LIGHT CRUDE OIL SLICK AS A FUNCTION OF TIME AFTER SPILL



Time after spill (hours)

Figure 7.6

SURFACE AREA OF A HEAVY CRUDE OIL SLICK AS A FUNCTION OF TIME AFTER SPILL



Time after spill (hours)

Figure 7.7

SURFACE AREA OF FUEL OIL #2 OIL SLICK AS A FUNCTION OF
TIME AFTER SPILL

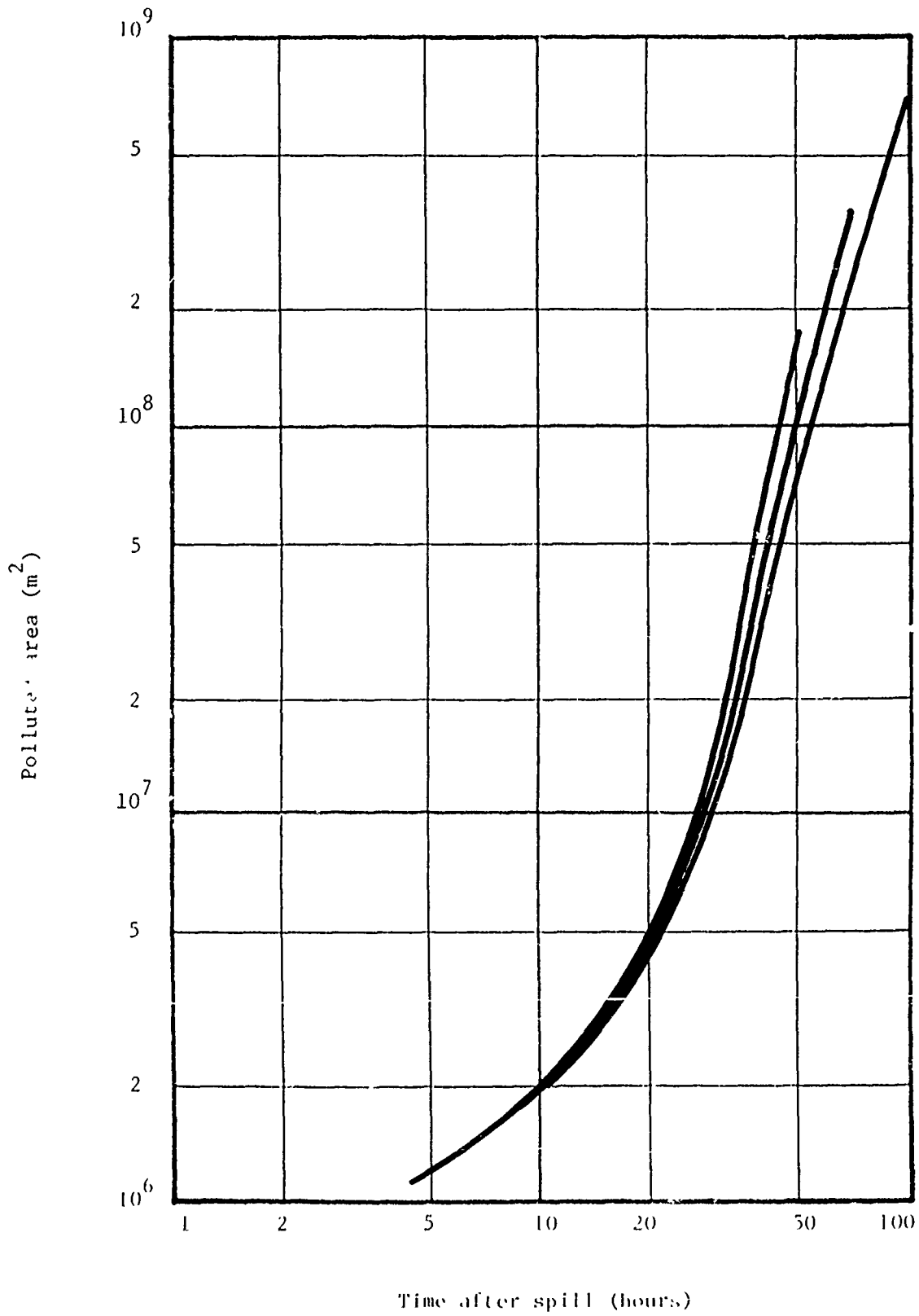


Figure 7.8

SURFACE AREA OF FUEL OIL #6 OIL SLICK AS A FUNCTION OF TIME AFTER SPILL

REFERENCES

1. Blokker, P. C., "Spreading and Evaporation of Petroleum Products on Water," 4th International Harbor Conference, Antwerp, 1964, p. 911.
2. Bowden, K. F., "Turbulence," The Sea, Volume 1, ed. by M. N. Hill, Interscience Publishers, New York, 1962.
3. Csanady, G. T., Turbulent Diffusion in the Environment, D. Reidel Publishing Company, Dordrecht, Holland, 1973.
4. Donelan, M. A., M. S. Longuet-Higgins and J. S. Turner, "Periodicity in Whitecaps," Nature, Volume 239, 1972, pp. 449-450.
5. Duncan, J. H., "The Dynamics of Breaking Surface Waves," Journal of Fluid Mechanics, 1979.
6. Fay, J. A., "Physical Processes in the Spread of Oil on Water Surface," Prevention and Control of Oil Spills, American Petroleum Institute, Washington, D. C., 1970, pp. 463-467
7. Forrester, W. P., "Distribution of Suspended Oil Particles Following the Grounding of the Tanker ARROW," Journal of Marine Research, Volume 29, 1971, p.151.
8. Hoult, D. P. and W. Suchon, "The Spread of Oil in a Channel," Stop Oil Pollution, Report 2, MIT, Department of Mechanical Engineering, Cambridge, Massachusetts, 1970.
9. Hoult, D. P., "Oil Spreading on the Sea," Annual Review of Fluid Mechanics, pp. 341-368, 1972.
10. Ichiye, T., "Upper Ocean Boundary Layer Flow Determined by Dye Diffusion," Physics of Fluids, Supplement, s270, 1967.
11. Leibovich, S., "A Natural Limit to the Containment and Removal of Oil Spills at Sea," Ocean Engineering, Volume 99, 1976, p. 809.
12. Levich, V. G., Physicochemical Hydrodynamics, Prentice-Hall, Englewood Cliffs, New Jersey, 1962.
13. Lin, J. T. Mohamed Gad-el-Hak, Hsien-Ta Liu, A Study to Conduct Experiments Concerning Turbulent Dispersion of Oil Slicks, Flow Research Company, Kent, Washington, April, 1978.
14. McIntyre, W. et al., "Investigation of Surface Films--Chesapeake Bay Entrance," report EPA - 67012-73-099, Office of R&D, USEPA, Washington, D.C., 1974.

15. McKay, D. and R. S. Matsugu, "Evaporation Rates of Liquid Hydrocarbon Spills on Land and Water," Canadian Journal of Chemical Engineering, Volume 51, 1973, p. 434.
16. Milgram, J. H., R. G. Donnelly, R. J. Van Houten & J. M. Camperman, "Effects of Oil Slick Properties on the Dispersion of Floating Oil into the Sea," report CG-D-64-78, U. S. Coast Guard, Washington, D. C., 1978.
17. Milgram, J. H., and R. J. Van Houten, "Hydrodynamics of the Containment of Oil Slicks," 10th Symposium on Naval Hydrodynamics, MIT, Cambridge, Massachusetts, June 1974.
18. Okubo, A., "Oceanic Diffusion Diagrams," Deep Sea Research, Volume 18, p. 789-802, 1971
19. Schlichting, H., Boundary Layer Theory, McGraw-Hill, New York, 1979.
20. Shuleikin, V. V., Soviet Research on the Theory of Wind Driven Waves," Atmospheric and Oceanic Physics, Volume 3, No. 11, pp.1137-1157, 1967.
21. Shonting, D., "Observations of Reynolds Stresses on Wind Waves," Journal of Pure and Applied Geophysics, Volume 81, Number 4, 1970, pp. 202-210.
22. Shonting, D., Report to the U. S. Coast Guard on the Measurements of Ocean Turbulence Off Gould Island (RI) - 1979, (Under Preparation).
23. Smith, F. B. and J. S. Hay, "The Expansion of Clusters of Particles in the Atmosphere," Quarterly Journal of the Royal Meteorological Society, Volume 87, 1961, pp. 82-101.
24. Van Dorn, W. G., Oceanography and Seamanship, Dodd, Mead & Company, New York, 1974.
25. Wiegel, R. L., Oceanographical Engineering, Prentice-Hall, Englewood Cliffs, New Jersey, 1964.
26. Wu, J. "Oceanic Whitecaps and Sea State," Journal of Physical Oceanography, Volume 9, pp. 1064-1068, 1979.

NOMENCLATURE

<u>Symbol</u>	<u>Definition</u>	<u>Equation No.</u>	<u>Units</u>
a	Ratio of r.m.s. turbulent velocity to mean current speed	A.1	
A	Area of the oil slick at time t	3.1	m ²
A*	Liuerson Moskowitz spectrum parameter		
A _o	Area of floating oil	6.15	m ²
A _s	Total surface area contaminated by oil	6.14	m ²
b	Wake thickness	5.3	m
B	Coefficient for turbulent dispersion	6.13	
C _d	Drag coefficient		
d	Droplet diameter	4.1	m
d _m	Maximum droplet diameter	4.4	m
d _{max}	Maximum droplet diameter	4.12	m
d _o	Minimum droplet diameter	6.13	m
d _s	Distance to shore	6.13	m
erfc	Complementary error function		
g	Acceleration due to gravity	3.3	m/sec ²
g(d)	Number density distribution of entrained oil vs. droplet diameter	5.16	
G	Effective acceleration	3.3	m/sec ²

<u>Symbol</u>	<u>Definition</u>	<u>Equation No.</u>	<u>Units</u>
h	Slick thickness	3.30	m
$H_{1/3}$	Significant wave height	4.16	m
i^2	Turbulent intensity	6.6	m^2/sec^2
I	Integral of the complementary error function	5.14	sec
k	Evaporation flux	3.1	kg/m^2sec
k_0	Evaporation constant	3.2	s^2/m^2
K^*	Wave steepness parameters	5.10	
K_t	Diffusion coefficient	5.12	m^2/sec
L	Length scale of largest eddies	6.13	m
M	Rate of loss of wave momentum flux	5.1	kg/sec^2
N	Frequency of occurrence of breaking waves within the slick	5.10	sec^{-1}
p^*	Turbulence pressure fluctuations	4.1	N/m^2
p	Vapor pressure of oil	3.2	N/m^2
Pr^*	Probability of wave breaking	5.10	
PDF	Probability density function	5.11	
r_o	Slick radius when thickness reaches 5 mm	6.7	m
$r(t)$	Slick radius at time t	B.4	m

<u>Symbol</u>	<u>Definition</u>	<u>Equation No.</u>	<u>Units</u>
R	ρ / ρ_0	3.6	
R_d	Reynolds number of droplet	5.8	
R(t)	Lagrangian autocorrelation function	6.2	
t	Time since spill	3.1	sec
t_c	Lagrangian time scale	5.7	sec
t_g	Time at which slicklet formation begins, i.e., end of gravity spreading regime	6.4	sec
t_G	Time at which slicklet distribution approaches a Gaussian distribution	6.13	sec
t_1	Thickness of the turbulent bore	4.9	m
t_5	Time at thickness = 5mm		sec
T	Characteristic time		sec
T_1	Observed wave period	5.10	sec
T_s	Slick temperature	3.12	$^{\circ}\text{C}$
$\overline{u'^2}$	Mean square velocity fluctuation of turbulence	4.2	m^2/s^2
U	Surface wind velocity	3.2	m/s
U_c	Current speed		m/sec
v(t)	Fluctuating Lagrangian velocity of a particle relative to the center of gravity of the slick at time t	6.4	m/sec

<u>Symbol</u>	<u>Definition</u>	<u>Equation No.</u>	<u>Units</u>
$v^2(t_0)$	Initial slick averaged velocity covariance	6.9	m^2/sec^2
V	Volume of the oil remaining in the slick	3.1	m^3
\bar{V}	Nondimensional volume		
\dot{v}	Entrainment rate	5.13	
v_d	r.m.s. velocity difference	4.10	m/sec
V_d	Dispersed oil volume	5.14	m^3
$V_d(d)$	Volume entrained as a function of diameter	5.15	m^3
V_0	Initial volume of the spill	3.4	m^3
V_1	Residual volume at the end of gravity-viscous region	3.8	m^3
W	Terminal velocity	5.8	m/s
We	Weber number	4.6	
We_η	Microscale Weber number	4.7	
z_0	Maximum depth of dispersion	5.5	m

GREEK LETTERS

Δ	ρ_o / ρ_w ; specific gravity of oil	3.16	
λ	Wave length		m
ν_o	Kinematic viscosity of oil	4.18	m^2/s
ν_{eff}	Effective kinematic viscosity	4.18	m^2/s

<u>Symbol</u>	<u>Definition</u>	<u>Equation No.</u>	<u>Units</u>
ν_w	Kinematic viscosity of water	3.19	m^2/s
ρ	Average density of the oil		kg/m^3
ρ_{max}	Density of the heaviest component in the oil	3.23	kg/m^3
ρ_0	Initial average density of the oil	3.16	kg/m^3
ρ_w	Density of water	3.16	kg/m^3
σ	Surface tension of oil	3.20	N/m
σ	Standard deviation of surface oil distribution at time when gravity spreading regime ends	6.12c	m
σ_g	Standard deviation of surface oil distribution at time when gravity spreading regime ends	6.12d	m
σ_1	Standard deviation of surface oil distribution at time when gravity spreading regime ends	6.12d	m
τ	Nondimensional time		
τ_c	nondimensional time limit for evaporation model	3.15	
τ_0	Nondimensional time for transition from gravity-inertia to gravity-viscous region	3.19	
τ_{max}	Nondimensional time to attain maximum density	3.14	
τ_1	Nondimensional time for transition from gravity-viscous to viscous-surface-tension region	3.20	
ω	Wave frequency	4.15	s^{-1}

APPENDIX A

RELATIONSHIP BETWEEN VARIOUS SEA STATE PARAMETERS AND CALCULATION OF OCEAN TURBULENCE

A.1 RELATIONSHIP BETWEEN VARIOUS SEA STATE PARAMETERS

In this appendix, we derive several sea state parameters from a spectral correlation for a fully developed sea. In deriving these parameters, we use the Pierson-Moskowitz spectral representation. The average energy per unit nominal surface area of the sea is given by (see Raj, 1977 for details):

$$E'' = \frac{1}{2} \rho_w g \int_0^{\infty} e(\omega) d\omega \quad (\text{A.1})$$

where $e(\omega)$ is the spectral energy density (m^2s) at frequency ω . The Pierson-Moskowitz spectra for $e(\omega)$ has the form:

$$e(\omega) = \frac{\alpha g^2}{\omega^5} \exp\left(-\beta (g/\omega u)^4\right) \quad (\text{A.2})$$

The commonly accepted values for the constants are:

$$\begin{aligned} \alpha &= 1.62 \times 10^{-2} \\ \beta &= 0.74 \end{aligned}$$

The amplitude of the water particle velocity is given by:

$$\overline{u^2} = \overline{\alpha^2 \omega^2} = \int_0^{\infty} \omega^2 e(\omega) d\omega \quad (\text{A.3})$$

Substituting for $e(\omega)$ from Equation (A.2) leads to:

$$\overline{u^2} = \frac{\pi^{1/2}}{4} \frac{\alpha}{\beta^{1/2}} u^2 \quad (\text{A.4})$$

For a Raleigh distribution of particle velocity amplitudes, we have:

$$u_s^2 = 2 \overline{u^2} \quad (\text{A.5})$$

This gives us:

$$u_s = \left(\frac{\pi \alpha^2}{4 \beta} \right)^{1/4} u \quad (\text{A.6})$$

If the heights of waves are Raleigh distributed, then it can be shown that

the significant wave height is related to the mean square amplitude by:

$$H_{1/3} = \left(\frac{2\alpha}{\beta} \right)^{1/2} \frac{U^2}{g} \quad (\text{A.7})$$

From Equations (A.4) and A.7), it can be shown that:

$$\overline{u^2} = \left(\frac{\alpha \pi}{32} \right)^{1/2} g H \quad (\text{A.8})$$

The modal frequency ω_0 , is that frequency at which the energy density is maximum. This is given by:

$$\omega_0 = \left(\frac{4}{5} \beta \right)^{1/4} g/U \quad (\text{A.9})$$

A.2 CALCULATION OF OCEAN TURBULENCE PARAMETERS FOR A SPECIFIED SEA STATE*

A definition sketch for the air and water boundary layers in a wind-waves flow field is drawn in Figure A.1. The air boundary layer is characterized by a thickness δ_a , and the water boundary layer by a thickness δ_w . The fetch x is measured from the beginning of the test-section in a laboratory wind-wave tank or is defined as the offshore distance in the field. The vertical coordinate z is positive upwards, and is measured from the undisturbed water surface. The dominant wavelength and height are denoted by λ and $H_{1/3}$, respectively. The free stream velocity in the laboratory or the reference velocity at 10 meters in the field are denoted by U_∞ . Fully developed sea state is assumed in the following computations.

For a turbulent air boundary layer over wind-waves, the growth of the air boundary layer thickness δ_a , and the air friction velocity** u_{*a} are correlated with the free stream velocity U_∞ and the fetch x as follows:

$$\frac{g \delta_a}{U_\infty^2} = 0.025 \left(\frac{gx}{U_\infty^2} \right)^{4/5} \quad \text{for } 0.2 < \frac{gx}{U_\infty^2} < 17 \quad (\text{A.10})$$

$$\frac{u_{*a}}{U_\infty} = 0.055 \left(\frac{gx}{U_\infty^2} \right)^{-1/10} \quad \text{for } 0.3 < \frac{gx}{U_\infty^2} < 200 \quad (\text{A.11})$$

* This work was performed by Flow Research Company, a subcontractor to Arthur D. Little, under the present USCG contract.

** Related to the surface skin friction coefficient by $C_f \equiv 2 \left(\frac{u_{*a}}{U_\infty} \right)^2$

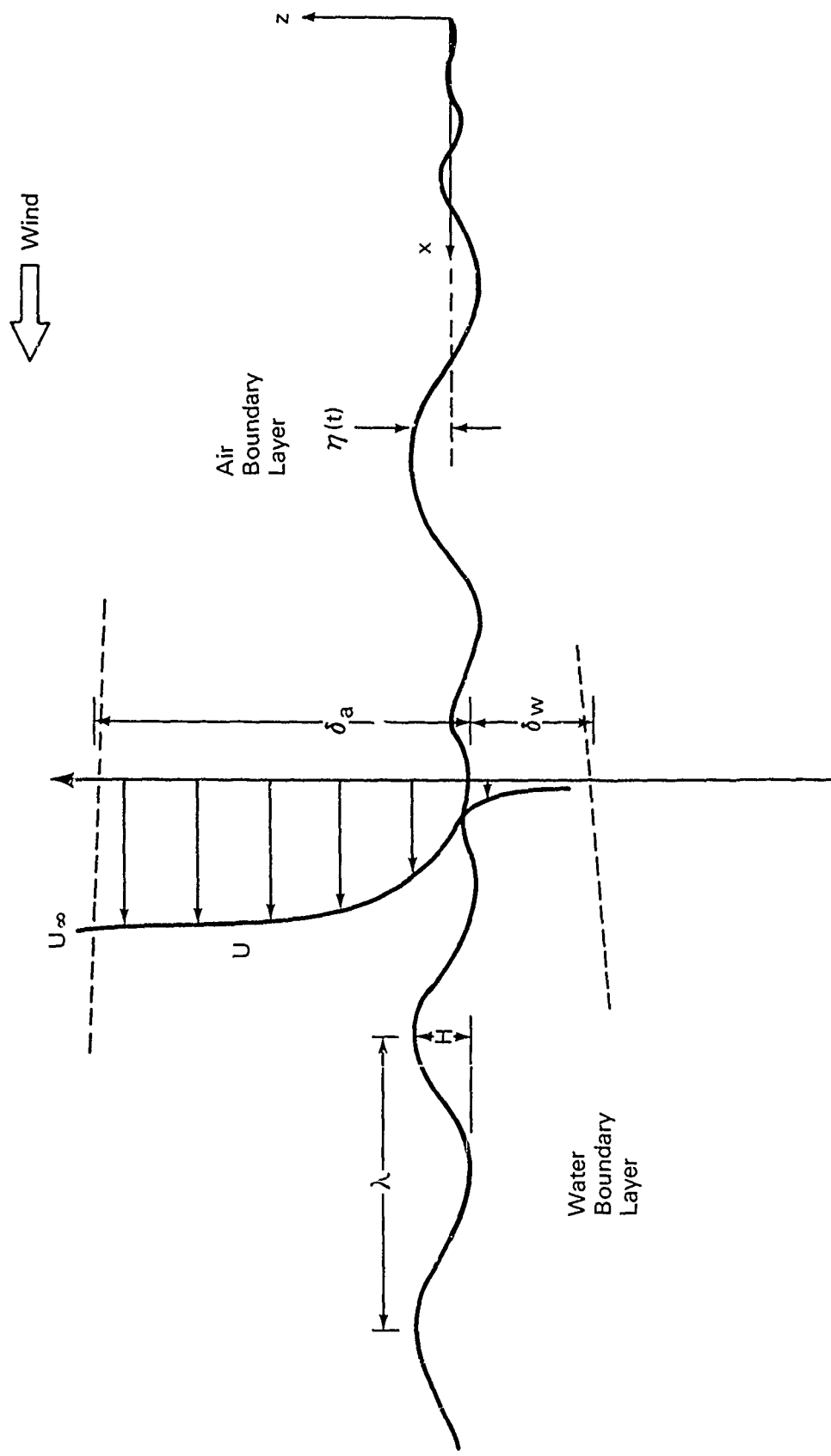


Figure A.1 Definition for Wind-Wave Field

$$\frac{u_*}{U_\infty} = 0.03 \quad \text{for } 200 < \frac{gx}{U_\infty^2} < 6 \times 10^4 \quad (\text{A.12})$$

where g is the gravitational acceleration.

The air velocity profile is approximately logarithmic and is given by:

$$\frac{\bar{U}(z)}{u_*} = 5.75 \log \frac{z}{z_0} \quad (\text{A.13})$$

where z_0 is the aerodynamic roughness. Hence, for a given free stream velocity U_∞ and fetch x , one could compute the air boundary layer thickness δ_a using Equation (A.10), and the air friction velocity u_* using Equation (A.11) or Equation (A.12). Equation (A.13) could then be used to compute z_0 by the relation:

$$\bar{U} \text{ (at 10 m)} \equiv U \quad (\text{A.14})$$

The root-mean-square of the water-surface-displacement η_{rms} , and the dominant wavelength λ are correlated with the free stream velocity U_∞ and the fetch x as follows:

$$\frac{g\eta_{rms}}{U_\infty^2} = 0.001 \left(\frac{gx}{U_\infty^2} \right)^{2/5} \quad \text{for } 0.3 < \frac{gx}{U_\infty^2} < 17 \quad (\text{A.15})$$

$$\frac{g\eta_{rms}}{U_\infty^2} = \left(6.9 \times 10^{-5} + 2.97 \times 10^{-7} \left(\frac{gx}{U_\infty^2} - 200 \right)^{1/2} \right) \quad \text{for } 200 < \frac{gx}{U_\infty^2} < 6 \times 10^4 \quad (\text{A.16})$$

$$\frac{g\lambda}{U_\infty^2} = 0.03 \left(\frac{gx}{U_\infty^2} \right)^{2/5} \quad \text{for } 0.3 < \frac{gx}{U_\infty^2} < 17 \quad (\text{A.17})$$

The significant wave height $H_{1/3}$ and the dominant phase speed for the wind-waves C_p are related to the rms displacement η_{rms} by:

$$H_{1/3} = 4\eta_{rms} \quad (\text{A.18})$$

$$C_p = 2.24 (g\eta_{rms})^{1/2} \quad (\text{A.19})$$

For a given free stream velocity U and fetch x , one could compute the root-mean-square of the water-surface displacement η_{rms} using Equation (A.15) or Equation (A.16), the dominant wavelength λ using Equation (A.17),

the significant wave height $H_{1/3}$ using Equation (A.18), and the dominant phase speed C_p using Equation (A.19). The significant wave height $H_{1/3}$ could be used as an input parameter in place of the fetch x , if desired. Equations (A.15) through (A.17) are consistent with field data compiled by Wiegel (1964).

The frequency spectrum of the water surface displacement (wave energy spectrum) follows the function:

$$S(f) = \alpha^2 g^2 f^{-5} \quad (\text{A.20})$$

from the dominant frequency to a frequency cut-off of about 10 Hz, where capillary waves become important. The constant α is in the order of 10^{-4} in typical laboratory tanks and 10^{-5} in the ocean. In the capillary wave regime the wave energy spectrum follows the function:

$$S(f) = \beta \gamma^{2/3} f^{-7/3} \quad (\text{A.21})$$

for f greater than 7.5 Hz. The constant β is the order of 10^{-2} in typical laboratory tanks. No information is available for the value of the constant β in the ocean.

The momentum transferred from the air boundary layer to the water is manifested as water waves and a drift layer in the water. About 90 percent of the air boundary layer momentum is transferred to the water boundary layer.* The equation

$$(\rho u_*^2)_{\text{water}} = 0.90 (\rho u_*^2)_{\text{air}} \quad (\text{A.22})$$

can be used to compute the water friction velocity u_{*w} . The surface drift velocity U_s is computed from

$$\frac{U_s}{U} = 0.032 \quad (\text{A.23})$$

or

$$\frac{U_s}{U} = 0.02 + \left\{ \left(\frac{\pi H_{1/3}}{\lambda} \right)^2 + 0.445 \frac{H_{1/3}}{\lambda} \right\} \frac{C_p}{U} \quad (\text{A.24})$$

where $H_{1/3}$ is the significant wave height, λ is the dominant wave length, and C_p is the dominant phase speed.

*Equivalently, the ratio of the wave drag coefficient to the wind drag coefficient is 0.1.

The water boundary layer thickness δ_w is correlated with the free air stream velocity U_∞ and the fetch x as follows:

$$\frac{g \delta_w}{U_\infty^2} = 0.025 \left(\frac{gx}{U_\infty^2} \right)^{4/5} \quad (\text{A.25})$$

The mean velocity profile in the water boundary layer is approximately logarithmic and is given by:

$$\frac{U_s - \bar{U}(z)}{u_{*w}} = 5.75 \log \left(\frac{-z}{z_0} \right) \quad (\text{A.26})$$

where u_{*w} is the water friction velocity which could be computed from Equation (A.21), and U_s is the surface drift velocity which could be computed from Equation (A.22) or Equation (A.23). The roughness height in the water boundary layer is usually smaller than the corresponding one in the air boundary layer, but could be considered the same for an order of magnitude estimate. The mean velocity defect shows that the water boundary layer under the water surface resembles the turbulent air boundary layer over the water surface, and the water boundary layer is produced as the result of the wind stress exerted on the water surface. Both air and water boundary layers resemble a turbulent boundary layer over a rough flat plate. For example, under weak sea states without wave breaking, the maximum root-mean-square of the longitudinal velocity fluctuations* is about two to three times the friction velocity and about 15-20 percent of the free stream velocity U_∞ in air or the mean surface drift velocity U_s in water. The maximum rms values occur near the water surface and monotonically decrease away from it. The rms of the vertical velocity fluctuations is about half the rms of the longitudinal velocity fluctuations. The dimensionless dissipation rate is, as expected on the order of one, and the Reynolds stress coefficient is typically 0.3.

*Contains in part the contribution from orbital motion of the waves.

In high sea states with intensive wave breaking (H/L on the order of 0.1), the maximum rms value of the longitudinal velocity fluctuations is as high as 60 percent of the mean surface drift velocity, and the rms value of the vertical velocity fluctuations. The (dimensional) dissipation rate is one to two orders of magnitude higher than in non-breaking waves.

In short, data on ocean turbulence parameters (especially close to the ocean surface) are scarce, and one has to use similar flow fields for an order of magnitude estimate. The information summarized in this report provides a few rules of thumb for obtaining such estimates. For accurate predictions of ocean turbulence parameters from laboratory measurements, systematic investigations will be required to establish appropriate scaling laws. These scaling laws should be validated with ocean data obtained from future field experiments.

APPENDIX B
DEVELOPMENT OF A MULTI-COMPONENT
OIL SLICK EVAPORATION MODEL

Here, we have developed a multi-component oil slick model which considers the combined effects of evaporation and spreading. The extent of spread is determined by the expressions given by Fay (1971). The resulting equations are coupled and nonlinear, and are solved using a digital computer.

B.1. FORMULATION OF THE MULTI-COMPONENT OIL SLICK MODEL

In formulating the mass transfer due to evaporation from a floating oil slick, we have made three assumptions:

- The slick is homogeneous in horizontal and vertical directions and is of uniform thickness.

- The evaporation flux of the individual components is given by the empirical relationship:

$$k_i = k_0 U p_i \quad (\text{B.1})$$

where k_0 is an empirical constant (s^2/m^2)

k_i = evaporation flux ($\text{kg}/\text{m}^2\text{s}$)

U = wind speed

p_i = partial pressure of i^{th} component (N/m^2)

- The slick is radially symmetric.

If $C_i(t)$ is the time varying mass concentration of the i^{th} component per unit volume (kg/m^3), then the conservation of mass leads to:

$$\frac{d}{dt} \left(C_i(t)V(t) \right) = -k_i A(t) \quad (\text{B.2})$$

$i = 1, 2, \dots, N$

Where A and V are the surface area and the remaining volume of the slick, respectively. If ρ_i is the density of an individual component, then the volumetric relationship leads to the following constraint on $C_i(t)$:

$$\sum_{i=1}^N C_i(t) / \rho_i = 1 \quad (\text{B.3})$$

Substituting $A = \pi r^2$ and $V = \pi r^2 h$ in Equation (B.2), dividing by ρ_i and summing over N components leads to:

$$r^2 h \sum_{i=1}^N \frac{1}{\rho_i} \frac{dC_i}{dt} + \frac{d}{dt} (r^2 h) \sum_{i=1}^N \frac{C_i}{\rho_i} = -r^2 \sum_{i=1}^N \frac{k_i}{\rho_i} \quad (\text{B.4})$$

Differentiating Equation (B.3) with respect to t leads to:

$$\sum_{i=1}^N \frac{1}{\rho_i} \frac{dC_i}{dt} = 0 \quad (\text{B.5})$$

Substituting Equations (B.3) and (B.5) into Equation (B.4) leads to an expression for the rate of change of volume:

$$\frac{d}{dt} (r^2 h) = - \sum_{i=1}^N \frac{k_i}{\rho_i} r^2 \quad (\text{B.6})$$

Substituting Equation (B.6) into Equation (B.2) leads to

$$\frac{dC_i}{dt} = \frac{C_i}{h(t)} \sum_{j=1}^N \frac{k_j}{\rho_j} - \frac{k_i}{h(t)} \quad (\text{B.7})$$

In Equation (B.7), the first term on the right-hand side represents the increase in the concentration of a component due to reduction in volume, and the second term indicates the decrease in the concentration of the component due to evaporation. Equation (B.7) shows that the concentration of a particular component may either increase or decrease depending on which one of the two phenomena dominates. The concentration of the lighter components decreases with time because of their higher vapor pressure, and the concentration of heavier hydrocarbons increases with time. The average density of the oil at any given time is:

$$\rho_{\text{ave}} = \sum_{i=1}^N C_i(t) \quad (\text{B.8})$$

The partial pressure of a component is related to the vapor pressure of the component and the molar concentration. If we assume that the mixture of the vapors behave like an ideal mixture of gases, then this relationship is given by Henry's Law, which is:

$$P_i = \frac{C_i / M_i}{\sum_{j=1}^N C_j / M_j} P_i(T_i) \quad (B.9)$$

Where M_i is the molecular weight of the i^{th} component and P_i is the vapor pressure at the saturation temperature T . Given a distillation curve for the oil or a breakdown by boiling point classifications, the value of the vapor pressure P_i can be found easily. From the average boiling point of a fraction, the average vapor pressure may be determined using the integrated form of the Clausius-Clapeyron equation. This leads to:

$$\log (P_i / P_o) = \frac{-qM_i}{4.57} \left(\frac{1}{T_s^*} - \frac{1}{T_i} \right) \quad (B.10)$$

Where P_o is the vapor pressure at the boiling point, (usually atmospheric pressure) T_s^* is the slick temperature in $^{\circ}\text{K}$ and q is the heat of evaporation. The quantity $(qM_i/4.57T_i)$ is nearly constant (5 ± 0.2) for hydrocarbons, and we can simplify Equation (B.10) to:

$$\log (P_i / P_o) = -5 \left(\frac{T_i - T_s^*}{T_s^*} \right) \quad (B.11)$$

The radius of the slick is calculated using Fay's (1971) expressions. In essence, the spreading is broken down artificially into three stages, i.e., gravity-inertia, gravity-viscous and the surface tension regions. The expressions for the radius of the slick in these regions are:

- Gravity-Inertia region:

$$0 < t < t_0$$

$$t_0 = 0.564 \left(v_o / g(1 - \rho_o / \rho_w) \right)^{1/3} \quad (B.12)$$

$$r = 1.14 \left(g(1 - \rho_o / \rho_w) v_o \right)^{1/4} t^{1/2} \quad (B.13)$$

Gravity-Viscous region:

$$t_0 < t < t_1$$

$$t_1 = 0.375 \frac{\rho_w}{\sigma} \left[g^2 (1 - \rho_o / \rho_w)^2 v^4 / \nu_w^2 \right]^{1/6} \quad (\text{B.14})$$

$$r = 0.98 \left(g^2 (1 - \rho_o / \rho_w)^2 v^4 / \nu_w \right)^{1/12} t^{1/4} \quad (\text{B.15})$$

Viscous-surface-tension region:

$$t > t_1$$

$$r = 1.6 \left(\sigma / \nu_w^{1/2} \rho_w^{3/2} \right)^{1/2} t^{3/4} \quad (\text{B.16})$$

The thickness of the slick is given by:

$$h = \frac{V(t)}{A(t)} = V(t) / \pi r^2(t) \quad (\text{B.17})$$

Milgram et al., (1978) contend that the spread law in the viscous regime discussed by Fay (1971) is theoretically not valid. Their reasoning is two-fold. First, Fay's model assumes that the water boundary layer is laminar. In actuality, the Reynold's number based on the mean interfacial velocity and slick radius is very large and the boundary layer is likely to be turbulent. Second, for the gravity-viscous region to be favored over surface-tension region, the ratio of surface tension forces to gravitational forces must be much smaller than unity. Milgram et al., (1978) have demonstrated, using an order of magnitude estimate, that this ratio is larger than unity. The gravity-viscous region should include the spread due to surface-tension effects as well. This would yield a faster rate for the spreading of the slick than the rate predicted using Fay's model. The inclusion of turbulent boundary layer effects do not change the spread law significantly. There are no simpler expressions which consider the combined gravity-surface tension effects. We have used Fay's (1971) expressions for spreading of the slick.

Substitution of the appropriate spread law with the evaporation flux, given by Equation (B.1) in Equations (B.6) and (B.7), leads to a set of nonlinear coupled equations to determine the remaining volume and the concentration of the individual components in the slick. These equations were solved numerically with the aid of a digital computer.

B.2: SOLUTION OF THE MULTI-COMPONENT OIL SLICK MODEL

The resulting nonlinear equations were solved numerically using a fourth order Ringe-Kutta technique. Figure B.1 shows the flow diagram of the computer program. The input to the program is :

- Initial volume of the spill,
- Wind speed and slick temperature, and
- Number of components and the following properties of each one of the components:
 - (1) Density,
 - (2) Initial concentration,
 - (3) Vapor pressure (or boiling temperature), and
 - (4) Molecular weight.

For simplicity, we assumed that there was no evaporation in the gravity-inertia region. The remaining volume of oil, area and thickness of the slick and the concentration of individual components as a function of time were computed in the gravity-viscous and the surface-tension region. The program was automatically terminated when the slick thickness was equal to 3 mm. The computations were performed over a range of parameters. The initial volume was varied from 100m^3 to $10,000\text{m}^3$. The wind velocity was varied from 5 m/s to 25 m/s and the slick temperature was varied from 10 C to 25°C. The specific outputs sought from this model were the variation of the average density and the vapor pressure with time. These are discussed in the next section. The various oils are given in Table B.1.

B.3. DISCUSSION OF RESULTS

To obtain the variation of the average density of the oil remaining in the slick with time, we nondimensionalized the density and the time by:

$$R = \rho / \rho_0 \quad (\text{B.18})$$

$$\tau = t/T \quad (\text{B.19})$$

Figure B.2 plots the variation of R with the nondimensional time difference $(\tau - \tau_0)$ for various initial volumes for light crude oil. A least-squares fit to the data points indicated in Figure B.2 leads to the following functional relationship for the variation of R.:

$$R = 1 + 1.43 \times 10^{-4} (\tau - \tau_0)^{0.62} \quad (\text{B.20})$$

Similar relationships were obtained for various wind velocities and slick temperatures. The final expression for variation of R with time, slick temperature and wind velocity is:

$$R = 1 + 4.17 \times 10^{-5} T_s^{0.22} U^{0.32} (\tau - \tau_0)^{0.62} \quad (\text{B.21})$$

Figure B.3 demonstrates the variation of vapor pressure of oil as a function of nondimensional time difference $\tau - \tau_0$. A least-squares curve fit leads to an expression for the variation of the vapor pressure P:

$$P = 2929 \exp -1.95 \times 10^{-4} (\tau - \tau_0) \quad (\text{B.22})$$

The final expression for the variation of P with dimensionless time and temperature is:

$$P = 350 T_s^{0.66} \exp -9.67 \times 10^{-5} T_s^{0.22} (\tau - \tau_0) \quad (\text{B.23})$$

Similar expressions were obtained for other types of oils. These are given in Table 3.1.

TABLE B.1
COMPOSITION OF VARIOUS TYPES OF OILS

Light Crude*:

<u>Specific Gravity</u>	<u>Yield Percent by Volume (%)</u>	<u>Boiling Point Temperature (°C)</u>
.700	10.0	73.9
.786	19.2	151.4
.850	20.7	265.8
.890	15.4	376.4
.965	34.7	426.7

Heavy Crude*:

<u>Specific Gravity</u>	<u>Yield Percent by Volume (%)</u>	<u>Boiling Point Temperature (°C)</u>
.72	11.00	121.1
.83	11.35	204.4
.89	12.76	323.9
.93	24.13	454.4
1.06	40.76	648.9

Fuel Oil #2**:

<u>Specific Gravity</u>	<u>Yield Percent by Volume (%)</u>	<u>Boiling Point Temperature (°C)</u>
.80	20.00	221.1
.83	20.00	240.6
.85	20.00	260.0
.87	20.00	276.7
.89	20.00	304.4

Fuel Oil #6:

The average density of fuel oil #6 is 970 kg/m³ and the boiling point temperature is greater than 325°C. Therefore, we have assumed that there is no evaporation.

* From Oil and Gas Journal, March 29, 1976.

** From Mark's Standard Handbook for Mechanical Engineers, 7th edition, 1966

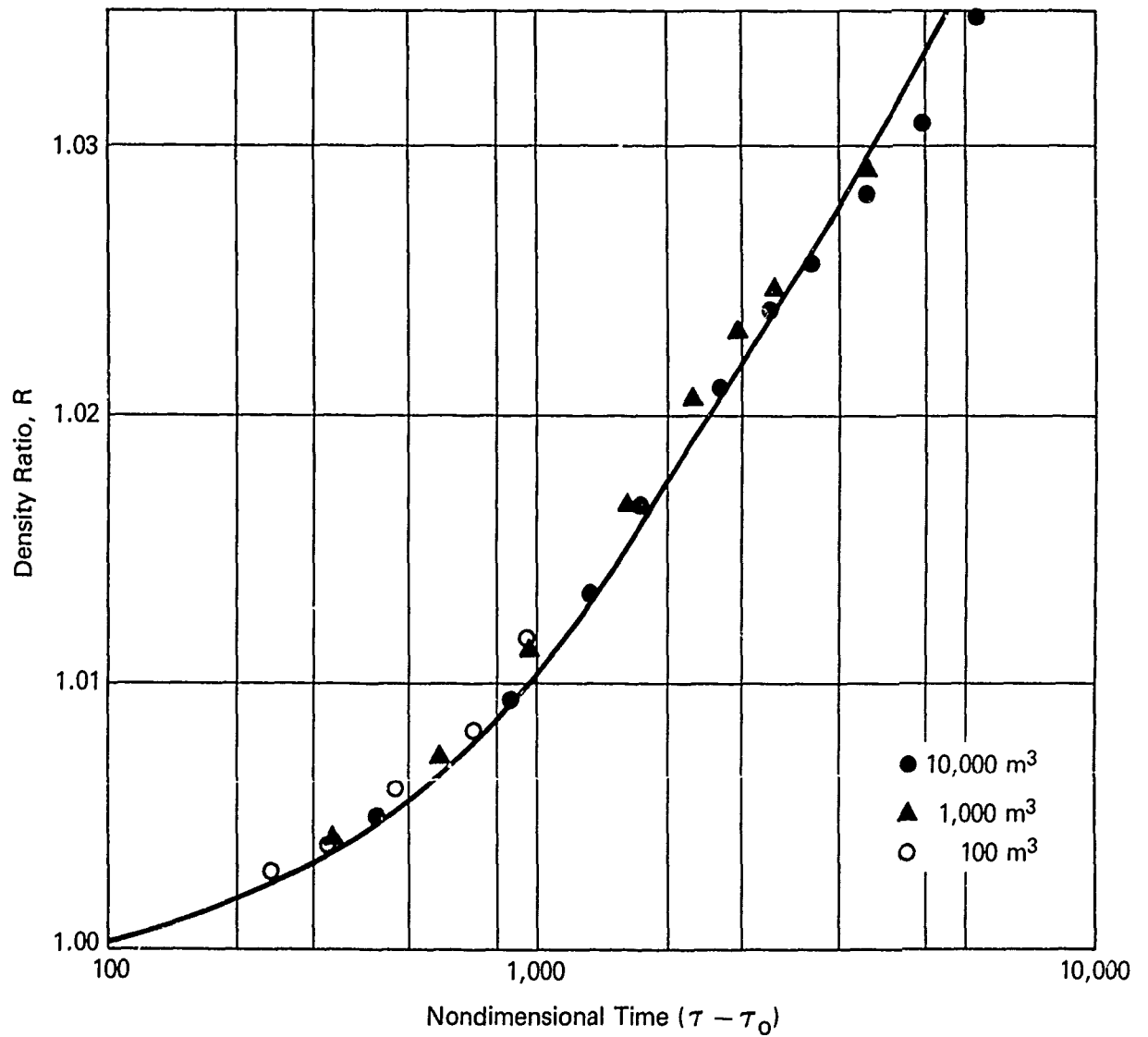


Figure B.2 Variation of the Density Ratio R of Light Crude Oil with Nondimensional Time; Slick Temperature $T_s = 25^\circ\text{C}$, Wind Velocity $U = 5 \text{ m/s}$

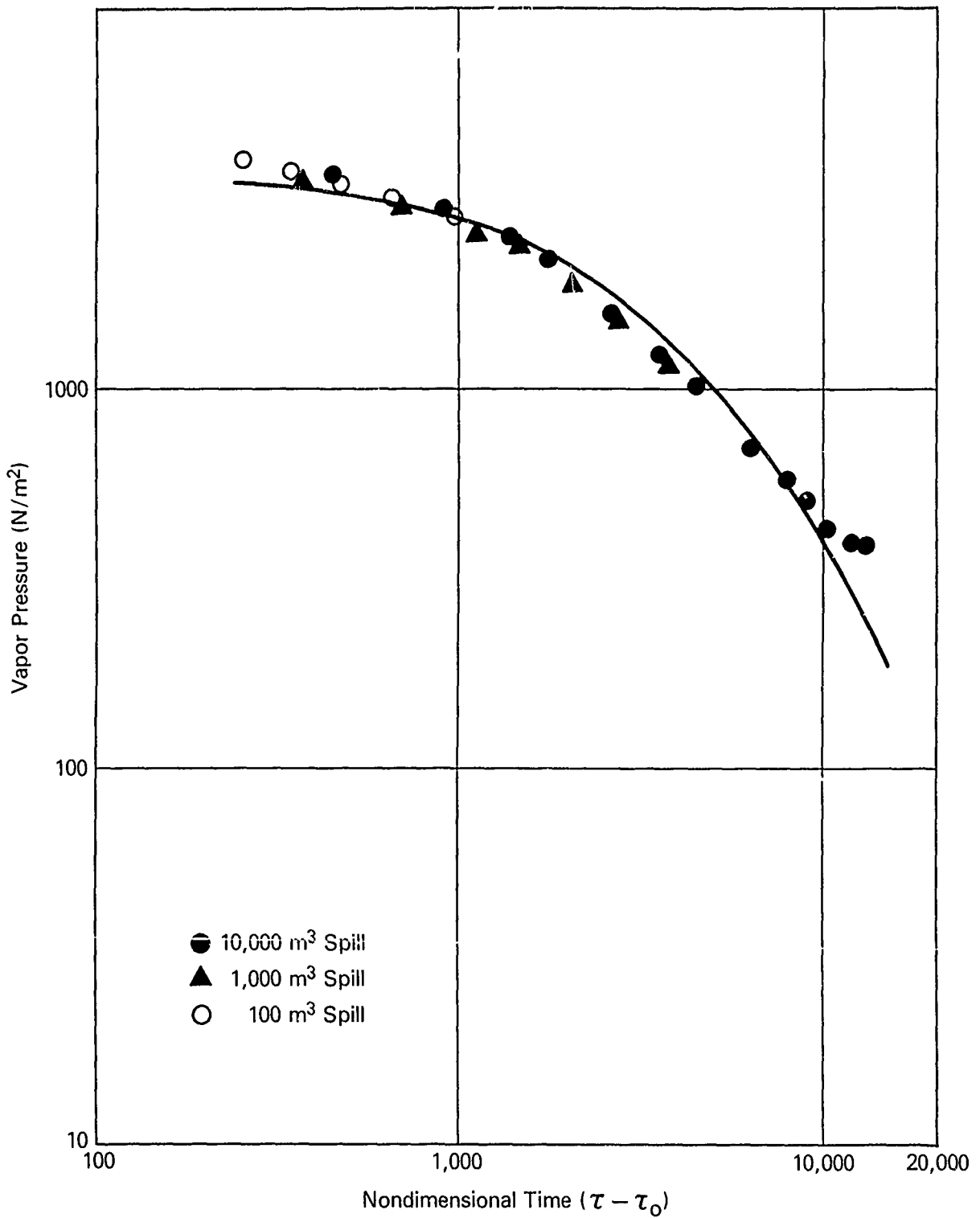


Figure B.3 Variation of the Vapor Pressure of Light Crude Oil with Nondimensional Time; Slick Temperature $T_s = 25^\circ\text{C}$, Wind Velocity $U = 5 \text{ m/s}$

APPENDIX C
THE EFFECT OF OIL VISCOSITY AND SLICK THICKNESS
ON THE DAMPING OF BREAKING WAVE TURBULENCE

The present droplet formation model is based on the assumption that the smallest droplet sizes will be determined by the energy spectrum of the turbulence generated by a breaking wave. Milgram, et. al. (1978) found that typically the smallest droplets had a length scale lying in the inertial subrange of the turbulence, in which case the droplet sizes were independent of the microscale. Since the energy dissipation rate is a function of the macro-length and time scales, the smallest droplet sizes predicted are dependent on oil slick characteristics insofar as they affect the macroscale; i.e., only as they affect the size of the breaking wave. However, in the experiments reported by Milgram, et. al. (1978) the presence of a thick oil slick was found to increase significantly the smallest droplet sizes, even for cases where the macroscale characteristics were substantially the same. Milgram, et. al. (1978) hypothesized that the existence of oil may increase the microscale of the turbulence to the point where droplet formation no longer stops within the inertial subrange, so that it may be affected by the size of the microscale.

Although the problem of a two-phase turbulent flow is extremely complex, a simple approach, which was outlined by Milgram, et. al. (1978), is to model the turbulence in a breaking wave as a single-fluid flow, but one whose viscosity is some weighted average of that of oil and that of water. For simplicity, a linear weighting may be used. The effective viscosity is then:

$$\nu_{\text{eff}} = (1 - h/t_1) \nu_w + h/t \nu_o \quad (\text{C.1})$$

where h is the thickness of the oil slick and t_1 is the thickness of the turbulent fluid which rides on the crest of a breaking wave. A good estimate for t_1 is:

$$t_1 = 0.001 \text{ g}/\omega^2 \quad (\text{C.2})$$

which is approximately 0.001 times the breaking wave height. Although the apparent thickness of a whitecap is somewhere between .01 and 0.1 times the wave height, t_1 is taken as less than this to account for the fact that the oil lies in the region of greatest shear between the forward moving bore and the rearward moving fluid beneath, so that it is extremely effective in damping the turbulence.

When the effective viscosity of the fluid is large enough for the microscale Weber number to be smaller than 10, or:

$$0.6 \frac{\sigma \omega^{1/4}}{\rho g^{1/2} \gamma_{\text{eff}}^{5/4}} \leq 10 \quad (\text{C.3})$$

the droplet splitting process will stop at the microscale (Levich, 1962), so that the smallest droplet sizes will be given by:

$$d_{\text{min}} = 0.6 \frac{\omega^{1/4} \gamma_{\text{eff}}^{3/4}}{g^{1/2}} \quad (\text{C.4})$$

The practical consequences of this model are that for small amounts of oil, the smallest droplet size is independent of oil thickness and viscosity; whereas for large amounts of oil, the smallest droplet size increases with both oil thickness and oil viscosity. These trends agree with available experimental evidence.

APPENDIX D

THE EFFECT OF WAVE DAMPING ON THE PROBABILITY OF BREAKING

Although the droplet distribution model assumes that the sea is unaffected by the existence of an oil slick, there is some evidence that this is not actually the case. Theoretically, an oil slick will cause ocean waves to be damped at a higher rate than in the absence of oil. The significant wave height within an oil slick might therefore be somewhat less than that in neighboring regions of the ocean. Since higher frequency waves are damped more strongly than lower frequency waves, the significant wave period will also be reduced. Both of these effects will tend to reduce the steepness parameter, and thereby the probability of wave breaking within an oil slick.

The difficulty in quantifying this effect is that theoretical investigations indicate that the effect is negligible; whereas field observations indicate otherwise. Often even relatively thin slicks appear to calm the sea, and reduce the number of breaking waves. However, no systematic field investigation of this effect has been carried out. In this appendix, an approach is outlined whereby experimental data on wave damping can be used to modify the droplet distribution model.

Assuming that wave damping is linear, and that the forces tending to generate waves are negligible during the time they are within an oil slick, we can take the local sea spectrum to be:

$$S(\omega, x) = S^*(\omega) e^{-\gamma(\omega, h, \nu) x} \quad (D.1)$$

$S^*(\omega)$ is the ambient spectrum and x is measured from the upwind edge. The damping constant γ can be determined experimentally. If the frequency dependence is taken to be the same as that of the theoretical damping constant in the case of clean water, γ has the form:

$$\gamma = \eta(h, \nu_0) \omega^5 \quad (D.2)$$

One can calculate the percentage of waves which break during one wave period in an oil slick as follows:

$$P_t = \frac{1}{l} \int_0^l P_b(x) dx \quad (D.3)$$

where l is the dimension of the oil slick in the direction of the wind. $P_b(x)$ represents the local probability of breaking and is given by:

$$P_b(x) = \frac{\mathcal{K}^2(x)}{\mathcal{K}^2(x) + 1} \quad (D.4)$$

where $\mathcal{K}(x)$ is the local steepness parameter:

$$\mathcal{K}(x) = \frac{1}{2.61 g} H_{1/3}(x) \omega^2(x) \quad (D.5)$$

where here the significant wave height and average frequency are spatially varying, and can be computed from the zeroth and second moments of the local spectrum, given in Equation (D.1).

Equation (D.3) can be computed numerically, or may be approximated as follows. One can linearize the probability of breaking about the ambient steepness parameter to obtain:

$$P_b(x) = \frac{\mathcal{K}^*}{\mathcal{K}^{*2} + 1} \mathcal{K}(x) \quad (D.6)$$

where the * superscript refers to the value in the absence of an oil slick. Furthermore, since the damping constant varies as the fifth power of the frequency, the second moment of the spectrum will change more than the zeroth moment; or in other words, the primary effect of the oil is to reduce the average frequency of waves, rather than to reduce their height. Therefore, one can approximate $\mathcal{K}(x)$ as:

$$\mathcal{K}(x) = \frac{6.13}{g H_{1/3}} \int_0^{\infty} \omega^2 S(\omega, x) d\omega \quad (D.7)$$

This gives an expression for the percentage of waves which break:

$$P_t = \frac{\mathcal{K}^*}{\mathcal{K}^{*2} + 1} \frac{6.13}{g H_{1/3}} \frac{1}{l} \int_0^{\infty} \omega^2 S(\omega) \int_0^l e^{-\eta \omega^5 x} d\omega dx \quad (D.8)$$

The inner integral can be evaluated, to give:

$$P_t = \frac{\mathcal{K}^*}{\mathcal{K}^{*2} + 1} \frac{6.13}{g H_{1/3}} \frac{1}{l} \int_0^{\infty} \omega^2 S(\omega) \frac{(1 - e^{-\eta \omega^5 l})}{\eta \omega^5} d\omega \quad (D.9)$$

If wave damping is large enough to suppress wave breaking in the interior of the slick, (or, mathematically, $\eta \omega^5 l \gg 1$), then:

$$P_t = \frac{\mathcal{K}^*}{\mathcal{K}^{*2} + 1} \frac{6.13}{g} \frac{H_{1/3}}{\eta l} \int_0^\infty \frac{S^*(\omega)}{\omega^3} d\omega \quad (D.10)$$

In the case of a Pierson-Moskowitz spectrum, S^* can be defined as:

$$S^*(\omega) = \frac{A}{\omega^5} e^{-B/\omega^4} \quad (D.11)$$

and one obtains:

$$P_t = 1.81 \frac{\mathcal{K}^*}{\mathcal{K}^{*2} + 1} \frac{H_{1/3}}{g l^B \eta T_1} \quad (D.12)$$

$$= \frac{\mathcal{K}^*}{\mathcal{K}^{*2} + 1} \frac{2.17}{\eta l \omega^5} \quad (D.13)$$

P_t , given by Equation (D.13), can be substituted for P_b in the droplet distribution model to incorporate the effects of wave damping. The factor in brackets in equation (D.13) represents the change in breaking probability due to the presence of oil. One must be careful in using this equation, since if $\eta l \omega^5$ is not much greater than unity, an assumption made in the derivation is violated. For these cases, the equation could predict breaking probabilities greater in the oil slick than in the surrounding sea. In these cases Equation (D.9) should be used.

The formula derived above for the probability of wave breaking in an oil slick was not used in the predictive model because of the lack of available data. Because wall boundary layers are much stronger than surface boundary layers, this data cannot readily be obtained in laboratory experiments, and must be obtained at sea. Any field investigations of oil spill behavior should include, at least, visual observations of wave damping and wave breaking within the slick, and ideally would include precise measurements of the sea spectrum both outside and inside the slick. Once data are available, the droplet distribution model can readily incorporate the effects of wave damping.

APPENDIX E

OIL SLICK SIMULATION PROGRAM

To relieve the user of having to perform the difficult and tedious calculations detailed in Sections 3 through 6, we have written an interactive BASIC program that performs these calculations more quickly, more accurately, and in more detail than is possible with a hand-held calculator.

Section E.1 contains a general discussion of the program, its structure, input and output. Section E.2 contains a listing of the program itself, the definitions of variables used in the program code, and some notes concerning the code and its installation on other systems.

E.1 PROGRAM DESCRIPTION AND FLOW CHART

A flow chart of the oil slick simulation program is given in Figures E-1 and E-2. The flow chart shows not nearly the level of detail actually contained in the program; however, it does describe the general structure of the program, and so serves as a useful guide. The simplest and probably the most effective way for us to describe the program is to follow the flow chart.

E.1.1 Overall Program Structure

The program is broken into four main sections: (1) the input section, which performs the obvious function; (2) the initialization section, which determines a variety of initial and constant values based on the input parameters; (3) the calculation section, which determines the evaporation, spreading, dispersion, and other physical characteristics on an hourly or semi-hourly basis; and, (4) the output section, which prints the results in summary or in detail according to the user's request. Each of these four main sections is composed of a number of subsections or subroutines.

FIGURE E.1
FLOW CHART OF OIL SLICK MODELLING PROGRAM

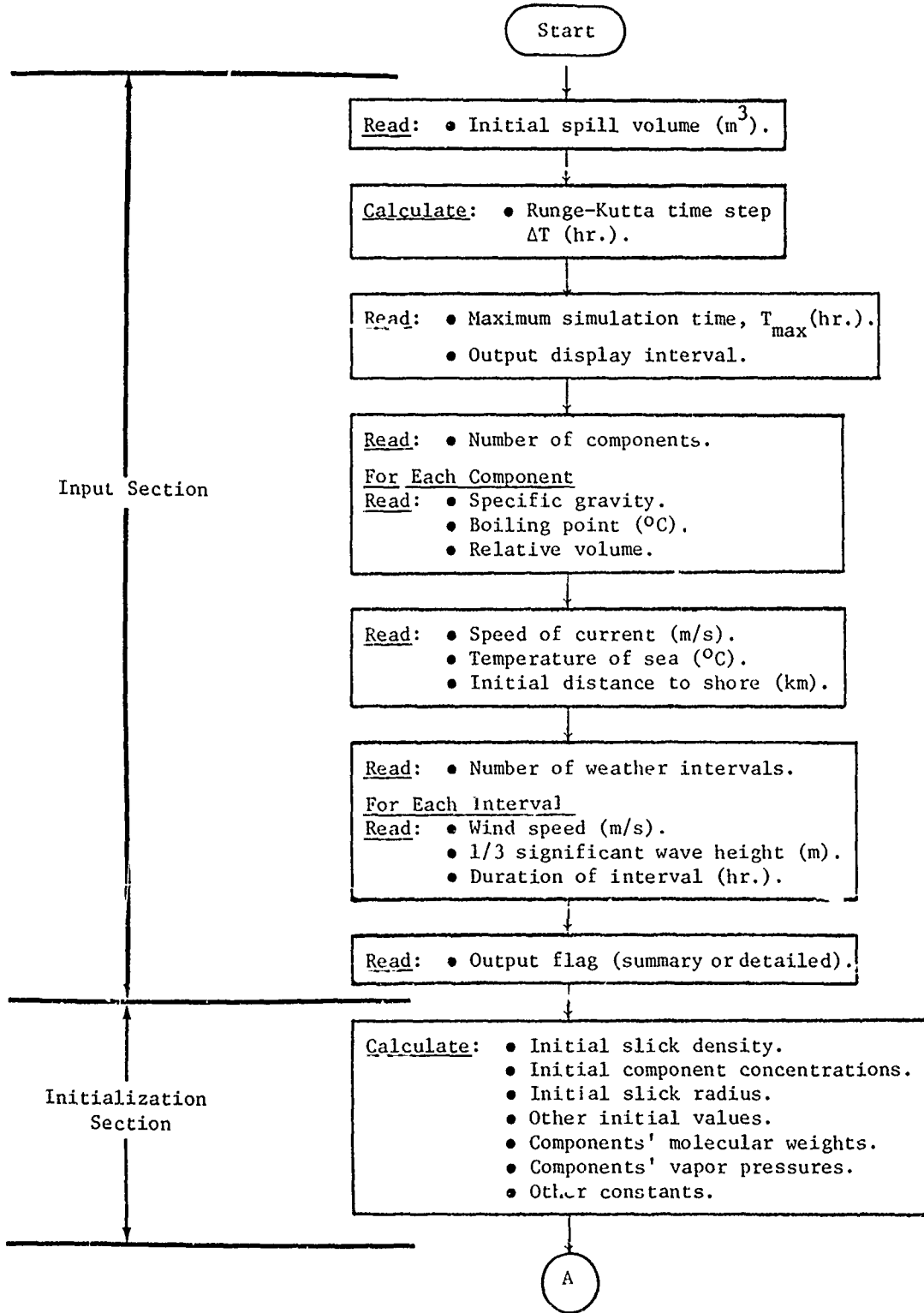
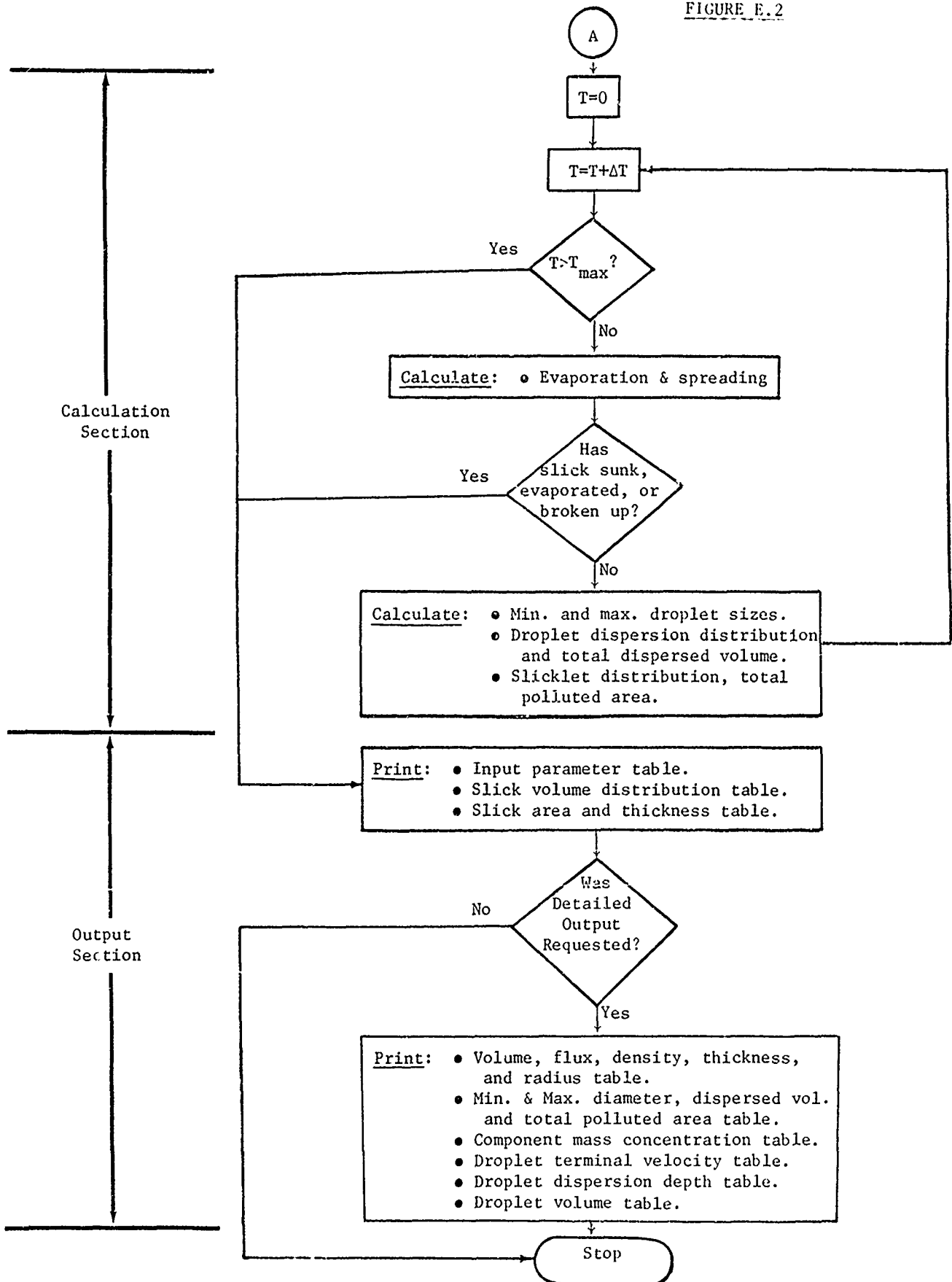


FIGURE E.2



E.1.2 Input Section

The input section of the program is fully interactive: the user is asked to supply all input necessary for the run, is told what units the input values must be in, and, when an input value is clearly incorrect, is asked to correct the error.

The required input is of two types: physical/environmental and program control. The physical/environmental input describes the physical characteristics of the oil slick (volume, specific gravity, boiling point, etc.) and the characteristics of its ocean environment (wind speed, wave height, current, etc.). The program control input determines how many iterations the program will perform and how detailed the output will be. The physical/environmental input describes the problem; the program control input describes in part how the problem should be solved and how the solution should be displayed.

The physical/environmental input parameters are described in Table E-1. This table gives the variables, their units, and any size restrictions (for example, the initial slick volume must be greater than 100 m^3 , and the ocean temperature must be between 0°C and 50°C). The program control parameters are described in Table E-2. This table describes the decisions the user must make and the consequences of those decisions.

One feature of the input section is not shown on the flow chart: after the user has entered the oil spill component data, these data may be saved in a file and read back in during subsequent runs, so the user can avoid repetitive and error-prone retyping. In the present version of the program, up to ten different component data sets may be stored. (This may easily be increased according to the capacity of the storage tape.)

TABLE E-1
PHYSICAL/ENVIRONMENTAL INPUT PARAMETERS

<u>Variable</u>	<u>Meaning</u>	<u>Units</u>	<u>Restrictions</u>
V \emptyset	Initial Spill Volume	m ³	V \emptyset \geq 100
R(I)	Specific Gravity of Component I	unit vol. component per unit vol. water	.4 \leq R(I) \leq 1.1
B(I)	Boiling Point of Component I	$^{\circ}$ C	B(I) \geq 40
V(I)	Relative Volume of Component I	parts component volume per part total slick volume	V(I) > 0
C \emptyset	Speed of Current	m/s	0 \leq C \emptyset \leq 5
T \emptyset	Ocean Temperature	$^{\circ}$ C	0 \leq T \emptyset \leq 50
D \emptyset	Initial Distance to Shore	km	D \emptyset > 0
W(I)	Wind Speed During Time Interval I	m/s	0 \leq W(I) \leq 60
@(I)	Wave Height During Time Interval I	m	must be compatible with wind speed*

*
$$\frac{.283}{G} [W(I) * .8]^2 \leq @(I) \leq \frac{.283}{G} [W(I) * 1.2]^2$$

See Section 5.4, Step 1.

TABLE E-2
PROGRAM CONTROL INPUT PARAMETERS

<u>Variable</u>	<u>Meaning</u>	<u>Comments</u>
T2	Total Simulation Time (hr.)	Must be between 10 and 140 times the Runge-Kutta time step determined by the program.
D1	Display Interval	A positive integer. Determines the number of Runge-Kutta time steps between displayed output lines of the summary tables. Must be small enough so that at least five output lines result.
F	File Number for Oil Spill Component Data	An integer between 1 and 10.
NØ	Number of Components in Spilled Oil	An integer between 1 and 5.
F3	Output Type Flag	Set according to whether the user requests summary or detailed output.
Y1	Number of Wind Speed/Wave Height Intervals	An integer between 1 and 10.
#(I)	Duration (hr.) of Wind Speed/Wave Height Interval I	Must be greater than 0, and sum of all durations must be greater than or equal to the maximum simulation time.

E.1.3 Initialization Section

The initialization section calculates a large number of initial and constant values used in the calculation section. (A few of these "constants" depend upon wind speed and wave height data that may change periodically according to the durations of the weather intervals defined by the user. When the weather changes, these "constants" are recalculated; this is not shown in the flow chart.)

E.1.4 Calculation Section

The calculation section is composed of four subroutines, corresponding to the procedures described in the four Chapters 3* through 6: (1) the evaporation and spreading subroutine; (2) the droplet diameter subroutine; (3) the droplet dispersion subroutine; and, (4) the slicklet distribution subroutine. These four subroutines are executed in sequence, once for each Runge-Kutta iteration, until either the maximum simulation time is reached or the spreading and evaporation subroutine indicates that the slick has entirely evaporated, broken up, or sunk.

The evaporation and spreading subroutine determines:

- component mass concentrations
- average slick density
- evaporated volume
- surface volume remaining
- slick thickness
- slick radius

*Actually, the more detailed spreading and evaporation procedure described in Appendix B is used, rather than that in Chapter 3.

The droplet diameter subroutine determines:

- minimum dispersed droplet diameter
- maximum dispersed droplet diameter

The droplet dispersion subroutine determines:

- incremental dispersed slick volume
- dispersed droplet volumes
- dispersed droplet terminal velocities
- dispersed droplet dispersion depths
- probabilities that droplets remain dispersed
- total dispersed volume

(The droplet dispersion subroutine also adjusts the oil slick thickness according to the increment of volume dispersed during one time step.)

The slicklet distribution subroutine determines:

- the total area polluted by oil slicklets
- the percentage of total polluted area covered with oil

The results generated by these four subroutines, along with some intermediate and constant values, are passed to the output section when one of the stopping criteria (e.g., maximum simulation time or break-up) is reached.

E.1.5 Output Section

The output section produces either three or nine output tables, depending upon whether the user has selected summary or detailed output. Tables E-3 through E-11 show examples of these output tables, produced by a run modelling a 100 m³ spill of light crude consisting of five components. The first three tables (see Tables E-3 through E-5) are always produced. (If detailed output were not requested, as it was in

TABLE E-3

TABLE 1--INPUT PARAMETERS:

INITIAL SPILL VOLUME (CUBIC METERS): 100

SPILL COMPONENTS:

COMPONENT NO. 1 :
 SPECIFIC GRAVITY: .7
 BOILING POINT (DEG. C): 73.9
 RELATIVE VOLUME: .1
 VAPOR PRESSURE: 12028.314590
 MOLECULAR WEIGHT: 101.178

COMPONENT NO. 2 :
 SPECIFIC GRAVITY: .786
 BOILING POINT (DEG. C): 151.4
 RELATIVE VOLUME: .192
 VAPOR PRESSURE: 572.373055
 MOLECULAR WEIGHT: 133.728

COMPONENT NO. 3 :
 SPECIFIC GRAVITY: .85
 BOILING POINT (DEG. C): 265.8
 RELATIVE VOLUME: .207
 VAPOR PRESSURE: 6.389410
 MOLECULAR WEIGHT: 181.776

COMPONENT NO. 4 :
 SPECIFIC GRAVITY: .89
 BOILING POINT (DEG. C): 376.4
 RELATIVE VOLUME: .154
 VAPOR PRESSURE: 8.281114E-2
 MOLECULAR WEIGHT: 228.228

COMPONENT NO. 5 :
 SPECIFIC GRAVITY: .965
 BOILING POINT (DEG. C): 426.7
 RELATIVE VOLUME: .347
 VAPOR PRESSURE: 1.147432E-2
 MOLECULAR WEIGHT: 249.354

CURRENT SPEED (M/S): .5

WIND SPEED/WAVE HEIGHT INTERVALS:

TEMPERATURE OF SEA (DEG. C): 20

INTERVAL NO. 1 :

INITIAL DISTANCE TO SHORE (KM): 10

WIND SPEED (M/S): 5
 1/3 SIG. WAVE HEIGHT (M): .5
 INTERVAL DURATION (HR): 5

RUNGE-KUTTA TIME STEP (HR): .25

DISPLAY INTERVAL: 2

INTERVAL NO. 2 :

MAXIMUM SIMULATION TIME (HR): 35

WIND SPEED (M/S): .5
 1/3 SIG. WAVE HEIGHT (M): 1E-2
 INTERVAL DURATION (HR): 35

TABLE E-4

TABLE 2---SLICK VOLUME DISTRIBUTION:

ELAPSED TIME (HR)	SURFACE VOLUME REMAINING (M**3)	PERCENT OF INITIAL VOLUME ON SURFACE	PERCENT OF INITIAL VOLUME EVAPORATED	PERCENT OF INITIAL VOLUME DISPERSED
0.00	1.000E+02	100.00	0.00	0.00
.50	9.587E+01	95.87	4.13	6.00
1.00	9.109E+01	91.49	8.51	.00
1.50	8.815E+01	88.15	11.84	.01
2.00	8.588E+01	85.88	14.06	.05
2.50	8.322E+01	83.22	16.61	.16
3.00	8.008E+01	80.08	19.51	.42
3.50	7.685E+01	76.85	22.42	.74
4.00	7.393E+01	73.93	24.98	1.09
4.50	7.156E+01	71.56	26.95	1.48
5.00	6.985E+01	69.85	28.28	1.88
5.50	6.995E+01	69.95	28.39	1.66
6.00	7.003E+01	70.03	28.50	1.47
6.50	7.009E+01	70.09	28.62	1.29
7.00	7.023E+01	70.23	28.74	1.03
7.50	7.034E+01	70.34	28.86	.80
8.00	7.032E+01	70.32	28.99	.70
8.50	7.032E+01	70.32	29.10	.58
9.00	7.030E+01	70.30	29.22	.49
9.50	7.030E+01	70.30	29.32	.38
10.00	7.027E+01	70.27	29.42	.30
10.50	7.025E+01	70.25	29.52	.23
11.00	7.039E+01	70.39	29.61	.00
11.50	7.031E+01	70.31	29.69	.00
12.00	7.023E+01	70.23	29.77	.00
12.50	7.016E+01	70.16	29.84	.00

SLICK BREAKS UP (AREA VS. VOLUME STOPPING CRITERION REACHED).

TABLE E-5

TABLE 3-- POLLUTED AREA AND SLICK THICKNESS

ELAPSED TIME (HR)	TOTAL AREA CONTAMINATED (KM*2)	PERCENT OF TOTAL AREA COVERED WITH OIL	SLICK THICKNESS (MM)
0.00	1.500E-02	100.00	6.667E+00
.50	2.864E-02	100.00	3.347E+00
1.00	5.212E-02	100.00	1.756E+00
1.50	1.277E-01	75.00	9.207E-01
2.00	3.277E-01	44.99	5.826E-01
2.50	6.117E-01	33.67	4.040E-01
3.00	9.818E-01	27.58	2.957E-01
3.50	1.439E+00	23.71	2.252E-01
4.00	1.986E+00	21.00	1.773E-01
4.50	2.622E+00	18.97	1.439E-01
5.00	3.350E+00	17.39	1.199E-01
5.50	4.170E+00	16.12	1.041E-01
6.00	5.083E+00	15.07	9.142E-02
6.50	6.089E+00	14.18	8.115E-02
7.00	7.191E+00	13.42	7.276E-02
7.50	8.388E+00	12.76	6.571E-02
8.00	9.681E+00	12.18	5.963E-02
8.50	1.107E+01	11.67	5.445E-02
9.00	1.256E+01	11.21	4.996E-02
9.50	1.414E+01	10.79	4.607E-02
10.00	1.583E+01	10.41	4.264E-02
10.50	1.761E+01	10.07	3.962E-02
11.00	1.949E+01	9.75	3.702E-02
11.50	2.147E+01	9.46	3.459E-02
12.00	2.356E+01	9.20	3.242E-02
12.50	2.574E+01	8.95	3.046E-02

SLICK BREAKS UP (AREA VS. VOLUME
STOPPING CRITERION REACHED).

TABLE E-6

TABLE 4--DETAILED SURFACE SLICK CHARACTERISTICS

I	SURFACE VOLUME (M**3)	EVAPORATION FLUX (KG/M**2/S)	AVERAGE DENSITY (KG/M**3)	SLICK THICKNESS (M)	SLICK RADIUS (M)
1	1.000E+02	1.168E-04	8.688E+02	6.667E-03	6.910E+01
2	9.821E+01	1.015E-04	8.717E+02	4.721E-03	8.137E+01
3	9.587E+01	8.059E-05	8.757E+02	3.347E-03	9.549E+01
4	9.362E+01	5.955E-05	8.797E+02	2.741E-03	1.043E+02
5	9.149E+01	3.938E-05	8.836E+02	1.756E-03	1.288E+02
6	8.959E+01	2.268E-05	8.869E+02	1.230E-03	1.523E+02
7	8.815E+01	1.318E-05	8.893E+02	9.207E-04	1.746E+02
8	8.698E+01	9.371E-06	8.901E+02	7.209E-04	1.960E+02
9	8.588E+01	7.674E-06	8.924E+02	5.826E-04	2.166E+02
10	8.463E+01	7.219E-06	8.939E+02	4.812E-04	2.366E+02
11	8.322E+01	6.695E-06	8.956E+02	4.040E-04	2.561E+02
12	8.168E+01	6.109E-06	8.975E+02	3.437E-04	2.750E+02
13	8.008E+01	5.471E-06	8.996E+02	2.957E-04	2.936E+02
14	7.844E+01	4.796E-06	9.017E+02	2.569E-04	3.118E+02
15	7.685E+01	4.105E-06	9.038E+02	2.252E-04	3.296E+02
16	7.533E+01	3.423E-06	9.059E+02	1.991E-04	3.471E+02
17	7.393E+01	2.775E-06	9.078E+02	1.773E-04	3.643E+02
18	7.266E+01	2.185E-06	9.096E+02	1.591E-04	3.812E+02
19	7.156E+01	1.671E-06	9.111E+02	1.439E-04	3.979E+02
20	7.063E+01	1.243E-06	9.123E+02	1.309E-04	4.144E+02
21	6.985E+01	9.027E-07	9.133E+02	1.199E-04	4.307E+02
22	6.922E+01	8.724E-08	9.134E+02	1.114E-04	4.467E+02
23	6.995E+01	8.411E-08	9.135E+02	1.041E-04	4.626E+02
24	6.993E+01	3.090E-08	9.136E+02	9.732E-05	4.783E+02
25	7.003E+01	7.762E-08	9.137E+02	9.142E-05	4.938E+02
26	7.009E+01	7.430E-08	9.138E+02	8.607E-05	5.091E+02
27	7.009E+01	7.096E-08	9.139E+02	8.115E-05	5.243E+02
28	7.024E+01	6.761E-08	9.140E+02	7.686E-05	5.394E+02
29	7.023E+01	6.427E-08	9.141E+02	7.276E-05	5.543E+02
30	7.021E+01	6.095E-08	9.142E+02	6.901E-05	5.691E+02
31	7.034E+01	5.768E-08	9.143E+02	6.571E-05	5.837E+02
32	7.036E+01	5.448E-08	9.144E+02	6.258E-05	5.983E+02
33	7.032E+01	5.135E-08	9.145E+02	5.963E-05	6.127E+02
34	7.030E+01	4.830E-08	9.146E+02	5.693E-05	6.270E+02
35	7.032E+01	4.536E-08	9.147E+02	5.445E-05	6.412E+02
36	7.032E+01	4.253E-08	9.148E+02	5.213E-05	6.553E+02
37	7.030E+01	3.983E-08	9.149E+02	4.996E-05	6.693E+02
38	7.029E+01	3.725E-08	9.150E+02	4.794E-05	6.831E+02
39	7.030E+01	3.481E-08	9.150E+02	4.607E-05	6.969E+02
40	7.029E+01	3.251E-08	9.151E+02	4.430E-05	7.107E+02
41	7.027E+01	3.036E-08	9.152E+02	4.264E-05	7.243E+02
42	7.025E+01	2.835E-08	9.153E+02	4.108E-05	7.378E+02
43	7.025E+01	2.649E-08	9.153E+02	3.962E-05	7.513E+02
44	7.043E+01	2.477E-08	9.154E+02	3.830E-05	7.647E+02
45	7.039E+01	2.319E-08	9.155E+02	3.702E-05	7.780E+02
46	7.035E+01	2.175E-08	9.155E+02	3.577E-05	7.912E+02
47	7.031E+01	2.044E-08	9.156E+02	3.459E-05	8.043E+02
48	7.027E+01	1.926E-08	9.156E+02	3.347E-05	8.174E+02
49	7.023E+01	1.819E-08	9.157E+02	3.242E-05	8.304E+02
50	7.019E+01	1.722E-08	9.147E+02	3.141E-05	8.434E+02
51	7.016E+01	1.622E-08	9.159E+02	3.046E-05	8.562E+02
52	7.014E+01	1.521E-08	9.159E+02	2.956E-05	8.690E+02

TABLE E-7

TABLE 5- DETAILED DROPLET DISPERSION AND
SLICKLET DISTRIBUTION RESULTS

I	SMALL DIAMETER (M)	LARGE DIAMETER (M)	VOLUME DISPENSED (M**3)	TOTAL POL. AREA (M**2)
1	0.000E+00	0.000E+00	0.000E+00	1.500E+04
2	1.140E-05	4.721E-03	0.000E+00	2.080E+04
3	1.140E-05	3.347E-03	0.000E+00	2.864E+04
4	1.140E-05	2.741E-03	0.000E+00	3.416E+04
5	1.140E-05	1.756E-03	1.725E-03	5.212E+04
6	1.140E-05	1.230E-03	4.165E-03	7.283E+04
7	1.140E-05	9.207E-04	6.875E-03	1.277E+05
8	1.140E-05	7.210E-04	1.756E-02	2.173E+05
9	1.140E-05	5.829E-04	5.262E-02	3.277E+05
10	1.140E-05	4.814E-04	9.091E-02	4.591E+05
11	1.140E-05	4.044E-04	1.646E-01	6.117E+05
12	1.140E-05	3.442E-04	2.817E-01	7.859E+05
13	1.140E-05	2.962E-04	4.156E-01	9.818E+05
14	1.140E-05	2.574E-04	5.715E-01	1.200E+06
15	1.140E-05	2.257E-04	7.355E-01	1.439E+06
16	1.140E-05	1.995E-04	9.071E-01	1.701E+06
17	1.140E-05	1.778E-04	1.093E+00	1.986E+06
18	1.140E-05	1.596E-04	1.288E+00	2.293E+06
19	1.140E-05	1.442E-04	1.484E+00	2.622E+06
20	1.140E-05	1.313E-04	1.681E+00	2.975E+06
21	1.140E-05	1.202E-04	1.875E+00	3.350E+06
22	2.493E-05	1.113E-04	1.846E+00	3.748E+06
23	2.493E-05	1.038E-04	1.658E+00	4.170E+06
24	2.493E-05	9.727E-05	1.626E+00	4.615E+06
25	2.493E-05	9.122E-05	1.473E+00	5.083E+06
26	2.493E-05	8.592E-05	1.353E+00	5.574E+06
27	2.493E-05	8.108E-05	1.292E+00	6.089E+06
28	2.493E-05	7.662E-05	1.076E+00	6.628E+06
29	2.493E-05	7.271E-05	1.027E+00	7.191E+06
30	2.493E-05	6.897E-05	9.878E-01	7.777E+06
31	2.493E-05	6.553E-05	7.999E-01	8.388E+06
32	2.493E-05	6.250E-05	7.127E-01	9.022E+06
33	2.493E-05	5.962E-05	6.960E-01	9.681E+06
34	2.493E-05	5.689E-05	6.556E-01	1.036E+07
35	2.493E-05	5.439E-05	5.782E-01	1.107E+07
36	2.493E-05	5.209E-05	5.241E-01	1.180E+07
37	2.493E-05	4.993E-05	4.876E-01	1.256E+07
38	2.493E-05	4.791E-05	4.381E-01	1.334E+07
39	2.493E-05	4.603E-05	3.812E-01	1.414E+07
40	2.493E-05	4.427E-05	3.378E-01	1.497E+07
41	2.493E-05	4.262E-05	3.037E-01	1.583E+07
42	2.493E-05	4.106E-05	2.727E-01	1.671E+07
43	2.493E-05	3.959E-05	2.294E-01	1.761E+07
44	2.493E-05	3.822E-05	1.268E-03	1.854E+07
45	2.493E-05	3.702E-05	1.325E-03	1.949E+07
46	2.493E-05	3.577E-05	1.382E-03	2.047E+07
47	2.493E-05	3.459E-05	1.438E-03	2.147E+07
48	2.493E-05	3.347E-05	1.494E-03	2.250E+07
49	2.493E-05	3.242E-05	1.549E-03	2.356E+07
50	2.493E-05	3.141E-05	1.605E-03	2.464E+07
51	2.493E-05	3.046E-05	1.659E-03	2.574E+07
52	2.493E-05	2.956E-05	1.714E-03	2.687E+07

TABLE E-8

TABLE 6 - COMPONENT MASS CONCENTRATIONS (KG COMPONENT
PER CUBIC METER OF SLICK)

I	COMP. 1	COMP. 2	COMP. 3	COMP. 4	COMP. 5
1	7.000E+01	1.509E+02	1.760E+02	1.371E+02	3.349E+02
2	5.942E+01	1.527E+02	1.791E+02	1.396E+02	3.410E+02
3	4.529E+01	1.547E+02	1.835E+02	1.430E+02	3.493E+02
4	3.153E+01	1.563E+02	1.879E+02	1.464E+02	3.577E+02
5	1.875E+01	1.568E+02	1.922E+02	1.498E+02	3.660E+02
6	8.501E+00	1.555E+02	1.962E+02	1.530E+02	3.737E+02
7	2.876E+00	1.517E+02	1.994E+02	1.555E+02	3.798E+02
8	0.000E+00	1.457E+02	2.020E+02	1.575E+02	3.849E+02
9	0.000E+00	1.381E+02	2.046E+02	1.597E+02	3.901E+02
10	0.000E+00	1.289E+02	2.070E+02	1.620E+02	3.957E+02
11	0.000E+00	1.186E+02	2.105E+02	1.645E+02	4.020E+02
12	0.000E+00	1.072E+02	2.140E+02	1.670E+02	4.090E+02
13	0.000E+00	9.492E+01	2.176E+02	1.705E+02	4.165E+02
14	0.000E+00	8.222E+01	2.210E+02	1.737E+02	4.243E+02
15	0.000E+00	6.946E+01	2.252E+02	1.769E+02	4.322E+02
16	0.000E+00	5.708E+01	2.288E+02	1.801E+02	4.399E+02
17	0.000E+00	4.552E+01	2.321E+02	1.830E+02	4.472E+02
18	0.000E+00	3.515E+01	2.350E+02	1.857E+02	4.537E+02
19	0.000E+00	2.625E+01	2.374E+02	1.880E+02	4.594E+02
20	0.000E+00	1.893E+01	2.392E+02	1.900E+02	4.642E+02
21	0.000E+00	1.318E+01	2.404E+02	1.916E+02	4.681E+02
22	0.000E+00	1.267E+01	2.405E+02	1.917E+02	4.685E+02
23	0.000E+00	1.214E+01	2.407E+02	1.919E+02	4.689E+02
24	0.000E+00	1.160E+01	2.408E+02	1.920E+02	4.692E+02
25	0.000E+00	1.105E+01	2.409E+02	1.922E+02	4.696E+02
26	0.000E+00	1.049E+01	2.410E+02	1.923E+02	4.700E+02
27	0.000E+00	9.930E+00	2.411E+02	1.925E+02	4.704E+02
28	0.000E+00	9.367E+00	2.411E+02	1.927E+02	4.708E+02
29	0.000E+00	8.808E+00	2.412E+02	1.928E+02	4.712E+02
30	0.000E+00	8.254E+00	2.413E+02	1.930E+02	4.716E+02
31	0.000E+00	7.707E+00	2.414E+02	1.932E+02	4.721E+02
32	0.000E+00	7.171E+00	2.414E+02	1.933E+02	4.725E+02
33	0.000E+00	6.649E+00	2.415E+02	1.935E+02	4.729E+02
34	0.000E+00	6.141E+00	2.415E+02	1.937E+02	4.733E+02
35	0.000E+00	5.651E+00	2.416E+02	1.938E+02	4.737E+02
36	0.000E+00	5.180E+00	2.416E+02	1.940E+02	4.740E+02
37	0.000E+00	4.730E+00	2.416E+02	1.941E+02	4.744E+02
38	0.000E+00	4.302E+00	2.416E+02	1.943E+02	4.748E+02
39	0.000E+00	3.897E+00	2.416E+02	1.944E+02	4.751E+02
40	0.000E+00	3.516E+00	2.416E+02	1.946E+02	4.755E+02
41	0.000E+00	3.159E+00	2.415E+02	1.947E+02	4.758E+02
42	0.000E+00	2.826E+00	2.415E+02	1.948E+02	4.761E+02
43	0.000E+00	2.518E+00	2.414E+02	1.950E+02	4.765E+02
44	0.000E+00	2.234E+00	2.413E+02	1.951E+02	4.768E+02
45	0.000E+00	1.974E+00	2.412E+02	1.952E+02	4.771E+02
46	0.000E+00	1.736E+00	2.411E+02	1.953E+02	4.774E+02
47	0.000E+00	1.521E+00	2.410E+02	1.954E+02	4.776E+02
48	0.000E+00	1.324E+00	2.409E+02	1.955E+02	4.779E+02
49	0.000E+00	1.150E+00	2.407E+02	1.956E+02	4.782E+02
50	0.000E+00	0.000E+00	2.405E+02	1.958E+02	4.784E+02
51	0.000E+00	0.000E+00	2.406E+02	1.961E+02	4.792E+02
52	0.000E+00	0.000E+00	2.404E+02	1.961E+02	4.794E+02

TABLE E-9

TABLE 7--DROPLET TERMINAL VELOCITIES (M/S)

I	SIZE 1	SIZE 2	SIZE 3	SIZE 4
1	0.000E+00	0.000E+00	0.000E+00	0.000E+00
2	2.518E-02	7.723E-02	9.958E-02	1.178E-01
3	1.243E-02	6.406E-02	8.255E-02	9.759E-02
4	8.149E-03	5.707E-02	7.351E-02	8.689E-02
5	3.340E-03	2.810E-02	5.792E-02	6.844E-02
6	1.652E-03	1.352E-02	3.683E-02	5.646E-02
7	9.439E-04	7.493E-03	2.028E-02	3.930E-02
8	6.001E-04	4.612E-03	1.239E-02	2.394E-02
9	4.023E-04	2.987E-03	7.965E-03	1.334E-02
10	2.845E-04	2.035E-03	5.383E-03	1.033E-02
11	2.083E-04	1.433E-03	3.756E-03	7.177E-03
12	1.569E-04	1.036E-03	2.688E-03	5.113E-03
13	1.209E-04	7.647E-04	1.963E-03	3.717E-03
14	9.522E-05	5.757E-04	1.462E-03	2.753E-03
15	7.645E-05	4.414E-04	1.107E-03	2.074E-03
16	6.254E-05	3.444E-04	8.533E-04	1.589E-03
17	5.209E-05	2.736E-04	6.689E-04	1.238E-03
18	4.414E-05	2.210E-04	5.332E-04	9.806E-04
19	3.802E-05	1.817E-04	4.322E-04	7.897E-04
20	3.327E-05	1.518E-04	3.561E-04	6.462E-04
21	2.953E-05	1.287E-04	2.978E-04	5.368E-04
22	6.025E-05	1.551E-04	2.940E-04	4.769E-04
23	5.705E-05	1.400E-04	2.596E-04	4.159E-04
24	5.436E-05	1.276E-04	2.317E-04	3.666E-04
25	5.190E-05	1.166E-04	2.071E-04	3.235E-04
26	4.980E-05	1.074E-04	1.868E-04	2.880E-04
27	4.791E-05	9.924E-05	1.691E-04	2.574E-04
28	4.619E-05	9.204E-05	1.535E-04	2.307E-04
29	4.471E-05	8.596E-05	1.406E-04	2.085E-04
30	4.332E-05	8.033E-05	1.287E-04	1.883E-04
31	4.206E-05	7.531E-05	1.182E-04	1.707E-04
32	4.095E-05	7.103E-05	1.093E-04	1.559E-04
33	3.992E-05	6.707E-05	1.012E-04	1.424E-04
34	3.895E-05	6.344E-05	9.386E-05	1.302E-04
35	3.807E-05	6.018E-05	8.734E-05	1.195E-04
36	3.727E-05	5.727E-05	8.155E-05	1.101E-04
37	3.652E-05	5.461E-05	7.631E-05	1.016E-04
38	3.583E-05	5.217E-05	7.156E-05	9.401E-05
39	3.520E-05	4.995E-05	6.728E-05	8.718E-05
40	3.461E-05	4.792E-05	6.340E-05	8.104E-05
41	3.405E-05	4.605E-05	5.986E-05	7.547E-05
42	3.354E-05	4.432E-05	5.661E-05	7.040E-05
43	3.306E-05	4.273E-05	5.364E-05	6.580E-05
44	3.261E-05	4.126E-05	5.093E-05	6.162E-05
45	3.222E-05	4.000E-05	4.863E-05	5.810E-05
46	3.182E-05	3.871E-05	4.629E-05	5.454E-05
47	3.144E-05	3.752E-05	4.413E-05	5.128E-05
48	3.109E-05	3.640E-05	4.214E-05	4.829E-05
49	3.075E-05	3.536E-05	4.029E-05	4.554E-05
50	3.080E-05	3.479E-05	3.903E-05	4.352E-05
51	3.009E-05	3.342E-05	3.693E-05	4.062E-05
52	2.982E-05	3.258E-05	3.547E-05	3.848E-05

TABLE E-10

TABLE E--DROPLET DISPERSION DEPTHS (M)

I	SIZE 1	SIZE 2	SIZE 3	SIZE 4
1	0.000E+00	0.000E+00	0.000E+00	0.000E+00
2	1.780E-01	5.804E-02	4.502E-02	3.807E-02
3	3.607E-01	6.998E-02	5.430E-02	4.593E-02
4	5.501E-01	7.855E-02	6.098E-02	5.159E-02
5	1.342E+00	1.595E-01	7.738E-02	6.550E-02
6	2.713E+00	3.315E-01	1.217E-01	7.939E-02
7	4.749E+00	5.982E-01	2.210E-01	1.140E-01
8	4.793E+00	9.720E-01	3.617E-01	1.872E-01
9	4.793E+00	1.501E+00	5.628E-01	2.923E-01
10	4.793E+00	2.202E+00	8.328E-01	4.341E-01
11	4.793E+00	3.127E+00	1.193E+00	6.246E-01
12	4.793E+00	4.328E+00	1.668E+00	8.768E-01
13	4.793E+00	4.793E+00	2.283E+00	1.206E+00
14	4.793E+00	4.793E+00	3.067E+00	1.628E+00
15	4.793E+00	4.793E+00	4.048E+00	2.161E+00
16	4.793E+00	4.793E+00	4.793E+00	2.821E+00
17	4.793E+00	4.793E+00	4.793E+00	3.621E+00
18	4.793E+00	4.793E+00	4.793E+00	4.571E+00
19	4.793E+00	4.793E+00	4.793E+00	4.793E+00
20	4.793E+00	4.793E+00	4.793E+00	4.793E+00
21	4.793E+00	4.793E+00	4.793E+00	4.793E+00
22	9.586E-02	9.586E-02	9.586E-02	9.586E-02
23	9.586E-02	9.586E-02	9.586E-02	9.586E-02
24	9.586E-02	9.586E-02	9.586E-02	9.586E-02
25	9.586E-02	9.586E-02	9.586E-02	9.586E-02
26	9.586E-02	9.586E-02	9.586E-02	9.586E-02
27	9.586E-02	9.586E-02	9.586E-02	9.586E-02
28	9.586E-02	9.586E-02	9.586E-02	9.586E-02
29	9.586E-02	9.586E-02	9.586E-02	9.586E-02
30	9.586E-02	9.586E-02	9.586E-02	9.586E-02
31	9.586E-02	9.586E-02	9.586E-02	9.586E-02
32	9.586E-02	9.586E-02	9.586E-02	9.586E-02
33	9.586E-02	9.586E-02	9.586E-02	9.586E-02
34	9.586E-02	9.586E-02	9.586E-02	9.586E-02
35	9.586E-02	9.586E-02	9.586E-02	9.586E-02
36	9.586E-02	9.586E-02	9.586E-02	9.586E-02
37	9.586E-02	9.586E-02	9.586E-02	9.586E-02
38	9.586E-02	9.586E-02	9.586E-02	9.586E-02
39	9.586E-02	9.586E-02	9.586E-02	9.586E-02
40	9.586E-02	9.586E-02	9.586E-02	9.586E-02
41	9.586E-02	9.586E-02	9.586E-02	9.586E-02
42	9.586E-02	9.586E-02	9.586E-02	9.586E-02
43	9.586E-02	9.586E-02	9.586E-02	9.586E-02
44	9.586E-02	9.586E-02	9.586E-02	9.586E-02
45	9.586E-02	9.586E-02	9.586E-02	9.586E-02
46	9.586E-02	9.586E-02	9.586E-02	9.586E-02
47	9.586E-02	9.586E-02	9.586E-02	9.586E-02
48	9.586E-02	9.586E-02	9.586E-02	9.586E-02
49	9.586E-02	9.586E-02	9.586E-02	9.586E-02
50	9.586E-02	9.586E-02	9.586E-02	9.586E-02
51	9.586E-02	9.586E-02	9.586E-02	9.586E-02
52	9.586E-02	9.586E-02	9.586E-02	9.586E-02

TABLE E-11

TABLE 9--VOLUME IN DROPLETS (M**3):

I	SIZE 1	SIZE 2	SIZE 3	SIZE 4
1	0.000E+00	0.000E+00	0.000E+00	0.000E+00
2	4.007E-03	7.437E-02	2.050E-01	1.869E-01
3	3.984E-03	7.282E-02	2.001E-01	1.822E-01
4	3.945E-03	7.127E-02	1.954E-01	1.777E-01
5	4.023E-03	7.013E-02	1.908E-01	1.730E-01
6	4.140E-03	6.923E-02	1.867E-01	1.687E-01
7	4.301E-03	6.873E-02	1.836E-01	1.651E-01
8	4.501E-03	6.849E-02	1.810E-01	1.620E-01
9	4.732E-03	6.837E-02	1.786E-01	1.591E-01
10	4.985E-03	6.815E-02	1.758E-01	1.557E-01
11	5.265E-03	6.788E-02	1.728E-01	1.521E-01
12	5.573E-03	6.755E-02	1.694E-01	1.482E-01
13	5.914E-03	6.718E-02	1.658E-01	1.440E-01
14	6.293E-03	6.683E-02	1.622E-01	1.398E-01
15	6.714E-03	6.653E-02	1.586E-01	1.355E-01
16	7.181E-03	6.630E-02	1.551E-01	1.314E-01
17	7.699E-03	6.619E-02	1.518E-01	1.274E-01
18	8.270E-03	6.620E-02	1.488E-01	1.237E-01
19	8.894E-03	6.634E-02	1.461E-01	1.203E-01
20	9.575E-03	6.662E-02	1.437E-01	1.171E-01
21	1.031E-02	6.703E-02	1.415E-01	1.142E-01
22	3.525E-05	1.040E-04	1.628E-04	1.121E-04
23	3.859E-05	1.060E-04	1.606E-04	1.085E-04
24	4.206E-05	1.081E-04	1.586E-04	1.052E-04
25	4.572E-05	1.100E-04	1.562E-04	1.016E-04
26	4.948E-05	1.119E-04	1.540E-04	9.832E-05
27	5.338E-05	1.137E-04	1.517E-04	9.496E-05
28	5.740E-05	1.153E-04	1.491E-04	9.151E-05
29	6.148E-05	1.171E-04	1.469E-04	8.845E-05
30	6.570E-05	1.185E-04	1.441E-04	8.508E-05
31	6.998E-05	1.198E-04	1.413E-04	8.175E-05
32	7.430E-05	1.212E-04	1.389E-04	7.881E-05
33	7.868E-05	1.224E-04	1.362E-04	7.573E-05
34	8.311E-05	1.234E-04	1.332E-04	7.259E-05
35	8.755E-05	1.243E-04	1.304E-04	6.959E-05
36	9.199E-05	1.252E-04	1.276E-04	6.675E-05
37	9.643E-05	1.259E-04	1.248E-04	6.395E-05
38	1.009E-04	1.265E-04	1.220E-04	6.122E-05
39	1.052E-04	1.271E-04	1.192E-04	5.861E-05
40	1.096E-04	1.276E-04	1.165E-04	5.611E-05
41	1.139E-04	1.280E-04	1.138E-04	5.369E-05
42	1.182E-04	1.283E-04	1.111E-04	5.134E-05
43	1.224E-04	1.285E-04	1.084E-04	4.909E-05
44	1.265E-04	1.286E-04	1.058E-04	4.695E-05
45	1.306E-04	1.291E-04	1.038E-04	4.518E-05
46	1.346E-04	1.290E-04	1.012E-04	4.315E-05
47	1.385E-04	1.290E-04	9.870E-05	4.121E-05
48	1.423E-04	1.288E-04	9.625E-05	3.936E-05
49	1.460E-04	1.286E-04	9.386E-05	3.760E-05
50	1.497E-04	1.284E-04	9.153E-05	3.592E-05
51	1.532E-04	1.281E-04	8.930E-05	3.433E-05
52	1.567E-04	1.278E-04	8.713E-05	3.282E-05

this example run, then the components' vapor pressures and molecular weights would not be given in the first table. Also, in this example run, the display interval was 2; hence, as the Runge-Kutta time step for a 100 m³ spill is .25 hours, results were printed every half hour in the second and third tables.) The last six tables (see Tables E-6 through E-11) are only produced when detailed output is requested. (In the detailed output tables, results are displayed for every iteration, regardless of the display interval or the time step.)

E.2 PROGRAM LISTING AND NOTES

E.2.1 Program Listing

The program code is divided into two files, due to capacity restrictions on the IBM 5100 on which the program was developed. The first file contains the input, initialization, and calculation sections; the second file contains the output section.

```

0010 REM *****
0020 REM
0030 REM THIS PROGRAM MODELS THE BEHAVIOR OF OIL SLICKS
0040 REM ON ROUGH SEAS, PARTICULARLY THEIR SPREADING,
0050 REM EVAPORATION, DISPERSION INTO THE WATER COLUMN,
0060 REM AND EVENTUAL BREAK-UP INTO SMALL SLICKLETS.
0070 REM
0080 REM THIS PROGRAM WAS WRITTEN FOR THE UNITED STATES
0090 REM COAST GUARD BY JOHN K. OSTLUND OF ARTHUR D.
0100 REM LITTLE, INC., JULY 20, 1981.
0110 REM
0120 DIM R(5),B(5),A(6),V(5),E(6),T(4),W(10),@ (10),#(10)
0130 DIM Y(6),G(5),I(141),J(141),S(141)
0140 DIM P(5),M(5),C(141,5),F(6),K(141)
0150 DIM L(141),H(141),N(141),D(141),U(141,4)
0160 DIM O(141,4),Z(141,4),X(31),Q(141)
0170 REM *****
0180 REM
0190 REM *** MAIN PROGRAM ***
0200 REM
0210 GOSUB 0370
0220 GOSUB 1680
0230 FOR I0=2 TO N
0240 PRINT 'ITERATION NUMBER: ';I0
0250 IF I0<#(Y2)IY2=Y1 GOTO 0280
0260 Y2=Y2+1
0270 GOSUB 2480
0280 GOSUB 2550
0290 IF F2<0 GOTO 0340
0300 GOSUB 3910
0310 GOSUB 4140
0320 GOSUB 4960
0330 NEXT I0
0340 GOSUB 5310
0350 CHAIN 'E80',1
0360 END
0370 REM *****
0380 REM
0390 REM ** INPUT **
0400 REM
0410 PRINT 'INITIAL VOLUME OF SPILL (CUBIC METERS)?';
0420 INPUT V0
0430 IF V0<100. GOTO 0460
0440 PRINT 'THE INITIAL VOLUME MUST BE 100 OR GREATER.'
0450 GOTO 0410
0460 IF V0>500 GOTO 0490
0470 T3=.25
0480 GOTO 0530
0490 IF V0>5000 GOTO 0520
0500 T3=.5
0510 GOTO 0530

```

```

0520 T3=1.
0530 PRINT 'THE RUNGE-KUTTA TIME STEP IS ';T3;' HOURS.'
0540 PRINT ' '
0550 PRINT 'TOTAL SIMULATION TIME (HR) (MUST BE ';140*T3
0560 PRINT 'OR LESS)?';
0570 INPUT T2
0580 IF T2>9.999*T3 GOTO 0610
0590 PRINT 'THE SIMULATION TIME MUST BE ';10*T3;' OR GREATER.'
0600 GOTO 0550
0610 IF T2>140.001*T3 GOTO 0550
0620 PRINT 'DISPLAY INTERVAL (INTEGER--NUMBER OF RUNGE-KUTTA'
0630 PRINT 'TIME STEPS BETWEEN DISPLAYED OUTPUT LINES)?';
0640 INPUT D1
0650 IF D1<1&D1=INT(D1) GOTO 0680
0660 PRINT 'THE INTERVAL MUST BE A POSITIVE INTEGER.'
0670 GOTO 0620
0680 IF D1*T3<T2/4.9999 GOTO 0720
0690 PRINT 'FEWER THAN 5 OUTPUT LINES WILL RESULT. CHOOSE'
0700 PRINT 'A SMALLER DISPLAY INTERVAL.'
0710 GOTO 0620
0720 PRINT 'BASED ON A ';T3;' HOUR TIME STEP AND A DISPLAY'
0730 PRINT 'INTERVAL OF ';D1;', THE SIMULATION RESULTS WILL'
0740 PRINT 'BE DISPLAYED EVERY ';T3*D1;' HOUR(S). IS THIS'
0750 PRINT 'SATISFACTORY?';
0760 INPUT A$
0770 IF STR(A$,1,1)='Y' GOTO 0800
0780 PRINT 'ENTER A DIFFERENT DISPLAY INTERVAL.'
0790 GOTO 0640
0800 PRINT 'DO YOU WISH TO ENTER THE OIL SPILL'
0810 PRINT 'COMPONENT MAKEUP FROM THE TERMINAL (ENTER ''T'')'
0820 PRINT 'OR FROM A FILE (''F'')?';
0830 INPUT A$
0840 IF A$='T' GOTO 0980
0850 PRINT 'ENTER FILE NO. IN WHICH DATA ARE STORED.';
0860 INPUT F
0870 IF F>0&F<11 GOTO 0900
0880 PRINT 'MUST BE BETWEEN 1 AND 10.'
0890 GOTO 0850
0900 OPEN FLO,'E40',F ,IN
0910 GET FLO,N0
0920 FOR I=1 TO N0
0930 GET FLO,R(I),K(I),V(I)
0940 NEXT I
0950 CLOSE FLO
0960 GOTO 1020
0970 PRINT
0980 PRINT 'NUMBER OF COMPONENTS IN SPILLED OIL?';
0990 INPUT N0
1000 IF N0>0&N0<6 GOTO 1040
1010 PRINT 'THERE MUST BE BETWEEN 1 AND 5 COMPONENTS.'
1020 GOTO 0980

```

```

1030 PRINT
1040 PRINT 'FOR EACH COMPONENT, ENTER THE SPECIFIC GRAVITY,'
1050 PRINT 'BOILING POINT (DEGREES C), AND RELATIVE'
1060 PRINT 'VOLUME (THAT IS, PARTS COMPONENT PER PART'
1070 PRINT 'SPILLED OIL).'
```

1080 V1=0

1090 FOR I=1 TO N0

1100 PRINT

1110 PRINT 'FOR COMPONENT ';I;': ';

1120 INPUT R(I),B(I),V(I)

1130 IF V(I)>0 GOTO 1160

1140 PRINT 'THE RELATIVE VOLUME MUST BE GREATER THAN ZERO.'

1150 GOTO 1100

1160 IF R(I)≥.4&R(I)≤1.1 GOTO 1190

1170 PRINT 'THE SPECIFIC GRAVITY MUST BE BETWEEN .4 AND 1.1.'

1180 GOTO 1100

1190 IF B(I)≥40. GOTO 1220

1200 PRINT 'THE BOILING POINT MUST BE GREATER THAN 40.'

1210 GOTO 1100

1220 V1=V1+V(I)

1230 NEXT I

1240 FOR I=1 TO N0

1250 V(I)=V(I)/V1

1260 NEXT I

1270 PRINT 'DO YOU WISH TO WRITE THE OIL SPILL'

1280 PRINT 'COMPONENT MAKEUP TO A FILE?';

1290 INPUT A\$

1300 IF STR(A\$,1,1)≠'Y' GOTO 1420

1310 PRINT 'ENTER FILE NO. IN WK.CH DATA ARE TO BE STORED.';

1320 INPUT F

1330 IF F>0&F<11 GOTO 1360

1340 PRINT 'MUST BE BETWEEN 1 AND 10.'

1350 GOTO 1310

1360 OPEN FLO,'E40',F ,OUT

1370 PUT FLO,N0

1380 FOR I=1 TO N0

1390 PUT FLO,R(I),B(I),V(I)

1400 NEXT I

1410 CLOSE FLO

1420 PRINT

1430 PRINT 'CURRENT SPEED (M/S)?';

1440 INPUT C0

1450 IF C0≥0&C0≤5. GOTO 1470

1460 PRINT 'THE CURRENT SPEED MUST BE BETWEEN 0 AND 5.'

1470 GOTO 1420

1480 PRINT

1490 PRINT 'TEMPERATURE OF THE SEA (DEGREES C)?';

1500 INPUT T0

1510 IF T0≥0&T0≤50 GOTO 1540

1520 PRINT 'THE TEMP. OF THE SEA MUST BE BETWEEN 0 AND 50.'

1530 GOTO 1480

```

1540 PRINT
1550 PRINT 'INITIAL DISTANCE TO SHORE (KM)?';
1560 INPUT D0
1570 IF D0>0 GOTO 1600
1580 PRINT 'INITIAL DISTANCE TO SHORE MUST BE GREATER THAN 0.'
1590 GOTO 1540
1600 GOSUB 5450
1610 PRINT 'DO YOU WISH SUMMARY OUTPUT ONLY (ENTER ''S'')'
1620 PRINT 'OR DETAILED OUTPUT (''D'')?',
1630 INPUT A$
1640 F3=0
1650 IF A$='S' GOTO 1670
1660 F3=1
1670 RETURN
1680 REM *****
1690 REM
1700 REM ** INITIALIZATION **
1710 REM
1720 G=9.81
1730 R1=1000.
1740 N1=1.E-06
1750 P0=1.E05
1760 K0=1.E-08
1770 S1=.03
1780 T0=T0+273
1790 FOR I=1 TO N0
1800 B(I)=B(I)+273
1810 NEXT I
1820 REM ** CALCULATE AVE. SLICK DENSITY **
1830 R0=0
1840 FOR I=1 TO N0
1850 R0=R0+R(I)*V(I)*R1
1860 NEXT I
1870 J(1)=R0
1880 T2=T2*3600.
1890 T3=T3*3600.
1900 S(1)=V0
1910 FOR I=1 TO N0
1920 C(1,I)=V(I)*R(I)*R1
1930 R2=B(I)/T0
1940 P(I)=10.†(-5.†(R2-1.))†P0
1950 M(I)=.42†(B(I)-106.)
1960 NEXT I
1970 T4=0
1980 N=INT(T2/T3)+1
1990 E0=N0+1
2000 N4=8.E-06
2010 Z0=(1.-R0/R1)*G
2020 T7=.546†(V0/(Z0*N1))†(.333333)
2030 IF T3/2.>T7 GOTO 2060
2040 N(1)=1.14†((Z0*V0)†.25)†SQR(T3/2.)

```

```

2050 GOTO 2070
2060 N(1)=.98*(Z0↑2.*V0↑4./N1)↑.0833333*(T3/2.)↑.25
2070 H(1)=S(1)/(3.1416*N(1)↑2.)
2080 F2=0
2090 I0=1
2100 K(1)=0
2110 L(1)=0
2120 I(1)=0
2130 FOR I=1 TO 4
2140 U(1,I)=0
2150 O(1,I)=0
2160 Z(1,I)=0
2170 NEXT I
2180 DATA .5,.5398,.5793,.6179,.6554,.6915
2190 DATA .7257,.758,.7881,.8159,.8413
2200 DATA .8643,.8849,.9032,.9192,.9332
2210 DATA .9452,.9554,.9641,.9713,.9773
2220 DATA .9821,.9861,.9893,.9918,.9938
2230 DATA .9953,.9965,.9974,.9981,.9987
2240 FOR J=1 TO 31
2250 READ X(I)
2260 NEXT I
2270 RESTORE
2280 L0=.4*I0*1000.
2290 IF L0≥100000. GOTO 2310
2300 L0=L0+100000.
2310 Q(1)=S(1)/H(1)
2320 L1=0
2330 L2=0
2340 S2=0
2350 D7=2
2360 T(1)=0
2370 T(2)=0
2380 T(3)=0
2390 T(4)=0
2400 FOR I=1 TO N0
2410 S2=S2+C(1,I)/M(I)
2420 NEXT I
2430 I(1)=0
2440 FOR I=1 TO N0
2450 G(I)=K0*W(1)*((C(1,I)/M(I))/S2)*P(J)
2460 J(1)=T(1)+G(I)/(R(I)*R1)
2470 NEXT I
2480 W=.7*G*SQR(.283/((Y2)*G))
2490 B0=.001*G/(W↑2.)
2500 W2=(6.83/(2.*3.1416))*W
2510 N2=1.7E-06*W(Y2)↑3.75*W2/(8.*3.14159*10.)
2520 Z1=2.*3.1416*(G/(W2↑2.*4.))
2530 K2=.004*W2*(Y2)↑2.
2540 RETURN
2550 REM *****

```

```

2560 REM
2570 REM ** EVAPORATION/SPREADING **
2580 REM
2590 F1=0
2600 FOR I=1 TO N0
2610 F(I)=C(I0-1,I)
2620 NEXT I
2630 F(E0)=S(I0-1)/3.1416
2640 REM
2650 REM ** RUNGE-KUTTA ROUTINE **
2660 F1=F1+1
2670 IF F1>1 GOTO 2700
2680 K1=1
2690 GOTO 3000
2700 IF F1>2 GOTO 2790
2710 FOR I=1 TO E0
2720 Y(I)=F(I)
2730 E(I)=A(I)
2740 F(I)=Y(I)+.5*A(I)*T3
2750 NEXT I
2760 T4=T4+.5*T3
2770 K1=1
2780 GOTO 3000
2790 IF F1>3 GOTO 2860
2800 FOR I=1 TO E0
2810 E(I)=E(I)+2.*A(I)
2820 F(I)=Y(I)+.5*A(I)*T3
2830 NEXT I
2840 K1=1
2850 GOTO 3000
2860 IF F1>4 GOTO 2940
2870 FOR I=1 TO E0
2880 E(I)=E(I)+2.*A(I)
2890 F(I)=Y(I)+A(I)*T3
2900 NEXT I
2910 T4=T4+.5*T3
2920 K1=1
2930 GOTO 3000
2940 FOR I=1 TO E0
2950 F(J)=Y(I)+(E(I)+A(J))*T3/6.
2960 NEXT I
2970 F1=0
2980 K1=0
2990 REM ** END OF R-K ROUTINE **
3000 IF F(E0)≥.001 GOTO 3090
3010 IF I0>2. GOTO 3050
3020 PRINT 'THE SLICK EVAPORATES IN LESS THAN ONE'
3030 PRINT 'TIME STEP.'
3040 STOP
3050 N=I0
3060 S(I0)=0

```

```

3070 F2=-3.
3080 RETURN
3090 REM ** SLICK RADIUS ROUTINE **
3100 S(I0)=F(E0)*3.1416
3110 R0=0
3120 FOR I=1 TO N0
3130 R0=R0+F(I)
3140 NEXT I
3150 Z0=G*(1.-R0/R1)
3160 IF Z0>0 GOTO 3200
3170 PRINT 'OIL DENSITY GREATER THAN WATER DENSITY'
3180 PRINT 'IN RADIUS CALCULATION IN STEP ';I0;','
3190 STOP
3200 T7=.546*(V0/(Z0*N1))↑(.333333)
3210 T8=.375*(R1/S1)*((Z0*N1)↑2.*S(I0)↑4.)↑(.1666666)
3220 IF T4>T3/2. GOTO 3310
3230 IF T3/2.>T7 GOTO 3260
3240 R4=1.14*((Z0*V0)↑.25)*SQRT(T3/2.)
3250 GOTO 3380
3260 IF T3/2.>T8 GOTO 3290
3270 R4=.98*(Z0↑2.*S(I0)↑4./N1)↑.0833333*(T3/2.)↑.25
3280 GOTO 3380
3290 R4=1.6*SQRT(S1/(SQRT(N1)*R1))*(T3/2.)↑.75
3300 GOTO 3380
3310 IF T4>T7 GOTO 3340
3320 R4=1.14*((Z0*V0)↑.25)*SQRT(T4)
3330 GOTO 3380
3340 IF T4>T8 GOTO 3370
3350 R4=.98*(Z0↑2.*S(I0)↑4./N1)↑.0833333*T4↑.25
3360 GOTO 3380
3370 R4=1.6*SQRT(S1/(SQRT(N1)*R1))*T4↑.75
3380 REM ** END OF RADIUS ROUTINE **
3390 D6=0
3400 FOR I=1 TO N0
3410 D6=D6+F(I)/(R(I)*R1)
3420 NEXT I
3430 FOR I=1 TO N0
3440 F(I)=F(I)/D6
3450 NEXT I
3460 S2=0
3470 FOR I=1 TO N0
3480 S2=S2+F(I)/M(I)
3490 NEXT I
3500 I(I0)=0
3510 FOR I=1 TO N0
3520 G(I)=K0*W(Y2)*((F(I)/M(I))/S2)*P(I)
3530 I(I0)=I(I0)+G(I)/(R(I)*R1)
3540 NEXT I
3550 H0=S(I0)/(3.1416*R4↑2.)
3560 IF K1≠1 GOTO 3620
3570 FOR I=1 TO N0

```

```

3580 A(I)=(F(I)/H0)*I(I0)-G(I)/H0
3590 NEXT I
3600 A(E0)=-I(I0)*R4↑2.
3610 GOTO 2650
3620 REM ** END OF R-K ITERATIONS **
3630 FOR I=1 TO E0
3640 IF F(I)≥1. GOTO 3660
3650 F(I)=0
3660 NEXT I
3670 J(I0)=0
3680 FOR I=1 TO N0
3690 C(I0,I)=F(I)
3700 J(I0)=J(I0)+F(I)
3710 NEXT I
3720 H(I0)=H0
3730 N(I0)=R4
3740 S(I0)=F(E0)*3.1416
3750 IF R1>J(I0) GOTO 3790
3760 N=I0
3770 F2=-1
3780 RETURN
3790 IF 3.1416*R4↑2.≤100000.*S(I0)↑.75 GOTO 3830
3800 N=I0
3810 F2=-2
3820 RETURN
3830 IF S(I0)/S(1)>.0001 GOTO 3870
3840 N=I0
3850 F2=-3
3860 RETURN
3870 IF J(I0)>.1 GOTO 3900
3880 N=I0
3890 F2=-3
3900 RETURN
3910 REM *****
3920 REM
3930 REM ** DROP DIAMETER **
3940 REM
3950 N3=(1.-H(I0)/B0)*N1+(H(I0)/B0)*N4
3960 IF N3≥N1 GOTO 3990
3970 N3=N1
3980 GOTO 4010
3990 IF N3≤N4 GOTO 4010
4000 N3=N4
4010 W1=(.6*S1*W↑.25)/(J(I0)*G↑.5*N3↑1.25)
4020 IF W1>10. GOTO 4050
4030 K(I0)=.6*W↑.25*N3↑.75/G↑.5
4040 GOTO 4080
4050 K(I0)=(.03*S1↑.6*W↑.4)/(R1↑.6*G↑.8)
4060 IF H(I0)≥K(I0) GOTO 4080
4070 K(I0)=H(I0)↑.333333*K(I0)↑.666666
4080 L(I0)=SQR((12.*S1)/(G*(R1-J(I0))))

```

```

4090 IF L(I0)≠H(I0) GOTO 4110
4100 L(I0)=H(I0)
4110 IF L(I0)≠K(I0) GOTO 4130
4120 L(I0)=K(I0)
4130 RETURN
4140 REM *****
4150 REM
4160 REM ** DROP DISPERSION **
4170 REM
4180 D3=N2*S(J0)*T3
4190 D4=9.52*N1↑.666667/((G*(1.-J(I0)/R1))↑.333333)
4200 IF K(I0)≠L(I0) GOTO 4380
4210 REM ** MIN AND MAX DIAMETERS THE SAME **
4220 FOR I=2 TO 4
4230 O(I0,I)=0
4240 U(I0,I)=0
4250 Z(I0,I)=0
4260 NEXT I
4270 Q(I0,1)=D3
4280 IF K(I0)≠0 GOTO 4310
4290 U(I0,1)=(8.*G*K(J0)*(1.-J(I0)/R1)/3.)↑.5
4300 GOTO 4320
4310 U(I0,1)=G*K(I0)↑2.*(1.-J(I0)/R1)/(18.*N1)
4320 Z2=.01*W2*θ(Y2)↑2./U(I0,1)
4330 IF Z2≦Z1 GOTO 4360
4340 Z(I0,1)=Z1
4350 GOTO 4370
4360 Z(I0,1)=Z2
4370 GOTO 4550
4380 REM ** MIN AND MAX DIAMETERS DIFFERENT **
4390 A=20.*D3/(L(I0)↑5.-5.*L(I0)*K(I0)↑4.+4.*K(I0)↑5.)
4400 FOR J=1 TO 4
4410 D5=K(I0)+(2.*I-1.)*((L(I0)-K(I0))/8.)
4420 O(I0,I)=A*(L(I0)-D5)*D5↑3.*((L(I0)-K(I0))/4.)
4430 IF D5≦D4 GOTO 4460
4440 U(I0,I)=SQR(8.*G*D5*(1.-J(I0)/R1)/3.)
4450 GOTO 4470
4460 U(I0,I)=G*D5↑2.*(1.-J(I0)/R1)/(18.*N1)
4470 IF T(I)=1 GOTO 4500
4480 Z2=.01*W2*θ(Y2)↑2./U(I0,I)
4490 IF Z2≦Z1 GOTO 4530
4500 Z(I0,I)=Z1
4510 T(I)=1
4520 GOTO 4540
4530 Z(I0,I)=Z2
4540 NEXT J
4550 REM ** CALCULATE TOTAL OIL REMAINING DISPERSED **
4560 D(I0)=0
4570 FOR I=D7 TO I0

```

```

4580 D9=0
4590 FOR J=1 TO 4
4600 IF Q(I,J)>0 GOTO 4630
4610 D9=D9+1
4620 GOTO 4880
4630 IF Z(I,J)=0 GOTO 4660
4640 D9=D9+1
4650 GOTO 4880
4660 IF U(I,J)=0 GOTO 4690
4670 D(I0)=D(I0)+O(I,J)
4680 GOTO 4880
4690 T1=(10-I+.5)*T3
4700 Q=(U(I,J)*T1-Z(I,J))/SQR(2.*K2*T1)
4710 I8=1
4720 IF Q<=0 GOTO 4740
4730 I8=-1
4740 IF Q<2. GOTO 4770
4750 D9=D9+1
4760 GOTO 4880
4770 IF Q<=-2. GOTO 4800
4780 D(J0)=D(J0)+O(J,J)
4790 GOTO 4880
4800 Q=ABS(Q)*1.4142
4810 Q1=INT(10.*Q)+1
4820 Q2=Q1+1
4830 P1=X(Q1)+((X(Q2)-X(Q1))/1)*(Q-.1*(Q1-1))
4840 IF D8=-1 GOTO 4870
4850 D(I0)=D(I0)+(1.-P1)*O(I,J)
4860 GOTO 4880
4870 D(I0)=D(I0)+P1*O(I,J)
4880 NEXT J
4890 IF D9<4 GOTO 4910
4900 D7=D7+1
4910 NEXT J
4920 S5=S(I0)
4930 S(I0)=S(I0)-(D(I0)-D(I0-J))
4940 H(I0)=H(I0)*(S(I0)/S5)
4950 RETURN
4960 REM *****
4970 REM
4980 REM ** SLJCKLET DISTRIBUTION **
4990 REM
5000 IF L1<=0 GOTO 5100
5010 IF H(I0)<=.001 GOTO 5040
5020 Q(I0)=S(I0)/H(I0)
5030 RETURN
5040 T5=(I0-1)*T3
5050 L1=1
5060 O2=N(I0)/2./3.
5070 T6=250.*O2+.44
5080 Q(I0)=4.*3.1416*O2

```

```

5090 RETURN
5100 T9=(I0-1)*T3
5110 IF T9>T6 GOTO 5160
5120 O2=N(I0)↑2./3.
5130 O2=O2+.23*N(I0)↑1.5*C0*(T9-T5)/SQR(L0)
5140 Q(I0)=4.*3.1416*O2
5150 RETURN
5160 O2=N(I0)↑2./3.
5170 O3=O2
5180 O2=O2+.23*N(I0)↑1.5*C0*(T9-T5)/SQR(L0)
5190 IF L2≠0 GOTO 5220
5200 R3=N(I0)
5210 L2=1
5220 O3=O3+.23*R3↑1.5*C0*(T6-T5)/SQR(L0)
5230 O3=O3+5.E-06*(T9↑2.3-T6↑2.3)
5240 IF O2<O3 GOTO 5290
5250 Q(I0)=4.*3.1416*O2
5260 R3=N(I0)
5270 T6=T6+T3
5280 RETURN
5290 Q(I0)=4.*3.1416*O3
5300 RETURN
5310 REM *****
5320 REM
5330 REM ** VARIABLE MAP **
5340 REM
5350 OPEN FL1,'E80',002,OUT
5360 MAT PUT FL1,I,J,S,K,L,H,N,D,Q,W,@,#
5370 MAT PUT FL1,O,U,Z,C,R,B,V,P,M
5380 PUT FL1,N0,T3,N,V0,C0,T0,D0,T2,D1,F2,F3,Y1
5390 CLOSE FL1
5400 RETURN
5410 REM *****
5420 REM
5430 REM ** WIND/WAVES **
5440 REM
5450 PRINT 'ENTER THE NUMBER OF WIND SPEED/WAVE HEIGHT'
5460 PRINT 'TIME INTERVALS (1-10).';
5470 INPUT Y1
5480 IF Y1>0&Y1<11 GOTO 5510
5490 PRINT 'MUST BE BETWEEN 1 AND 10.'
5500 GOTO 5450
5510 PRINT 'FOR EACH INTERVAL, ENTER THE WIND SPEED (M/S).';
5520 PRINT 'THE ONE-THIRD SIGNIFICANT WAVE HEIGHT (M).';
5530 PRINT 'AND THE DURATION (HR) OF THE INTERVAL.'
5540 FOR I=1 TO Y1
5550 PRINT '
5560 PRINT 'SPEED, HEIGHT, AND DURATION FOR INTERVAL';I;'';
5570 INPUT W(I),@ (I),#(I)
5580 IF W(I)≥0&W(I)≤60 GOTO 5610
5590 PRINT 'THE WIND SPEED MUST BE BETWEEN 0 AND 60.'

```

```

5600 GOTO 5560
5610 A9=.283/9.81
5620 IF @ (I) ≥ A9*(W(I)*.8)↑2.&@ (I) ≤ A9*(W(I)*1.2)↑2. GOTO 5680
5630 PRINT 'THE GIVEN WAVE HEIGHT IS NOT COMPATIBLE'
5640 PRINT 'WITH THE GIVEN WIND SPEED. THE WAVE HEIGHT'
5650 PRINT 'MUST BE BETWEEN';A9*(W(I)*.8)↑2.;' AND'
5660 PRINT A9*(W(I)*1.2)↑2.;' METERS.'
5670 GOTO 5560
5680 IF #(I) > 0 GOTO 5710
5690 PRINT 'DURATION (HR) MUST BE GREATER THAN 0.'
5700 GOTO 5560
5710 #(I)=INT( #(J)/T3)
5720 NEXT I
5730 Y2=2
5740 FOR I=1 TO Y1
5750 Y2=Y2+#(I)
5760 #(I)=Y2
5770 NEXT I
5780 Y2=1
5790 RETURN

```

```

0010 REM *****
0020 REM
0030 REM ** OUTPUT ROUTINE **
0040 REM
0050 DIM R(5),B(5),A(6),V(5),E(6),W(10),@ (10),#(10)
0060 DIM Y(6),G(5),I(141),J(141),S(141)
0070 DIM P(5),M(5),C(141,5),F(6),K(141)
0080 DIM L(141),H(141),N(141),D(141),U(141,4)
0090 DIM Q(141,4),Z(141,4),X(31),Q(141)
0100 REM
0110 GOSUB 0140
0120 GOSUB 0240
0130 END
0140 REM *****
0150 REM
0160 REM ** REVERSE MAP **
0170 REM
0180 OPEN FL1,'E80',002,IN
0190 MAT GET FL1,I,J,S,K,L,H,N,D,Q,W,@,#
0200 MAT GET FL1,O,U,Z,C,R,B,V,P,M
0210 GET FL1,N0,T3,N,V0,C0,T0,D0,T2,D1,F2,F3,Y1
0220 CLOSE FL1
0230 RETURN
0240 REM *****
0250 REM
0260 REM ** OUTPUT SUBROUTINE **
0270 REM
0280 PRINT FLP,'TABLE 1--INPUT PARAMETERS:'
0290 PRINT FLP,'-----'
0300 PRINT FLP,' '
0310 PRINT FLP,'          INITIAL SPILL VOLUME (CUBIC METERS): ';V0
0320 PRINT FLP,' '
0330 PRINT FLP,'          SPILL COMPONENTS:'
0340 FOR I=1 TO N0
0350 PRINT FLP,' '
0360 PRINT FLP,'          COMPONENT NO. ';I;' '
0370 PRINT FLP,'          SPECIFIC GRAVITY:          ';R(I)
0380 PRINT FLP,'          BOILING POINT (DEG. C):    ';B(I)-273
0390 PRINT FLP,'          RELATIVE VOLUME:          ';V(I)
0400 IF F3=0 GOTO 0430
0410 PRINT FLP,'          VAPOR PRESSURE:            ';P(I)
0420 PRINT FLP,'          MOLECULAR WEIGHT:          ';M(I)
0430 NEXT I
0440 PRINT FLP,' '
0450 PRINT FLP,'          CURRENT SPEED (M/S):      ';C0
0460 PRINT FLP,' '
0470 PRINT FLP,'          TEMPERATURE OF SEA (DEG. C): ';T0-273
0480 PRINT FLP,' '
0490 PRINT FLP,'          INITIAL DISTANCE TO SHORE (KM): ';D0
0500 PRINT FLP,' '
0510 PRINT FLP,'          RUNGE-KUTTA TIME STEP (HR): ';T3/3600.

```

```

0520 PRINT FLP, ' '
0530 PRINT FLP, ' DISPLAY INTERVAL: ';D1
0540 PRINT FLP, ' '
0550 PRINT FLP, ' MAXIMUM SIMULATION TIME (HR): ';T2/3600.
0560 PRINT FLP, ' '
0570 PRINT FLP, ' WIND SPEED/WAVE HEIGHT INTERVALS: '
0580 PRINT FLP, ' '
0590 Y2=2
0600 FOR I=1 TO Y1
0610 PRINT FLP, ' '
0620 PRINT FLP, ' INTERVAL NO.,I;':''
0630 PRINT FLP, ' '
0640 PRINT FLP, ' WIND SPEED (M/S): ';W(I)
0650 PRINT FLP, ' 1/3 SIG. WAVE HEIGHT (M):';@ (I)
0660 H(I)=H(I)-Y2
0670 Y2=Y2+H(I)
0680 X9=H(I)*T3/3600.
0690 PRINT FLP, ' INTERVAL DURATION (HR): ';X9
0700 NEXT I
0710 FOR I=1 TO 8
0720 PRINT FLP, ' '
0730 NEXT I
0740 PRINT FLP, 'TABLE 2---SLICK VOLUME DISTRIBUTION: '
0750 PRINT FLP, '-----'
0760 PRINT FLP, ' '
0770 PRINT USING FLP,0780
0780 : SURFACE PERCENT OF PERCENT OF PERCENT OF
0790 PRINT USING FLP,0800
0800 : ELAPSED VOLUME INITIAL INITIAL INITIAL
0810 PRINT USING FLP,0820
0820 : TIME REMAINING VOLUME ON VOLUME VOLUME
0830 PRINT USING FLP,0840
0840 : (HR) (M**3) SURFACE EVAPORATED DISPERSED
0850 PRINT USING FLP,0860
0860 : -----
0870 F4=D1
0880 FOR I=1 TO N
0890 IF I<NIF220 GOTO 0920
0900 GOSUB 2640
0910 GOTO 1030
0920 IF F4#D1 GOTO 1000
0930 X1=(I-1)*T3/3600.
0940 X2=S(I)
0950 X3=S(I)/S(1)*100.
0960 X4=(1.-(S(I)+D(I))/S(1))*100.
0970 X5=D(I)/S(1)*100.
0980 PRINT USING FLP,1020,X1,X2,X3,X4,X5
0990 F4=0
1000 F4=F4+1
1010 NEXT I
1020 : #####.## #.##### ||| ###.## ###.## ###.##

```

```

1030 FOR I=1 TO 8
1040 PRINT FLP, ' '
1050 NEXT I
1060 PRINT FLP, 'TABLE 3---POLLUTED AREA AND SLICK THICKNESS:'
1070 PRINT FLP, '-----'
1080 PRINT FLP, ' '
1090 PRINT USING FLP,1100
1100 :          TOTAL          PERCENT OF
1110 PRINT USING FLP,1120
1120 :ELAPSED      AREA      TOTAL AREA      SLICK
1130 PRINT USING FLP,1140
1140 : TIME      CONTAMINATED  COVERED      THICKNESS
1150 PRINT USING FLP,1160
1160 : (HR)      (KM**2)      WITH OIL      (MM)
1170 PRINT USING FLP,1180
1180 :-----
1190 F4=D1
1200 FOR I=1 TO N
1210 IF I<NIF2=0 GOTO 1240
1220 GOSUB 2640
1230 GOTO 1340
1240 IF F4#D1 GOTO 1310
1250 X1=(I-1)*T3/3600.
1260 X2=Q(I)/1.E06
1270 X3=(S(J)/H(I))/Q(I)*100.
1280 X4=H(I)*1000.
1290 PRINT USING FLP,1330,X1,X2,X3,X4
1300 F4=0
1310 F4=F4+1
1320 NEXT I
1330 :####.##      #.###|1111      ###.##      #.###|1111
1340 FOR I=1 TO 8
1350 PRINT FLP, ' '
1360 NEXT I
1370 IF F3=1 GOTO 1390
1380 RETURN
1390 PRINT FLP, ' *****'
1400 PRINT FLP, ' *** DETAILED OUTPUT TABLES ***'
1410 PRINT FLP, ' *****'
1420 FOR I=1 TO 4
1430 PRINT FLP, ' '
1440 NEXT I
1450 PRINT FLP, 'TABLE 4---DETAILED SURFACE SLICK CHARACTERISTICS'
1460 PRINT FLP, '-----'
1470 PRINT FLP, ' '
1480 PRINT USING FLP,1490
1490 :          SURFACE EVAPORATION  AVERAGE      SLICK      SLICK
1500 PRINT USING FLP,1510
1510 : VOLUME      FLUX      DENSITY      THICKNESS      RADIUS
1520 PRINT USING FLP,1530
1530 : J      (M**3)      (KG/M**2/S)      (KG/M**3)      (M)      (M)

```

```

1540 PRINT USING FLP,1550
1550 -----
1560 FOR I=1 TO N
1570 IF I<NIF2<=0 GOTO 1600
1580 GOSUB 2640
1590 GOTO 1630
1600 PRINT USING FLP,1620,I,S(J),I(I)*J(I),J(I),H(I),N(J)
1610 NEXT J
1620 :### #.##### #.##### #.##### #.##### #.#####
1630 FOR I=1 TO 5
1640 PRINT FLP,' '
1650 NEXT I
1660 PRINT FLP,'TABLE 5--DETAILED DROPLET DISPERSION AND'
1670 PRINT FLP,' Slicklet DISTRIBUTION RESULTS:'
1680 PRINT FLP,'-----'
1690 PRINT FLP,' '
1700 PRINT USING FLP,1710
1710 : SMALL LARGE VOLUME TOTAL
1720 PRINT USING FLP,1730
1730 : DIAMETER DIAMETER DISPERSED POL. AREA
1740 PRINT USING FLP,1750
1750 : I (M) (M) (M**3) (M**2)
1760 PRINT USING FLP,1770
1770 :-----
1780 FOR J=1 TO N
1790 IF I<NIF2<=0 GOTO 1820
1800 GOSUB 2640
1810 GOTO 1850
1820 PRINT USING FLP,1840,I,K(I),L(J),D(I),Q(I)
1830 NEXT J
1840 :### #.##### #.##### #.##### #.#####
1850 FOR I=1 TO 5
1860 PRINT FLP,' '
1870 NEXT I
1880 PRINT USING FLP,1910
1890 PRINT USING FLP,1920
1900 PRINT USING FLP,1930
1910 :TABLE 6--COMPONENT MASS CONCENTRATIONS (KG COMPONENT
1920 : PER CUBIC METER OF SLICK:
1930 :-----
1940 PRINT FLP,' '
1950 PRINT USING FLP,1960
1960 : I COMP. 1 COMP. 2 COMP. 3 COMP. 4 COMP. 5
1970 PRINT USING FLP,1980
1980 :-----
1990 FOR I=1 TO N
2000 IF I<NIF2<=0 GOTO 2030
2010 GOSUB 2640
2020 GOTO 2060
2030 PRINT USING FLP,2050,I,C(I),J),C(I,2),C(I,3),C(I,4),C(I,5)
2040 NEXT I

```

```

2050 .### #.##### #.##### #.##### #.##### #.#####
2060 FOR I=1 TO 5
2070 PRINT FLP, ' '
2080 NEXT I
2090 PRINT USING FLP,2110
2100 PRINT USING FLP,2120
2110 :TABLE 7--DROPLET TERMINAL VELOCITIES (M/S)
2120 :-----
2130 PRINT FLP, ' '
2140 PRINT USING FLP,2150
2150 : I      SIZE 1      SIZE 2      SIZE 3      SIZE 4
2160 PRINT USING FLP,2170
2170 :-----
2180 FOR I=1 TO N
2190 IF I<NIF2<=0 GOTO 2220
2200 GOSUB 2640
2210 GOTO 2250
2220 PRINT USING FLP,2240,I,U(I,1),U(I,2),U(I,3),U(I,4)
2230 NEXT I
2240 .### #.##### #.##### #.##### #.#####
2250 FOR I=1 TO 5
2260 PRINT FLP, ' '
2270 NEXT I
2280 PRINT USING FLP,2300
2290 PRINT USING FLP,2310
2300 :TABLE 8--DROPLET DISPERSION DEPTHS (M)
2310 :-----
2320 PRINT FLP, ' '
2330 PRINT USING FLP,2340
2340 : I      SIZE 1      SIZE 2      SIZE 3      SIZE 4
2350 PRINT USING FLP,2360
2360 :-----
2370 FOR I=1 TO N
2380 IF I<NIF2<=0 GOTO 2410
2390 GOSUB 2640
2400 GOTO 2440
2410 PRINT USING FLP,2430,I,Z(I,1),Z(I,2),Z(I,3),Z(I,4)
2420 NEXT I
2430 .### #.##### #.##### #.##### #.#####
2440 FOR I=1 TO 5
2450 PRINT FLP, ' '
2460 NEXT I
2470 PRINT USING FLP,2490
2480 PRINT USING FLP,2500
2490 :TABLE 9--VOLUME IN DROPLETS (M^3)
2500 :-----
2510 PRINT FLP, ' '
2520 PRINT USING FLP,2530
2530 : I      SIZE 1      SIZE 2      SIZE 3      SIZE 4
2540 PRINT USING FLP,2550
2550 :-----

```

```

2560 FOR I=1 TO N
2570 IF J=NIF2=0 GOTO 2600
2580 GOSUB 2640
2590 GOTO 2630
2600 PRINT USING FLP,2620,I,O(I,1),O(I,2),O(I,3),O(I,4)
2610 NEXT I
2620 :### #.##### #.##### #.##### #.#####
2630 RETURN
2640 REM *****
2650 REM
2660 REM ** SLICK EVAP/SINK/BREAK-UP MESSAGES **
2670 REM
2680 IF F2=-1 GOTO 2730
2690 PRINT FLP,' '
2700 PRINT FLP,' THE AVERAGE DENSITY OF THE SLICK BECOMES'
2710 PRINT FLP,' GREATER THAN THE DENSITY OF WATER.'
2720 RETURN
2730 IF F2=-2 GOTO 2780
2740 PRINT FLP,' '
2750 PRINT FLP,' SLICK BREAKS UP (AREA VS. VOLUME'
2760 PRINT FLP,' STOPPING CRITERION REACHED).'
2770 RETURN
2780 PRINT FLP,' '
2790 PRINT FLP,' THE SLICK HAS ENTIRELY EVAPORATED OR'
2800 PRINT FLP,' DISPERSED IN THE WATER COLUMN.'
2810 RETURN

```

E.2.2 Definitions of Variables in Program Code

Arrays

- A(K) - Intermediate Runge-Kutta function value for equation K.
- B(J) - Boiling point (initially °C, later °K) of oil component J.
- C(I,J) - Mass concentration (kg of component/m³ of slick) of component J at beginning of interval I.
- D(I) - Total volume remaining dispersed in water column at beginning of interval I.
- E(K) - Intermediate Runge-Kutta routine value for equation K.
- F(K) - Intermediate value of differential equation K in Runge-Kutta routine.
- G(J) - Mass flux (kg of component/m² of slick/sec.) of component J.
- H(I) - Slick thickness (m) at beginning of interval I.
- I(I) - Average volume flux of all components (m³/m²/s) at beginning of interval I.
- J(I) - Average slick density (kg/m³) at beginning of interval I.
- K(I) - Minimum droplet diameter (m) at beginning of interval I.
- L(I) - Maximum droplet diameter (m) at beginning of interval I.
- M(J) - Molecular weight of component J.
- N(I) - Radius of slick (m) at beginning of interval I.
- O(I,L) - Volume (m³) of oil dispersed during interval I and contained in droplets of diameter given by L, K(I), and L(I), where L varies from 1 to 4.
- P(J) - Vapor pressure of component J.
- Q(I) - Total area polluted (m²) at beginning of interval I.
- R(J) - Specific gravity of component J.
- S(I) - Volume of surface slick (m³) at beginning of interval I.

Arrays (Cont.)

- T(L) - Flag in maximum dispersion depth calculation for droplets of diameter given by L, K(I), and L(I).
- U(I,L) - Terminal velocity (m/s) of droplets of diameter given by L, K(I), and L(I) that were dispersed during interval I.
- V(J) - Relative volume (parts component per one part slick) of component J.
- W(M) - Wind speed (m/s) during wind speed/wave height interval M.
- X(N) - Normal distribution table values.
- Y(K) - Intermediate Runge-Kutta variable for old values of equation K.
- Z(I,L) - Dispersion depths for droplets of diameter given by L, K(I) and L(I) and dispersed during interval I.
- @(M) - Wave height (m) during wind speed/wave height interval M.
- #(M) - Interval number at which wind speed/wave height interval M begins.

Scalar Variables

- A - Weighting factor for diameters in dispersion routine.
- A9 - Intermediate value in wind speed/wave height input routine.
- A\$ - Answer to query.
- BØ - Thickness of turbulent bore.
- CØ - Current speed (m/s).
- DØ - Initial distance to shore (km).
- D1 - Display interval.
- D3 - Increment of surface volume dispersed during an interval (m³).
- D4 - Droplet critical diameter (m).
- D5 - Droplet diameter (m).
- D6 - Temporary variable.

Scalar Variables (Cont.)

- D7 - Counter in dispersion routine.
- D8 - Sign flag in dispersion routine.
- D9 - Counter in dispersion routine.
- E0 - Total number of differential equations: $N0 + 1$.
- E1 - Evaporation time.
- F - Data file number.
- F1 - Runge-Kutta flag/step number.
- F2 - Slick evaporation/break-up/sink flag.
- F3 - Output type (summary or detailed) flag.
- F4 - Line count flag
- G - Acceleration due to gravity (m/s).
- H0 - Slick thickness (m) (temporary variable).
- I0 - Time step counter.
- K0 - Constant in component flux equation.
- K1 - Flag in Runge-Kutta routine.
- K2 - Turbulence diffusivity.
- L0 - Constant in distribution routine.
- L1 - Flag in distribution routine.
- L2 - Flag for checking slick radius at T6.
- N - Total number of time steps/intervals.
- N0 - Number of components in spilled oil.
- N1 - Viscosity of water.
- N2 - Fraction of surface oil dispersed per unit time (s^{-1}).
- N3 - Effective viscosity of water/oil boundary.
- N4 - Viscosity of oil

Scalar Variables (Cont.)

- O2 - Variance of slicklet distribution before T6.
- O3 - Variance of slicklet distribution after T6.
- P0 - Atmospheric pressure.
- P1 - Probability value in dispersion routine.
- Q - Temporary variable in probability calculation in dispersion routine.
- Q1 - Index for probability calculation.
- Q2 - Index for probability calculation.
- R0 - Average slick density (kg/m^3).
- R1 - Density of water (kg/m^3).
- R2 - Ratio of component boiling point ($^{\circ}\text{K}$) to ocean temperature ($^{\circ}\text{K}$).
- R3 - Slick radius (m) at time T6.
- R4 - Slick radius (m) (temporary value).
- S0 - 1/3 significant wave height (m).
- S1 - Surface tension of water/oil boundary.
- S2 - Intermediate variable.
- S5 - Volume variable.
- T0 - Ocean temperature (initially $^{\circ}\text{C}$, later $^{\circ}\text{K}$).
- T1 - Elapsed time since dispersion (s) in dispersion routine.
- T2 - Maximum simulation time (initially in hours, later in seconds).
- T3 - Runge-Kutta time step (initially in hours, later in seconds).
- T4 - Total elapsed time (s) in Runge-Kutta routine.
- T5 - Time when slick reaches 1 mm thickness.
- T6 - Time for transition to Gaussian distribution for slicklets.

Scalar Variables (Cont.)

- T7 - Time to end of gravity-inertia regime.
- T8 - Time to end of gravity -viscous regime.
- T9 - Present time (temporary).
- V0 - Initial spill volume (m³).
- V1 - Component relative volume normalizing factor.
- W - Wave frequency.
- W0 - Initial wind speed (m/s).
- W1 - Microscale Weber number.
- W2 - Wave crossing frequency.
- X1-X9 - Temporary output variables.
- Y1 - Time until weather update.
- Y2 - Index for weather update.
- Z0 - Intermediate variable in slick radius calculations.
- Z1 - Maximum dispersion depth (m).
- Z2 - Velocity-dependent dispersion depth (m).

E.2.3 Notes on Program Code

While the program code is quite complicated, it does, for the most part, follow the algorithms detailed in Sections 3 through 6 and Appendix B. Below are some notes concerning parts of the code either that depart somewhat from the given algorithms or that are in some other way confusing.

1. In line 580, 9.999 should be 10. (For some reason, our machine believes that $10 > 9.999 * 1.$, but does not believe that $10 \geq 10 * 1.$) Similarly in lines 610 and 680.
2. The code in lines 5450 through 5790 should really be moved up to line 1600. In an earlier version, there was a reason for this separation; in the present version, it's only confusing.
3. The matrix X contains a normal distribution table (lines 2180-2260). This is used in the droplet dispersion routine to calculate the error function:

$$\text{erf}(x) = 2F(\sqrt{2}x) - 1,$$

where F is the cumulative normal distribution.

4. Lines 2480-2530 contain the "constants" that change when the wind speed and wave height change; hence, the conditional GOSUB at line 270 in the main routine.
5. In line 4390, A is a constant such that

$$V_{\text{disp}} = \int_{d_{\text{min}}}^{d_{\text{max}}} A(d_{\text{max}} - d) d^3 dd,$$

where V_{disp} is the volume dispersed during a time interval, d_{min} is the minimum droplet diameter, and d_{max} is the maximum droplet diameter. Thus, $A(d_{\text{max}} - d)$ is the linear probability density distribution for droplets of size d .

6. At line 4690, the elapsed time since the oil was dispersed is given by $(I\theta - 1 + .5) * T3$. The .5 enters into the equation because we assume that the oil dispersed during a time interval is dispersed in the middle of the interval.
7. Line 4830 is an interpolation calculation using the normal distribution table values at intervals of .1:

$$P_{\text{interp}} = P_{\text{low}} + \left(\frac{P_{\text{high}} - P_{\text{low}}}{Q_{\text{high}} - Q_{\text{low}}} \right) (Q_{\text{actual}} - Q_{\text{low}}).$$

8. The value of $D(I)$ is the total volume of oil dispersed at, or as of, the beginning of time interval I . That is,

$$D(I) = \sum_{k=1}^I \left(\sum_{j=1}^4 P(I-k, j) \cdot O(k, j) \right),$$

where $P(I-k, j)$ is the probability that a droplet of the j^{th} diameter is still dispersed after time $I-k$, and $O(k, j)$ is the total volume of oil dispersed during time interval k and in droplets of the j^{th} diameter. In lines 4920-4940, the change in dispersed volume, $D(I)-D(I-1)$, is subtracted from the surface volume and the thickness of the surface slick is adjusted accordingly.

E.2.4 Installation on Other Systems

The version of BASIC that runs on the IBM 5100 is sufficiently primitive that converting this program to another version of BASIC for some other system should not be difficult (though it may be tedious).

Apart from I/O (input/output) incompatibilities (which plague all program conversions), there are only three immediately obvious potential problems:

- 1) The 5100's version of BASIC limits array names to a single character. Since the program requires 28 arrays, we were forced to use "@" and "#" as names for two of them. These are probably not legal names on most systems, and so will have to be changed. Since most systems do not require single character names, however, this should not prove too difficult.
- 2) The syntax of the IF statements will probably be different on other systems. Most systems use "<>" for "is not equal to," rather than "≠", for example. Many systems may require a THEN prior to the GOTO in an IF statement.

- 3) Some systems may require LET statements (such as "LET T3 = .25"). Most systems do not.

Most system incompatibilities will arise from the I/O statements: PRINT, PRINTUSING, OPEN, CLOSE, PUT, GET and CHAIN. It's fairly obvious what the objectives of these statements are (in the context of the program code), but, depending upon the system, these objectives will range from easy to impossible to achieve.

Any BASIC system has a PRINT statement, but the syntax will usually differ.

Most, if not all, versions of BASIC have a statement equivalent to PRINTUSING (a formatted output statement). Again, the syntax will usually differ.

Some machines or some versions of BASIC may be unable to handle multiple I/O devices, in which case the OPEN, CLOSE, PUT, and GET statements will either have to be replaced with hard-coded options or will have to be deleted. (For example, if it were not possible to read the oil spill component make-up from a file, then the component data for some types of oil could be stored in DATA statements within the program, and the user could be asked to select one of these oil types or to enter the component data from the terminal.) If the machine is able to handle multiple I/O devices, it will still be necessary to change the syntaxes of these statements.

If the system has a large enough core capacity, the CHAIN statement at the end of the main program can be changed to a GOSUB, and the output program can be made a subroutine of the main program, rather than a separate unit. This would eliminate the need for saving data in and retrieving data from a storage file. If, on the other hand, the system has too little core capacity, the input and initialization sections can be made a separate program unit and executed prior to the calculation section, through use of another CHAIN statement or its equivalent. (Note

that a small portion of the initialization section may occasionally be called by the calculation section. See Section E.1.3.)

APPENDIX F
DROPLET NUMBER DISTRIBUTION FUNCTIONS

To determine the volume fraction of oil dispersed in the water column, it is necessary to adopt an assumption regarding the size distribution of droplets. There are no reliable observations or theoretical estimates of actual size distribution of droplets formed by breaking wave-slick interaction. In Chapter 4, we presented an algorithm to estimate the diameter of largest and smallest droplets formed. In Chapter 5, a simple linear number density distribution was assumed to determine the fractional volume of oil dispersed in the water column as a function of time. In this Appendix, we will generalize the expressions obtained in Chapter 5 for an arbitrary number density distribution of droplets.

Let the droplet number density distribution be given by the following equation

$$g(d) = a d_{\max} f(\delta) \quad (\text{F.1})$$

Where $f(\delta)$ is the distribution function and δ is the nondimensional diameter d/d_{\max} . The most general form of the distribution function can be either a polynomial in δ or a known function (such as exponential function). However, certain closure conditions must be satisfied by the chosen function. These conditions are:

- It has been observed that in a given volume of water containing oil droplets, large numbers of small droplets are found. Hence the droplet distribution function should be a monotonically decaying function.
- The smallest diameter was determined by the Weber number criterion described in Chapter 4. Therefore, the distribution function should have a maximum at the minimum diameter, d_{\min} .

Some of the possible distributions are shown in Figure F.1. The elementary volume of droplets of diameter d is given by

$$dV(d) = a d_{\max} f(\delta) d^3$$

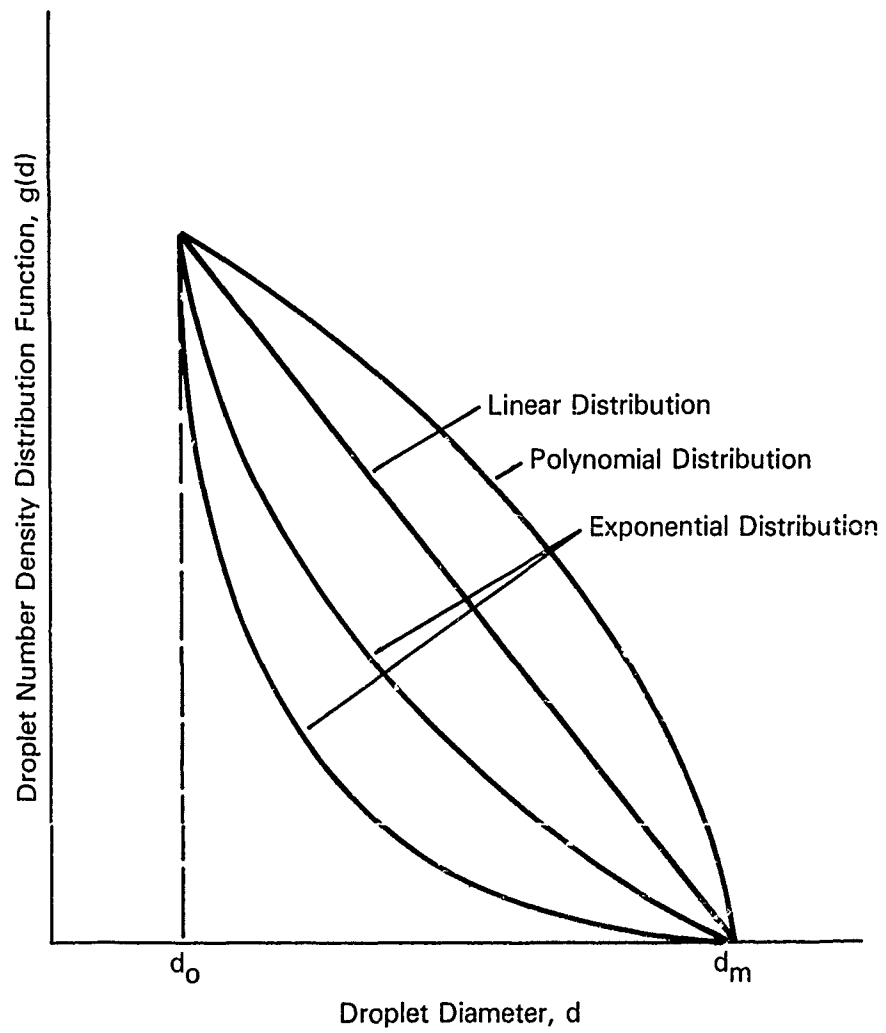


Figure F.1 Droplet Number Density Distribution Model

The total volume is:

$$\int_{d_{\min}}^{d_{\max}} f(\delta) d^3 dd$$

The parameter W^* , defined by Equation (5.22) may be redefined as:

$$W^* = d_{\max} \int_{d_{\min}}^{d_{\max}} f(\delta) d^3 dd \quad (F.2)$$

The fractional volume in the diameter range d and $d + \Delta d$ is given by:

$$F_d = W^* \int_d^{d + \Delta d} d_{\max} f(\delta) d^3 dd \quad (F.3)$$

Once the functional form of $f(\delta)$ is known, W^* and F_d may be readily determined. These results for some simple functions are given here.

1. Linear Function

Let $f(\delta)$ be given by

$$f(\delta) = 1 - \delta \quad (F.4)$$

Therefore

$$W^* = \frac{d_{\max}^5}{20} - \frac{d_{\max} d_{\min}^4}{4} + \frac{d_{\min}^5}{5} \quad (F.5)$$

$$F_d = \frac{1}{W^*} \left(\frac{d_{\max} d^4}{4} - \frac{d^5}{5} \right) \Bigg|_d^{d + \Delta d}$$

These expressions were used in the droplet distribution model developed in Chapter 5.

2. 2nd degree polynomial

Let $f(\delta)$ be given by:

$$f(\delta) = c_0 + c_1 \delta + c_2 \delta^2 \quad (F.6)$$

Since $f(\delta)$ should be maximum at $d = d_{\min}$ and steadily decrease, we will assume $c_0 = 1$, $c_1 = -0.5$ and $c_2 = -0.5$, which yields:

$$f(\delta) = 1 - \frac{\delta}{2} - \frac{\delta^2}{2}$$

The corresponding expressions for W^* and F_d are:

$$\begin{aligned}
 W^* &= \frac{d_{\max}^5}{15} - \frac{d_{\max} d_{\min}^4}{4} + \frac{d_{\min}^5}{10} + \frac{d_{\min}^6}{12d_{\max}} \\
 F &= \frac{1}{W^*} \left(\frac{d_{\max} d^4}{4} - \frac{d^5}{10} - \frac{d^6}{12d_{\max}} \right) \left| \begin{array}{c} d + \Delta d \\ d \end{array} \right.
 \end{aligned} \tag{F.7}$$

3. Exponential Function

Let the distribution function be exponential with a value of unity at $d = d_{\min}$. This is given by

$$f(d) = c_0 \exp\left(-\delta \frac{d - d_{\min}}{d_{\min}}\right) \tag{F.8}$$

where $c_0 = e$. Substituting this in Equations (F.2) and (F.3), we obtain the following expressions for W^* and f_d .

$$\begin{aligned}
 W^* &= d_{\max} d_{\min}^4 \left\{ 16 - \exp\left(1 - \frac{d_{\max}}{d_{\min}}\right) \left[\left(\frac{d_{\max}}{d_{\min}}\right)^3 + 3\left(\frac{d_{\max}}{d_{\min}}\right)^2 + 6\left(\frac{d_{\max}}{d_{\min}}\right) + 6 \right] \right\} \\
 F_d &= \frac{d_{\max} d_{\min}^4}{W^*} \left\{ -e^{(-d/d_{\min})} \left[\left(\frac{d}{d_{\min}}\right)^3 + 3\left(\frac{d}{d_{\min}}\right)^2 + 6\left(\frac{d}{d_{\min}}\right) + 6 \right] \right| \begin{array}{c} d + \Delta d \\ d \end{array} \right\}
 \end{aligned} \tag{F.9}$$

Similar expressions can be obtained for any distribution function and can be used in the algorithm developed in Chapter 5.

END

**DATE
FILMED**

9-82

DTIC